TECHNICAL REPORT

IN-SITU TREATMENT OF SURFACTANT-CONTAMINATED AQUIFER BY ELECTROCHEMICAL PROCESSES

submited to

Du Pont Company

and

Delaware State Research Partnership

March, 1994

by

C. P. Huang (Principal Investigator)

Chieh-Sheng Chu (Graduate Research Assistant)

Luis R. Takiyama (Graduate Research Assistant)

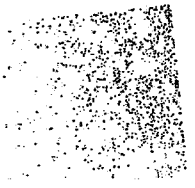

Table of Contents

List of Figures

List of Tables

Summary

During the project period, four major tasks were completed to study the feasibility of the removal of ammonium perfluoro-octanoate (C8) from contaminated soils. These tasks included:

- characterization of the plant production groundwater,
- characterization of soil samples at the anaerobic ponds,
- adsorption/desorption experiments, and
- electro-osmosis tests.

Characterization of the site groundwater was the first task accomplished. A water sample was taken from a tap on the plant site above the anaerobic ponds. The source of this water is from on-site production wells. Properties such as pH, alkalinity, conductivity, total dissolved solids (TDS), and concentration of major cations (Ca^{2+}, Mg^{2+}, Na^{+}, K^{+}), minor cations (Fe(II), Mn(II)), trace heavy metals (Pb(II), Cu(II), Cd(II), Ni(II), Zn(II), Co(II)), anions (HCO_3^-, CO_3^{2-}, Cl^-, NO_3^-, SO_4^-), and CO_2 were analyzed. Concentration of ammonium perfluoro-octanoate (C8) in the groundwater was also determined. The results demonstrated that Ca^{2+}, Na^{+}, HCO_3^-, Cl^-, and SO_4^- are the major ionic species present in the water. C8 was detected at a concentration of about 113 ppb.

Soil samples from two locations (ADPS-1 and ADPS-2) at various depths were received and physical-chemical properties, such as pH, specific surface area, moisture content, organic matter, cation exchange capacity (CEC), pH at zero point of charge (pH_{ZPC}), composition, hydraulic permeability, and C8 concentration were determined. The composition analysis showed a high percentage of clay (about 40%) in the top soil zones at both locations (depth < 10 feet). Therefore, the shallow zone is the most suitable region where the electro-osmosis process can be effectively applied. The highest concentrations of C8 were also found in these shallow soil samples in the top 10 feet; Around 5 to 16, and 5

to 33 ppm of C8 were detected in the shallow soils at ADPS-1 and ADPS-2 sites, respectively. As expected, specific surface area, organic matter content, cation exchange capacity and hydraulic permeability produced results consistent with the composition analysis (i.e., higher percentage of clay corresponds to higher specific surface area, organic matter content, cation exchange capacity, C8 concentration, and lower hydraulic permeability). The soil pH analysis showed that most of the subsurface soils are in the neutral pH region (pH = 5.5 ~ 7.5) and the variation with depth is not significant. The pH_{ZPC} of the soil samples from the ADPS-2 site are in the range of 2.0 to 2.7, indicating that at higher pH values, the soil particles will be negatively charged.

To examine the behavior of C8 in the soil water system, batch adsorption/desorption experiments were conducted at various pH values, C8 concentrations, temperatures, and soil/water ratios. Continuous flow adsorption experiments under an electrical field were performed to verify influence on C8 adsorption. The results demonstrated that the C8 adsorption varies substantially with pH. Because the acidity constant of C8 is $10^{-2.9}$ and the pH_{zpc} of the soil is in the range of 2.0 to 2.5, an electrostatic repulsion between anionic C8 and negatively charged soil surfaces occurs at pH values higher than 3. As a result, C8 adsorption to the soil decreases with increasing pH, and the higher the pH, the greater the amount of soil desorption.

Batch adsorption/desorption experiments were conducted at different temperatures (0°C, 25°C, and 45°C). The results showed that the temperature is inversely proportional to the extent of C8 adsorption and directly proportional to the amount of C8 desorbed. C8 soil adsorption capacity decreases with increasing temperature.

When the initial C8 concentration is below 50 ppm, the extent of soil adsorption is diminished significantly at pH greater than 5.0 (at least for soil/water ratio of 0.05 g/mL). However, when the initial C8 concentration is greater than 50 ppm, the percentage of C8 adsorbed is higher because the hydrophobic interactions become significant to the adsorption process.

Continuous flow apparatus were constructed to investigate the adsorption behavior under electrical fields. Three adsorption systems were adopted according to the voltage applied and the positions of electrodes. They were as follows:

Type **A**: without voltage applied (control);

Type **B**: anodes placed at the influent side and cathodes located at the effluent side;

Type **C**: cathode positioned at the influent side and anode at the effluent side.

Three parameters (effluent pH, effluent volume and C8 concentration) were monitored to evaluate the performance of these three reactors. The results show that type **C** exhibited the highest C8 retaining capacity and lowest effluent pH. Inversely, type **B** adsorption system produced the highest effluent pH and the lowest adsorption capacity. No differences were detected in the effluent volume between the three systems. The changes in pH of the solutions in the vicinity of electrodes were caused by the water redox reactions.

A total of six electro-osmosis tests under various conditions were conducted to evaluate the C8 removal from the contaminated subsurface anaerobic pond soils. The following **Table I** summarizes some of the experimental conditions of the tests.

Table I: Some experimental conditions of the electro-osmosis tests conducted.

Test #	Soil sample	Potential gradient (V/cm)	pH control
I	ADPS-2 0-5'	1.0	NO
II	ADPS-2 0-5'	1.5	NO
III	ADPS-2 5-10'	1.5	NO
IV	ADPS-2 0-5'	1.5	YES (NaOH, pH=10)

V	ADPS-2 0-5'	1.5	YES ($Ca(OH)_2$, pH=10)
VI	mixed soils	1.5	YES ($CaCO_3$, pH=6.0)

The results demonstrated that it is practical to remove the C8 by electro-osmosis under pH controlled conditions at influent and effluent solutions. A 97 % removal of the C8 originally present in the soil was achieved in Test IV under pH control (pH = 10) with NaOH/HCl. Other tests using $Ca(OH)_2$ and $CaCO_3$, did not yield the same results possibly due to the following reasons: a) high pH conditions caused precipitation of some salts, e.g., $CaCO_3$ that coated the surface of the electrodes, yielding low efficiency of the electro-osmosis process; b) By introducing calcium (instead of sodium) into the system, the ionic strength increases substantially, causing a diminishing of the zeta potential (ζ) and consequently the fluid velocity through the soil towards the cathode. Electro-osmosis experiments performed without pH conditioning showed little C8 removal. In these tests, a significant amount of C8 remained in the soil presumably caused by the low fluid velocity and the build up of strong pH gradients across the soil core.

ASH010612

I. Introduction

Electro-osmosis, an electro-kinetic phenomenon, has been one of the emerging techniques for in-situ treatment of contaminated subsurface soil and groundwater. This is the same process used by geological engineers to consolidate foundations for construction. The electro-osmosis process relies on externally voltage applied to a soil matrix system to induce water movement. The cations migrate toward the cathode and the anions toward the anode. Because there is an excess of solvated cations near the negatively charged soil surface, a net movement of water towards the cathode is observed.

The study included the following specific objectives:

- Investigated the influence of various physical-chemical properties of the soil matrix on the removal process;
- Evaluated the factors controlling the removal process;
- Obtained parameters needed for the design of the electrokinetic process for in-situ removal.

I.2. Theoretical background:

I.2.1. Electro-osmosis:

Electro-osmosis has found broad application in colloid characterization, particle separation and engineering construction (foundation consolidation). In an electrical field,

water will flow from the positive end (anode) to the negative end (cathode). Casagrande (1949) has pioneered some of the first successful field application of this technique.

Two theories have been proposed to described the electro-osmosis water flow; the Helmholtz-Smoluchowski (1879) and the Schmid (1952). According to the Helmholtz-Smoluchowski theory, the flow rate of water (Qe) moving in a capillary of length, L under electrostatic field, Φ, is

$$Q_e = \frac{\varepsilon \zeta \Phi}{4\pi\eta L}$$

where ε, Φ, ζ, and η are the dielectric constant, field strength, electrokinetic potential and viscosity. However, according Schmid (1952) the water flow rate is :

$$Q_e = \frac{r^2 q F \Phi}{8\eta L}$$

where **r**, **q**, **F** are the radius, volume charge density in the pore, and Faraday constant. Apparently, the Helmholtz-Smoluchowski theory predicts a flow rate that is independent of pore size whereas the Schmid theory predicts that the flow rate is proportional to the cross sectional area of the pores. Neither theory allows for an exchange of electrolytes in the pores beyond the number of cations needed to balance the negative charge of the clay particles. However, Esrig and Majtenyi (1965) have proposed the following equation:

$$Q_e = \frac{1}{2}\ln(1+\frac{\kappa}{r})(\frac{r^2}{\eta})\rho(\frac{\Phi}{L})$$

where ρ, κ are the average mobile surface charge density and the parameter characterizing the double layer. The above equation is able to accommodate both the Helmholtz-

Smoluchowski and the Schmid theories. Nevertheless, in field practice, the water flow rate is found to be a function of the cross-sectional area of the flow:

$$Q_e = k_e i_e A$$

where k_e and i_e are the electro-osmotic permeability, the electrical potential gradient, and electrode surface area. Casagrande has determined the electro-osmotic permeability of various soil and found that the K_e value varies only within one order of magnitude with an average value of 5×10^{-5} cm^2/sec-v. Chappel and Burton (1975) reported that a flow of 550 l per day was achieved with steel electrodes at a spacing of 3 meters and applied DC voltage of 40 V.

II. Experimental Procedures

II.1. Analysis of the site groundwater quality:

Alkalinity, pH and conductivity were measured immediately upon receiving the groundwater samples in our laboratory. The addition of 50 mL concentrated HNO_3 to 1 gallon of water sample was used to preserve it for future chemical analysis.

Atomic absorption spectrophotometry technique was employed to determine the concentration of all metals in the water. The major cation concentrations such as potassium, calcium, sodium, and magnesium were determined by direct aspiration into air-acetylene flame while the minor cations and trace heavy metals were analyzed by the graphite furnace (electrothermal atomic absorption method).

Potentiometric method using a chloride ion selective electrode was used to determine the concentration of Cl^- in the process water.

A turbidimetric method was employed to determine the sulfate concentration in the water sample.

For the analysis of nitrate, an ultraviolet spectrophotometric method was used.

Other anion concentrations such as CO_3^{2-} and HCO_3^- were calculated from the alkalinity and pH measurements.

All chemical analysis (except Cl^-) were performed according to the Standard Methods for the Examination of Water and Wastewater(1985).

II.1.1. Alkalinity:

The alkalinity was determined according to the Standard Methods for the Examination of Water and Wastewater (SMEWW, method No. 403) by titrating the water sample with hydrochloric acid (0.02 N) to a preselected pH value of 4.5. The procedure was as follows:

i) Take 100 mL of the water sample and transfer it to an Erlenmeyer flask.

ii) Prepare the titration assembly (i.e. a 25 mL buret, magnetic stirrer and pH meter apparatus) and fill the buret with standard HCl (0.02 N).

iii) Titrate the sample to the end point, pH of 4.5, without recording the intermediate pH values and without undue delay.

iv) As the end point is approached, make smaller additions of acid and be sure that the equilibrium pH is reached before adding more titrant.

v) Record the total volume of acid consumed.

vi) Calculate the alkalinity (in mg $CaCO_3$/L) as follows:

$$\text{Alkalinity, (mg } CaCO_3 \text{ / L)} = \frac{A \times N \times 50{,}000}{V}$$

where, A, N, and V are the volume of titrant, normality of the acid consumed, and volume of the sample, respectively.

II.1.2. Conductivity:

The conductivity of the water sample was determined by a conductivity meter (Markson Sci. Inc., model ElectroMark analyzer). The procedure was as follows:

i) Record the conductivity of deionized water before sample measurement. This is to be substracted from sample measurements.

ii) Insert the probe into the water sample and stir for 3 minutes. Read and record (in triplicate) the conductivity in µmho/cm.

II.1.3. Total dissolved solids:

The total dissolved solids was determined following method No. 208.B described in the Standard Methods for the Examination of Water and Wastewater (SMEWW). The procedures are presented as follows:

i) Heat the evaporating dish to 180°C for 1 hour in an oven; store the evaporating dish in the desiccator until needed, weigh the dish immediately before use.

ii) Filter the well mixed aliquot sample with No. 40 filter paper (Whatman), transfer the filtrate to the evaporating dish. Dry 100 mL of the filtrate in an oven at 180°C until all the water is vaporized.

iii) Cool the sample in a desiccator and weigh until a constant weight is obtained. Calculate the total dissolved solids by the following equation:

$$\text{mg of total dissolved solids/L} = \frac{1000 \times (A - B)}{\text{sample volume (mL)}}$$

where: A= weight of dried residue plus dish (mg), and

B= weight of empty dish (mg).

II.1.4. Analysis of the major cations:

The air-acetylene flame atomic absorption spectrophotometry method (SMEWW, method No. 303A) was followed for the analysis of Na^+, K^+, Mg^{+2} and Ca^{+2} in the water samples. Atomic absorption spectrophotometer (Perkin Elmer model Zeeman 5000 with a A-50 auto sampler) was used. The experimental procedures were as described below:

i) Prepare a calibration curve using known concentrations of the desired metal to be analyzed. Read and record (following the instructions of the operation's mannual) the absorbances of the standard solutions.

ii) Read and record the absorbance of the water samples (generally in triplicate) and check if the absorbances fit in the range obtained for the calibration curve.

iii) If the recorded absorbance is higher than the calibration curve limits, further dilution of the water samples is performed.

iv) Calculate the concentration of the element in question using the linear regression equation obtained from each calibration curve.

II.1.5. Analysis of the minor cations:

Essentially, the same method (SMEWW, method No. 304) described above was used to determine the concentrations of minor cations and trace heavy metals (Fe(II), Mn(II), Pb(II), Cu(II), Cd(II), Ni(II), Zn(II), and Co(II)). Due to the low concentration of these species in the water samples, it was necessary to use the electrothermal atomic absorption method (graphite furnace). An atomic absorption spectrophotometer (Perkin Elmer Zeeman 5000) equipped with a graphite furnace (model HGA 560) was employed for these analyses.

Detailed procedures are essentially the same as described above for the analyses of major cations.

II.1.6. Determination of carbonates:

The Standard Methods for the Examination of Water and Wastewater (SMEWW, method No. 406C) was used to calculate the concentrations of carbonate species, i.e. CO_2, CO_3^-, and HCO_3^- based on the chemical equilibrium relationship among these carbonate species in natural water systems.

The concentration of bicarbonate is calculated by the following equation:

$$B = [HCO_3^-]\ (\text{mg } CaCO_3 / L) = \frac{T - 5.0 * 10^{(pH-10)}}{1 + 0.94 * 10^{(pH-10)}}$$

where T and pH are alkalinity (mg $CaCO_3$/L) and original pH of the water sample.

The free CO_2 is calculated by the equation:

$$A = [CO_2]_{free}\ (\text{mg } CaCO_3 / L) = 2.0 * B * 10^{(6-pH)}$$

The carbonate concentration is calculated by the equation:

$$C = [CO_3^{2-}] \text{ (mg } CaCO_3 / L) = 0.94 * B * 10^{(pH-10)}$$

The total carbonate concentration is calculated by the equation:

$$[CO_2]_{total} \text{ (mg } CaCO_3 / L) = A + 0.44 * (2B + C)$$

II.1.7. Analysis of chloride:

The chloride ion concentration was measured by the Potentiometric method, using a chloride ion selective electrode (Orion Company, model 94-17B). The experimental procedure was as presented below:

i) Set up the potentiometric apparatus, which includes the potentiometer, the reference electrode (e.g. Orion Model 90-02 double junction reference electrode), the Cl^- ion selective electrode and the magnetic stirrer system.

ii) Prepare a calibration curve using known concentrations of NaCl solutions under constant ionic strength of 0.1 M of $NaNO_3$.

iii) Read and record the potential (in mV) for each solution while keeping the sample stirred.

iv) Plot the logarithmic of potential (millivolt) measured as a function of the chloride concentration.

v) Read and record the potential of the samples and by linear regression analysis of the calibration curve, find the concentration of Cl^- in the water samples.

II.1.8. Analysis of sulfate:

The analysis of sulfate was executed by a turbidimetric method described in the Standard Methods for the Examination of Water and Wastewater (SMEWW, method No.

426C). The basic principle of the method is the precipitation of sulfate ion (SO_4^{2-}) in acetic acid medium with barium chloride so as to form barium sulfate crystals of uniform size. Light absorbance of the $BaSO_4$ was measured by a photometer at 420 nm and the SO_4^{2-} concentration was determined by comparison of the reading with a standard curve. The procedures were as follows:

i) Prepare the buffer solution dissolving 30 g of $MgCl_2.6H_2O$, 5 g of $CH_3COONa.3H_2O$, 1.0 g of KNO_3 and 20 mL of acetic acid (99%) in 1000 mL of distilled water.

ii) Prepare the a calibration curve using known concentrations of Na_2SO_4 solutions.

iii) Mix 100 mL of sulfate containing solution with 20 mL of the buffer solution

iv) Add a spoonful of $BaCl_2$ crystals, begin timing and stir for 60 seconds at constant speed.

iii) Pour the solution into a cell and read the absorbance of the calibration curve solutions and samples (in triplicate) at 420 nm in the spectrophotometer (Hach Company, model DR/2000).

II.1.9. Analysis of nitrate:

The NO_3^- analysis were done by using UV spectrophotometric method described in the Standard Methods for the Examination of Water and Wastewater (SMEWW, method No. 418A). Measurement of UV absorption at 220 nm enables rapid determination of nitrate ions. The experimental procedures were as below:

i) Treat the sample by filtering it through a 45 µm membrane filter and adding 1 mL of HCl 1N.

ii) Prepare calibration standards in the range of 0 to 7 mg NO_3^-/L.

iii) Read absorbance against redistilled water set at zero absorbance using a UV-VIS spectrophotometer (Perkin Elmer, model 139) at wavelength of 220 nm.

II.1.10. C8 analysis in the liquid phase:

The concentration of C8 in the aqueous solution was measured by Gas Chromatograph equipped with an Electron Capture Detector (Hewllet-Packard 5880 II Gas Chromatograph with HP 19303 Electron capture detector). All aqueous samples were concentrated by freeze and drying (lyophilization) process to remove the water and permit the derivatization. Methanolic HCl was added to the dried residual as the esterification agent along with perfluorodecanoic acid (C10) as an internal standard. Hexane was added to the solution mixture to extract the methyl ester from the aqueous solution. The organic phase was then ready for the gas chromatograph (GC) analysis.

The detailed procedures were as follows:

i) Place 1 mL of aqueous sample into a lyophilizer (Labconco, bench-top freeze and drying chamber). A vacuum pump (Maxima, Model D8A) is connected to the drying chamber to reduced the pressure to around 3×10^{-4} torr.

ii) Dry the samples completely. This process takes about 12 hours. The dried samples are then ready for the derivatization.

iii) To the dried residual, add 1 mL of methanolic HCl (3% HCl in methanol) along with 0.2 mL of a 10 ppm C10 solution as an internal standard to begin the derivatization process.

iv) Keep the sample in a thermostat for 1 hour at 65 °C to allow a complete esterification reaction.

v) After cooling the sample down to room temperature, add 1 mL of distilled water and 2 mL of hexane. Shake the mixture well to allow the extraction of the C8 from the aqueous phase. The organic phase is then ready for the GC analysis.

vi) To analyze the hexane extract, set the GC conditions as follows:

- Column: DB-210 (50% trifluoropropyl, 50% methyl) 30 m x 0.25 mm internal diameter, 0.5 mm film thickness (J & W Scientific).
- Temperatures: Injection port 200 °C
  Detector 225 °C

Oven	initial	60 °C
	rate	20 °C /min
	final	200 °C

- Carrier gas: 90% argon/10% methane
  Column head pressure 12 psi
- Injection volume: 1 µL
- Run time: 25 min

vii) Prepare a calibration curve with known concentrations of C8 and plot the peak area ratio of the C8 to the internal standard C10 (area counts C8/area counts C10) versus concentration of C8. The statistical method of linear regression is then utilized to compute the concentration of the ammonium perfluoro-octanoate in the samples.

II.2. Characterization of the soil samples:

With exception of specific surface area, pH_{ZPC}, hydraulic permeability and C8 analysis in the soil samples, all the other characterization procedures were extracted from the Methods of Soil Analysis, provided by the Agricultural Experimental Station of University of Delaware (1991).

II.2.1. Composition analysis:

The composition of site clay material was analyzed by the sedimentation (hydrometer) method as described below.

i) Pretreat the soil samples by grinding and sieving to make sure that the diameter of the soil particles does not exceed 2 mm.

ii) Take 50 grams of the ground soil sample and add 100 mL of 5% sodium hexametaphosphate.

iii) Transfer the suspension to a sedimentation cylinder, insert a plunger and mix the contents thoroughly.

iv) About 15 seconds after mixing the suspension, lower the hydrometer into suspension, and after 40 seconds, read the scale at the top of the meniscus. Record the hydrometer value. Also record temperature of the sample and a blank without soil at the 40 seconds time mark. From these values, the percentage of sand can be calculated.

v) After 2 hours of standing, lower the hydrometer into the sedimentation cylinder again and record the hydrometer value, then record the temperature of sample and blank. From these values, the percentage of clay can be calculated.

The equations for the calculation of the soil composition are as follows:

$$\% \text{ Sand} = 100 - \left[\frac{100 \times (\text{hydrometer reading at 40 seconds})}{(\text{corrected weight of soil})}\right]$$

$$\% \text{ Clay} = \frac{100 \times (\text{hydrometer reading at 2 hours})}{(\text{corrected weight of soil})}$$

$$\% \text{ Silt} = 100 - (\% \text{ Sand} + \% \text{ Clay})$$

where: corrected weight of soil $= \dfrac{\text{oven dry weight of subsample} \times 50\text{g}}{\text{air} - \text{dried weight of subsample}}$

II.2.2. Soil pH:

The pH measurements were made in 0.01 M $CaCl_2$ solution. The procedures were as follows.

i) Air-dry the soil sample and sieve through 2 mm sieve to remove the coarse soil fraction.

ii) Weigh 10 grams of the pretreated soil sample and mix with 10 mL of 0.01 M $CaCl_2$. Mix thoroughly and let the sample stand for at least 1/2 hour but not more than 1 hour.

iii) Record the pH value with a pH meter.

II.2.3. Soil organic matter:

Soil organic matter was determined by the loss of weight on ignition (L. O. I.) method. The method is described below:

i) Take 1 cm^3 of air dried soil sample, sieve through 2 mm sieve and place it into a 30 mL beaker.

ii) Dry the soil sample at 105 °C for two hours and record the weight of soil sample plus beaker with an accuracy of ±0.001 g.

iii) Place the sample in an oven at 360 °C for two hours. Let the sample cool down to 105 °C and maintain at this temperature until weighing.

iv) Weigh the beaker with the ash in a draft-free environment to ±0.001 g.

$$O.M.(\%) = \frac{(W_{bs} - W_b) - (W_{ba} - W_b)}{W_{bs} - W_b} \times 100$$

where:

W_b = weight of beaker,

W_{bs} = weight of beaker plus soil before ashing,

W_{ba} = weight of beaker plus ashed soil.

II.2.4. Soil effective cation exchange capacity:

a) Determination of the exchangeable cations:

i) Weigh 10 g of soil sample into a 100 mL polyethylene cup and add 50 mL of 1 N ammonium acetate (NH_4OAc) to the cup as a buffer solution to maintain the solution pH at 7.0.

ii) Shake the cup for 30 minutes. Filtrate the suspension through No. 40 filter paper (Whatman) and use 25 mL of 1 N NH_4OAc again to wash the filter paper.

iii) Collect the filtrate and determine the potassium, calcium and magnesium concentration by atomic absorption spectrophotometer.

b) Determination of exchangeable acidity:

i) Weigh 10 g of soil sample into a 125 mL Erlenmeyer flask, add 25 mL of 1 N KCl solution and mix well.

ii) Filtrate the suspension into a 300 mL Erlenmeyer flask.

iii) Add 4 drops of phenolphthalein indicator and titrate the KCl solution with the standard 0.01 N NaOH. At the end point of titration, record the volume of NaOH used.

iv) Get the exchangeable acidity in (meq/100g).

c) Effective cation exchangeable capacity (ECEC):

The sum of the concentrations of exchangeable potassium, calcium and magnesium and the exchangeable acidity is the effective cation exchangeable capacity (ECEC).

II.2.5. Moisture content:

The moisture content determination was done as follows.

i) Weigh 1 ± 0.0001g of soil on a tared aluminum plate.

ii) Put the soil sample in oven at 105 °C for 24 hours to dry.

iii) Take the sample from the oven and place to a desiccator to let cool down to room temperature. Measure the weight of the dried soil.

iv) The moisture content can be calculated as the follows:

$$M(\%) = \frac{W_{wet\ soil} - W_{dry\ soil}}{W_{wet\ soil} - W_{plate}} \times 100$$

where M(%) = moisture content, percentage by weight

$W_{wet\ soil}$ = weight of original soil sample + aluminum plate

$W_{dry\ soil}$ = weight of the ashed soil + aluminum plate

W_{plate} = weight of the aluminum plate

II.2.6. Specific surface area:

The specific surface area of the soil sample was determined by the BET-N_2 gas adsorption method using a model QS-7 Quantasorb surface area analyzer (Quantachrom Co., Greenvale, NY. model QS-7 Quantasorb).

The multipoint BET equation (Brunauer, Emmett, and Teller, 1938) is used to calculate the specific surface area.

$$\frac{1}{X(\frac{P_o}{P}-1)} = \frac{(C-1)}{X_m C}\frac{P}{P_o} + \frac{1}{X_m C}$$

where X = mass of adsorbate (N_2) adsorbed at relative pressure P/P_o,

P = partial pressure of adsorbate (N_2),

P_o = saturate vapor pressure of adsorbate (N_2),

X_m = mass of monolayer coverage of adsorbate adsorbed, and

C = a constant relates to the heat of the adsorbate condensation and heat of adsorption.

Because the adsorption data from Quantasorb is often accompanied by a non-Gaussian tailing pattern, particularly on porous samples, e.g., soil at high N_2 concentrations, the desorption signals are always preferable and used in the analysis of specific surface area and pore size distribution. The desorption signal is calibrated by injecting a known volume of nitrogen gas into the machine with signal obtained accordingly. Based on adsorption and desorption data, the specific surface area can be obtained.

II.2.7. pH_{ZPC}:

The pH of zero point of charge was determined as follows:

i) Take the soil samples from the containers, dry at 105 °C, grind and sieve through U.S. mesh No. 100 (150 μm).

ii) For each sample, prepare solutions of 0.05 g/L of the pretreat soil under three different ionic strengths e.g. 1×10^{-3}, 1×10^{-2}, 1×10^{-1} M of $NaClO_4$.

iii) Measure the zeta potential (ζ) with a zetameter (Laser Zee model 500) as a function of pH values ranging from 2 to 9. Adjust the pH of the solutions using $HClO_4$ and/or NaOH at various concentrations.

iv) Plot the ζ values vs. pH for the three different ionic strengths. The pH_{ZPC} is then obtained at pH of zero zeta potential.

II.2.8. Hydraulic permeability:

The hydraulic permeabilities of the soil samples were measured by the constant head method (Fetter, 1980). The soil samples were collected from DuPont Washington Works ADPS-1 site depth (23'-25') and ADPS-2 site depths (0'-5'), (5'-10'), (15'-20'), (20'-25'). The constant-head permeameter apparatus is shown in **Figure 1** and the following procedures were employed to obtain the hydraulic permeability:

i) Air dry the samples at room temperature.

ii) Fill the bottom section of the column with the dried soil.

iii) Supply water to the regulated reservoir in order to keep the liquid level constant.

iv) Collect the water overflow from the column after passing upward through the soil media.

v) Let enough water flow through the soil media until a constant flow rate is obtained.

vi) Record and plot the volume of water as a function of time.

vii) Compute the hydraulic permeability by Darcy's law. The equation is as follows:

$$K = \frac{VL}{Ath}$$

where: K = permeability coefficient (cm/sec)

V = effluent volume in time t (cm^3)

L = length of the soil sample (cm)

A = cross sectional area of the cylinder (cm^2)

h = hydraulic head (cm)

t = elapsed time (sec)

II.2.9. C8 analysis in the soil:

The C8 in the soil was determined according to procedures developed by CH_2M Hill Company.

The experimental procedure was as follows:

i) Weigh 10 grams of homogenized soil sample into a tared 400 mL beaker. Extract the sample with 100 mL of methanol/methylene 1:1 (V/V).

ii) Sonicate the sample (sonication unit from Fisher Company, Sonic dismembrator, Model 300) for 180 seconds using the pulsed mode of operation with 50 % duty cycle.

iii) Prepare a filter funnel for each sample. Place a small piece of glass wool on the bottom of the funnel and transfer approximately 50 of anhydrous powdered sodium sulfate into the funnel. Take a vacuum flask only to prewash the filter funnel with methanol/methylene 1:1 (V/V) immediately before use. Attach a clean 500 mL vacuum flask to the funnel and decant the extract from the first sonication. Extract the sample remaining in the beaker once again as described previously, adding 100 mL of fresh extracting

solvent. After the second sonication, pour the entire sample from the beaker into the filter funnel and rinse with few milliliters of extracting solvent to complete the transfer.

iv) Assemble a Kuderna-Danish (KD) apparatus (500 mL evaporative flask, 10 mL concentrator tube and three ball macro Snyder column) and transfer it to the filtered sample extract along with 2 boiling chips. Place the unit on a steam bath with the concentrator tube partially immersed in the hot water. Concentrate the sample until the apparent volume in the concentrator tube is nearly 1 mL.

v) Remove the KD apparatus from the steam bath and add 100 mL of fresh dichloromethane directly down the Snyder column. Reconcentrate the extract again to an apparent volume of 1 mL, remove the KD apparatus from the steam bath and allow the glassware to cool for 5 minutes.

vi) Disassemble the KD apparatus (replacing the Snyder column by a 24/40 stopper) and transfer the methylene chloride concentrate to a 4-dram vial. Add 6 mL of 1M NaOH to the concentrator tube before reconnecting it to the KD flask. Gently rotate the apparatus to rinse the interior walls. Collect the rinse liquid to the 4-dram vial.

vii) Secure the cap on the 4-dram vial and shake vigorously for 30 seconds. Briefly centrifuge the vial to assure a good phase separation and discard the dichloromethane phase.

viii) Adjust the pH of the sample extract to less than 1.5 using 1+1 sulfuric acid. Verify the pH with pH indicator paper.

ix) Add 5 mL of ether into the vial containing the acidified sample. Recap the vial and shake vigorously for 30 seconds. Transfer the upper ether phase to a micro KD apparatus (25 mL evaporative flask, 2 mL receiver and two-ball micro Snyder column). Repeat the last step, combine the ether extract with the previous ether extract and add 0.1 mL of concentrated ammonium hydroxide. Take the KD apparatus to a steam bath and concentrate to approximately 0.5 mL. Remove the sample from the steam bath and allow to cool.

ASH010630

x) Transfer the concentrated solution quantitatively using 0.5 mL of acetone to a 4-dram vial and further concentrate the sample to dryness using a nitrogen gas stream.

xi) To the dried residual, add 1 mL of methanolic HCl (3% HCl in methanol) along with 0.2 mL of a 10 ppm C10 solution as an internal standard to begin the derivatization process. Keep the sample in a thermostat for 1 hour at 65 °C to allow a complete esterification reaction.

xii) After cooling the sample to room temperature, add 1 mL of distilled water and 2 mL of hexane. Shake well to allow the extraction of the C8 from the aqueous phase. The upper organic phase is then ready for the GC analysis.

xiii) Analyze the samples using the same GC conditions as described in section II.1.10.

II.3. Adsorption/desorption experiments:

In order to study the affinity between the C8 and site soil materials, batch adsorption/desorption experiments were conducted. The influence of an electrical field on the adsorption was also investigated by continuous flow experiment.

II.3.1. Soil sample preparation:

The soil was collected from DuPont Washington Works ADPS-2 site, depth range from 0.5 feet to 30 feet. The samples were air dried at room temperature and sieved to collect particles with a mesh size of 150 μm (ASTM No.100) or smaller. The sieved soil samples were preserved in labeled plastic bags until used.

II.3.2. Batch adsorption experiments:

The influence of pH, temperature, initial surfactant concentration, and soil/water ratio on the C8 adsorption onto the soil samples were studied. The batch adsorption experiments were conducted as follows:

a) The pH effect:

i) To a series of plastic bottles, add the desired amount of soil and 90 mL of C8 solution in 0.1 M $NaClO_4$ as electrolyte.

ii) Adjust the pH of each bottle from 2 to 10 with NaOH (0.1 M) and $HClO_4$ (0.1 M). Complete the volume to 100 mL with the C8 solution.

iii) Place the bottles in a shaker and shake for 24 hours.

iv) Measure and record the final pH of the suspensions.

v) Collect and filter the supernatants through a 0.45 μm membrane.

vi) Analyze the filtrates for residual C8 concentration.

b) Temperature effect:

To study the temperature influence on the C8 adsorption, the same experimental procedures as decribed above were applied; except that a thermostatic shaker was used. Experiments at temperatures of 10°C and 45°C and two different soil/water ratios (0.01 and 0.05) were accomplished.

c) Soil/water ratio effect:

Five different soil/water ratios (g of soil/mL of solution) including 0.005, 0.01, 0.02, 0.05 and 0.1 were adopted to examine their effects on C8 adsorption. Once more, the same above procedures were employed.

d) Initial concentration effect:

Seven different initial C8 concentrations (10, 20, 30, 50, 100, 150, and 200 ppm) were used to test the influence of C8 concentration on the C8 adsorption behavior. The same experimental procedures as described previously were utilized.

II.3.3. Batch desorption experiments:

Desorption experiments were done using the soil samples from the ADPS-2 site, depth 0.5 to 5 feet. The procedures were as follows:

i) To a series of plastic bottles, add 5 g of soil and 90 mL of C8 solution in 0.1 M $NaClO_4$ as electrolyte.

ii) Adjust the pH of each bottle to 2 with NaOH (0.1 M) and $HClO_4$ (0.5 M). Complete the volume to 100 mL with the C8 solution.

iii) Place the bottles in a shaker and shake for 24 hours.

iv) Separate the water and the solid phase by centrifugation (5,000 rpm for 5 minutes) and discard the liquid phase.

v) To each bottle, add 90 mL of $NaClO_4$ (0.1 M) solution.

vi) Adjust the pH of each bottle from 2 to 10 with NaOH (0.1 M) and $HClO_4$ (0.1 M). Complete the volume to 100 mL with the sodium perchlorate solution (0.1 M).

vii) Shake the plastic flasks for 48 hours.

viii) Take aqueous samples at 6, 24, and 48 hours.

ix) Filtrate the aliquots through a 45 µm membrane and analyze them for C8 concentration.

II.3.4. Adsorption study under the electrical field:

Adsorption study under electrical field was conducted by continuous flow experiments using the soil sample from ADPS-2 site, depth 0 to 5 feet.

Three types of configurations were set up according to the placement of the elctrodes. The schematic diagram of continuous flow apparatus types **A, B,** and **C** are shown in **Figure 2a, 2b** and **2c,** respectively. The continuous flow adsorption experiment for type **A** was performed without application of any electrical field. Configuration **B** had the anode (positively charged electrode) installed at the influent side and the cathode positioned at the effluent extremity while type **C** presented opposite arrangement. The tests were conducted by passing a 50 ppm C8 solution (in $NaClO_4$ 0.1 M) through the soil samples (approximately 200 g of soil were placed in the cell). The effluent was collected in graduate cylinder flasks and its volume was recorded. Effluent pH and C8 concentration were determined and plotted as a function of time. Graphite rod electrodes (Ultra Carbon Co. U7/SPK ultra "F" grade graphite) and a power supply (Power/Mate Corporation, model E-12/158) were used to provide a potential gradient of 1.0 V/cm over the soil samples.

II.3.5. Analytical methods:

All the analysis of ammonium perfluoro-octanoate in the aqueous phase were conducted following the same procedures previously described in section II.1.10.

II.4. Electro-osmosis tests:

II.4.1. Soil sample preparation:

Soil sample from ADPS-2 site, depth 0 to 5 feet was employed for the electro-osmosis **Tests I, II, IV** and **V.** Sample from the same location and depth range of 5 to 10 feet was used for the electro-osmosis **Test III.** A section of 10 cm in length of undisturbed soil sample was taken from the column (6.8 cm of internal diameter) and placed in the central cylinder (also with dimensions of 10 cm in length and 6.8 cm of internal diameter)

of the electro-osmosis cell (**Figure 3**). The electro-osmosis **Test VI** was executed with a mixture of soils from the ADPS-2 (0 to 17 feet) and BGMW6 (0 to 2 feet).

Some properties of the soil sample core and experimental conditions are shown in **Appendices A, B, C, D, E,** and **F** for **Tests I, II, III, IV, V,** and **VI,** respectively.

II.4.2. Electro-osmosis apparatus set up and testing:

Figure 3 shows the typical electro-osmosis apparatus employed in the experiment. The electro-osmosis cell consisted of three parts - anode container, central cylinder where the soil sample was held and cathode container.

The volume of the containers were 650 mL for the electro-osmosis **Test I** and 125 mL for the **Tests II** and **III**. For the tests with pH control (**IV, V** and **VI**), the anode container was 650 mL to allow the insertion of pH probe and feeding solution tubes while the cathode reservoir volume was 125 mL.

To separate the soil from the water solution, a set of two nylon meshes with a filter paper in between were used both in the cathodic and anodic reservoirs. The graphite electrodes were placed right behind the membranes. It was suggested for the tests under pH control that some space should be left between the electrodes and membranes at the anode container. The reason was to provide better mixing to the anode solution near the electrodes.

After assembling the cell, both anode and cathode compartments were filled with electrolyte solution (process water). Then the electrodes were connected to the power supply to begin the test. The electro-osmosis **Test I** was an exception, where initially only the anode container was filled with electrolyte solution and the cathode reservoir was empty; moreover, in the three first days of experiment, no voltage was applied to verify the magnitude of the hydraulic permeability.

For all the tests, parameters such as water flow, current, pH at the cathode and anode reservoirs were monitored as a function of time. Water samples from the effluent and influent were taken and analyzed for C8 concentration.

At the end of the test, the soil samples were removed from the cell and sliced into 10 sections. Each section was analyzed for water content, pH and C8 concentration.

II.4.3. Electro-osmosis experiments with pH control:

The soil sample preparation, set up and testing for the electro-osmosis experiment with pH control were essentially the same as for the other tests. **Figure 4** presents the schematic diagram of the system used for the experiment. The pH was maintained constant at both the anode and cathode reservoir using a pH controller equipment (model pH-22, New Brunswick Scientific Co., Inc., Edison, NJ). **Table II** below outlines the different reagents (acids and bases) utilized and the pH in the electro-osmosis experiments.

Table II. Reagents used in the electro-osmosis experiments with pH control.

Test #	anode		cathode	
	pH	reagents	pH	reagents
IV	10	NaOH, HCl	10	NaOH, HCl
V	10	$Ca(OH)_2$, HCl	10	NaOH, HCl
VI	6	$CaCO_3$, HCl	10	NaOH, HCl

II.4.4. Moisture content effect on the electro-osmotic flow:

Soil samples from RBLMW2 and RBLMW11 at depth from 10 feet to 12 feet were utilized for the moisture content study. The soil samples were dried in the oven at 52°C for 12 hours and placed into a desiccator for 2 hours. Afterward, the dried samples were

ground with mortar and pestle. The moisture content was determined right before packing the soil in the electro-osmosis cell (**Figure 3**). The anode compartment was filled with process water and the cathode container was initially empty. The electrodes were then connected to the power supply. The time required to saturate the soil column was recorded and the effluent volume emerged at the cathodic reservoir was monitored as a function of time.

II.4.5. Analytical methods:

The soil moisture content was measured using the same procedure described in section II.2.5.

Soil pH was determined by the same procedures as in section II.2.2.

C8 concentration in the soil was determined by the procedure developed by CH_2M Hill Co.. This method is thes wae as described in section II.1.10.

III. Results and Discussions

III.1. Analysis of the site groundwater quality:

Table III summarizes the results obtained for the analysis of the groundwater. As expected, calcium and sodium, as well as HCO_3^-, SO_4^{2-} and Cl^- are present at high concentrations and heavy metals are present at trace amounts (ppb levels). The C8 concentration in the water sample was 113 ± 2 ppb.

Table III. Characterization of the site groundwater quality:

Characteristics	Results*
pH	7.1
alkalinity (mg $CaCO_3$/L)	133
conductivity (μmho/cm)	420**
total dissolved solids (mg/L)	345
major cations (ppm):	
Ca^{2+}	62.9
Mg^{2+}	13.8
Na^+	25.9
K^+	3.12
minor cations (ppb):	
Fe(total)	161
Mn(II)	1000
Pb(II)	<1
Cu(II)	<1
Cd(II)	1.8
Ni(II)	4.6
Zn(II)	1.7
Co(II)	1.0
Hg(II)	-
major anions (ppm):	
HCO_3^- (as mg $CaCO_3$/L)	132
CO_3^{2-} (as mg $CaCO_3$/L)	0.2
Cl^-	70.3
NO_3^-	0.6
SO_4^{2-}	49.1
CO_2 (as mg $CaCO_3$/L)	137
C8 (ppb)	113 ± 2***

* all results expressed as an average of 3 determinations, unless indicated.
** average of 5 determinations.
*** average of 6 determinations.

Figures 5 and **6** show the concentration of the major cations and trace heavy metals, respectively. **Figure 7** presents the anion concentration in the process water sample.

The equivalent bar chart of the major ionic species present in the process water is illustrated in **Figure 8.** From the diagram, it is observed that the electroneutrality is satisfied among the cations and anions.

III.2. Characterization of the soil samples:

III.2.1. Composition analysis:

Figures 9 a, b and **10 a, b** show the soil composition obtained from sedimentation method of two different sites -- ADPS-1 and ADPS-2. Composition data from both sites show that the percentage of sand increases with the depth. The results of the composition analysis of the soil sample is listed in the **Table IV.** Clay is the major component at the top soil zone (depth < 10 ft) indicating that electro-osmosis technology will be feasible for this region.

III.2.2. Soil pH:

The soil pH values were measured using 0.01 M $CaCl_2$ as electrolyte. The soil pH profiles (**Figures 11** and **12**) indicate that most of the soil is in the neutral pH region (pH from 5.5 to 7.5) and the variation over depth is insignificant.

III.2.3. Soil organic matter:

Soil organic matter is an important component of the soil system. It can affect other soil physical properties such as specific surface area, adsorption capacity, and CEC.

Figures 13 and **14** show organic matter content as a function of soil depth for ADPS-1 and ADPS-2 soil samples, respectively. The results indicate that the soil organic matter content decreases with increasing depth in both sites. The percentage of organic matter is closely related to percentage of clay as well. This suggests that the organic matter is strongly adsorbed by the clay portion.

III.2.4. Soil effective cation exchange capacity:

Figures 15 a, b and **16 a, b** show the depth distribution of effective exchange capacity and exchangeable cations for the samples from the ADPS-1 and ADPS-2 sites. In both locations, the exchangeable calcium is the predominant component in all sections of the soil profile.

III.2.5. Moisture content:

The moisture content vs. depth for both sites, ADPS-1 and ADPS-2 is illustrated in **Figures 17** and **18**, respectively. At the ADPS-1 location the moisture content is high at the top soil zone (about 18 percent) and low (about 2 to 5 percent) at the subsurface section, then increasing again to about 15 percent just above the water table. At the ADPS-2 site, the highest water content of about 15 percent was found at the section from 5 to 10 feet deep.

III.2.6. Specific surface area:

Figure 19 to 24 show the BET plots of all soil samples analyzed. **Table IV** summarizes the results of specific surface area of the samples tested. The specific surface areas of the soil samples from the ADPS-2 site are from 10 to 22 m^2/g.

III.2.7. pH_{zpc}:

Figure 25 shows the variation of pH_{ZPC} with depth at the ADPS-2 site. The profile indicates that the pH_{ZPC} has a value approximately 2.0 to 2.7 over the entire depth.

Figures 26 to **31** show the zeta potential as a function of pH for all soil samples tested. The pH of zero point of charge is obtained at the pH value where ζ is equal to zero.

Since the application of electro-osmosis will be investigated in this project, it is crucial to know the microscopic electrical properties of the soil samples. It has been reported in the literature that the electro-osmotic water flow is directly proportional to the zeta potential:

$$Q_e = \frac{\varepsilon \zeta \phi}{4\pi\eta L}$$

where ε, ϕ, ζ, η and **L** are the dielectric constant, field strength, zeta potential, viscosity and length. This equation shows that the electrical property of the soil will influence directly the electro-osmotic process.

The other important aspect of soil ζ is the adsorption capacity for ionic species which is closely related to ζ of the soil particles.

III.2.8. Hydraulic permeability measurements:

Constant head permeameter was used to determine the hydraulic permeability for the soil samples from both ADPS-1 and ADPS-2. For each soil sample, results of the relationship between the cumulative effluent volume and elapsed time are shown in **Figure 32** to **36.**

The statistical method of linear regression technique was adopted to obtain the average slope and hence, the hydraulic permeability. The depth profile for ADPS-2 site is shown in **Figure 37.** As expected, the soil samples in the top 10 feet present very low hydraulic permeability (~10^{-6} cm/sec)due to the high clay content present in this area.

III.2.9. C8 analysis:

The concentrations of C8 in the unsaturated soil below the anaerobic digestion ponds are shown in **Table IV.** There is a general trend for the upper soil zone to have higher concentrations of C8 as illustrated in **Figures 38** and **39.** Concentrations up to 33 ± 10 ppm were detected at ADPS-2 site and 16 ± 1 ppm in ADPS-1 site.

Table IV. Characterization of the soil samples.

sample*	Composition analysis			pH	O.M.	BCEC	M.C.	Surf. area	pH_{ZPC}	hydr. perm.	C8 conc.
	sand (%)	silt (%)	clay (%)		(%)	(meq/100g)	(%)	(m^2/g)		(cm/sec)	(ppm)
ADPS-1											
0.5'-2.5'	36	34	31	7.5	1.9	8.0	17.8	-	-	-	16±1
5'-7'	5	45	50	5.6	2.2	7.6	2.3	-	-	-	4±1
9'-11'	28	34	38	5.9	2.1	6.9	4.1	-	-	-	5±1
11'-13'	24	44	32	6.7	1.6	7.1	7.8	-	-	-	-
15'-17'	52	22	26	5.8	1.3	4.4	8.0	-	-	-	-
20'-22'	44	31	25	7.1	0.9	6.0	7.4	-	-	-	-
23'-25'	88	6	6	6.4	0.1	2.2	11.6	-	-	$4x10^{-5}$	-
25'-27'	89	4	7	6.0	0.3	3.0	9.8	-	-	-	12±02
28'-30'	88	0	12	6.1	0.5	2.6	11.5	-	-	-	-
30'-32'	90	5	5	7.1	0.2	2.2	11.6	-	-	-	-
32'-34'	92	4	4	6.6	0	1.9	15.4	-	-	-	-
ADPS-2											
0'-5'	36	35	29	7.5	1.9	9.9	7.9	18.0	2.1	$4x10^{-6}$	33±10
5'-10'	5	49	46	5.5	1.5	6.3	15.3	21.9	2.1	$2x10^{-6}$	16±5
10'-15'	5	51	44	6.2	1.5	7.4	9.7	21.9	2.7	-	5±2
15'-20'	50	30	20	5.4	1.3	5.2	4.8	10.8	2.5	$6x10^{-5}$	5±2
20'-25'	46	42	12	5.5	0.6	8.3	5.9	17.2	2.4	$4x10^{-4}$	5±2
25'-30'	54	28	18	6.2	0.9	8.2	13.9	9.5	2.0	-	6±2

* Each section represent the depth in feet below ground surface.

III.3. Adsorption/desorption experiments:

III.3.1. The effect of pH on C8 adsorption/desorption:

a) Adsorption:

Figures 40 to 45 show the residual C8 concentration in aqueous phase as a function of pH for soil samples from the ADPS-2 site, from 0 to 30 feet of depth, and **Figures 46 to 51** present the percentage of C8 adsorbed as a function of pH. From these diagrams, it is concluded that the adsorption varies substantially with pH. At low pH values (pH<2) the surfactant is highly adsorbed onto the soil and there is decreasing adsorption with increasing pH. The acidity constant of C8 is 2.9 and the pH_{zpc} of the soil is between 2.0 to 2.5. The distribution diagrams of soil surface protonated species and C8 is shown in **Figures 52, and 53** respectively. From these illustrations, one can observe that the negatively charged soil particles repel the perfluoro-octanoate ion at pH values higher than 3.0. As a result, the amount of C8 adsorbed decreases as pH increases. The adsorption can be attributed to chemical interactions (probably hydrogen bonding) that are represented by the following equations:

$$\underline{S}OH + C_7F_{15}COO^- \rightarrow \underline{S}OH \cdots\cdots^- OOCC_7F_{15}$$

or

$$\underline{S}O^- + C_7F_{15}COOH \rightarrow \underline{S}O^- \cdots\cdots HOOCC_7F_{15}$$

where $\underline{S}OH$ and $\underline{S}O^-$ represent neutral and negatively charged soil surface species, respectively.

b) Desorption:

Figure 54 a, b, and Figure 55 a, b show the C8 desorption results for the ADPS-2 site, section 0 to 5 and 5 to 10 feet, respectively. The amount of surfactant

desorbed was determined by analyzing the aqueous samples at 6, 24 and 48 hours of equilibrium time. The results demonstrated that a great amount of C8 was desorbed under alkaline conditions (pH>8), decreasing its concentration as pH decreased. This is in agreement with the results obtained in the adsorption experiment described previously.

The kinetic study indicated that the system reached an equilbrium within 6 hours and the C8 concentrations detected in the aliquots were almost the same as for 24 hours and 48 hours.

III.3.2 Effect of soil/water ratio:

a) At constant pH:

Figure 56 shows the results of C8 adsorption under different soil/water ratios. A total of six sections of the soil depth profile (ADPS-2) were tested. The pH was adjusted to 7.0 and the initial C8 concentration was 50 ppm. A slight increase in the quantity of C8 adsorbed was observed by increasing the soil/water ratio.

b) At varying pH :

The influence of soil/water ratio (0.005, 0.01, 0.05, 0.1 g/mL) on C8 adsorption under various pH was investigated. The soil sample ADPS-2 (0'-5') was used for these experiments. The results are shown in **Figure 57**. The C8 adsorption behavior as a function of pH follows the same trend for all the soil/water ratios studied except at soil/water ratio of 0.1 g/mL, when C8 is adsorbed even in the alkaline pH region.

III.3.3 Temperature effect on the C8 adsorption/desorption:

a) Adsorption:

Three different temperatures (10°C, 25°C and 45°C) were chosen to conduct the batch adsorption and desorption experiments. The plots of percentage of adsorption as a function of pH for each temperature are shown in **Figures 58** to **60**. Two different soil/water ratios (0.01 and 0.05 g/mL) were used to conduct the test. **Figures 61** and **62** show the results of the adsorption study under the three different temperatures (10°C, 25°C, 45°C). From these graphs, it is viewed that there is a slight increase in the adsorption capacity with decrease in temperature.

b) Desorption:

Figure 63 shows the C8 desorption under three different temperatures - 10°C, 25°C and 45°C. The results indicate that more of the surfactant was desorbed with increases of temperature, or C8 adsorption capacity decreases with increasing temperature.

III.3.4 Initial C8 concentration:

Seven different initial C8 concentrations (10, 20, 30, 50, 100, 150 and 200 ppm) were used to test their effect on the behavior of adsorption at soil/water ratio of 0.05 g/mL. **Figures 64** and **65** show the residual C8 in the aqueous phase vs. pH at various initial surfactant concentrations. At C8 below 50 ppm, the extent of adsorption reached 100% at pH value ≤ 2.0. This is in agreement with the fact that the maximum adsorption only occurs when the solution pH is lower than pH_{ZPC} of the solid surface. At pH values higher than 5, almost no C8 was uptaken due to electrostatic repulsion between the anionic C8 and the negative surface charge of the soil particle.

A noteworthy observation is that the percentage of adsorption for initial C8 concentrations above 50 ppm is higher than that below 50 ppm within the pH range from 3

to 9 (**Figures 66** and **67**). This can be attributed in part to the hydrophobic-hydrophilic nature of the ammonium perfluoro octanoate. At high C8 concentrations, the adsorption process is brought by nonpolar interaction, in addition to specific chemical bonding, between C8 and the soil surface. Therefore, the percentage of adsorption for initial C8 concentrations above 50 ppm is higher than those for 10, 20, 30 ppm.

Figure 68, and **69** illustrate the partition coefficient of C8 as a function of pH. The partition coefficient of C8 was calculated by the following equation:

$$K_d = \frac{q}{C}$$

Where q = accumulated concentration of C8 in soil (mg/Kg),

C = C8 concentration in the bulk solution (mg/L),

K_d = partition coefficient (L/Kg).

III.3.5. Adsorption under electrical field:

In order to study the effect of electrical field on the adsorption of C8, a continuous flow method was employed. **Figure 70** shows the pH of the effluent for the 3 types of adsorption systems. The effluent solution in system **A** did not show any pH variations during the entire experiment. A gradual increase of pH was observed for the solution effluent obtained in the adsorption system type **B**. The pH of the effluent in system **C** dropped from 7.0 to 2.4 within 6 hours of the test. The reasons for the pH changes were attributed to the redox reactions of water at the electrodes.

As indicated above, pH plays an important role in C8 adsorption. Therefore changes in pH under the electrical field can alter the extent of C8 adsorption. **Figure 71** demonstrates that during the 6 hours of adsorption experiment under electrical field, the amount of C8 retained in the system **C** was higher than that for the systems **A** and **B**.

Figure 72 shows the plot of accumulated flow as a function of time. The three types of adsorption systems did not exhibit appreciable differences in effluent volume, indicating that the electrical potential had little influence on the flow rate. The only important effect of the electrical field was the pH modification which in turn affects the C8 adsorption.

III.4. Electro-osmosis tests:

III.4.1. Electro-osmotic water flow:

Figure 73 shows the cumulative electro-osmotic water flow as a function of time for all the tests performed.

For **Test I**, no voltage was applied during the first 3 days and consequently no water flow was observed. This indicates that the soil has low hydraulic permeability. Thus, the subsequent water flow could be attributed exclusively to the electro-osmosis process. However, no water flow was found at a period of four days after the voltage was applied possibly because the soil system needed to be adjusted to some conditions such as, moisture content and ionic distribution. It is important to remember that initially the cathode compartment was empty and the moisture was provided entirely from the anode side. Among all the tests, **Test I** presented the smallest amount of water flow. In 30 days of experiment, about 160 mL of liquid was collected at the cathode compartment.

Test II produced higher amount of flow than the previous test. For this test, a potential gradient of 1.5 V/cm was used. The electro-osmotic cell was modified in a way that both cathodic and anodic reservoirs were initially filled with electrolyte solution. The necessity of this procedure was to better simulate real field conditions and it was utilized in further tests. Water flow emerged at the first day of experiment and around 900 mL of liquid was passed through the soil core in 54 days.

Figure 73 shows that nearly 330 mL of water was collected at the cathode side for **Test III.** This value is small when compared to the water flow obtained in **Test II.** One of the reasons is that the soil sample from ADPS-2, depth 5 to 10 feet contained a considerable amount of wax that had been used to seal the drill core during sample collection.

A high amount of flow was observed in **Test IV** during the 23 days of experiment when compared to previous tests. This test was executed under pH controlled conditions (see **Table III**) and 1100 mL of water was passed through the soil sample core. At high pH values, the soil surface is negatively charged (pH_{ZPC} = 2.5 - 2.7) and more solvated cations (that are responsible for the net water movement towards the cathode) are present near the surface. Thus, higher water flow is expected at high pH values as the zeta potential of the soil is higher at higher pH. According to Casagrande (1949), the electro-osmosis flow is proportional to zeta potential.

The cumulative electro-osmotic water flow as a function of time (**Figure 73**) shows that in **Test V**, almost 500 mL of water was passed through the soil core. According to the results of the electro-osmosis **Test IV**, by maintaining the pH at 10, high water flow would be predicted. Two of the reasons for the observed contrasts can be speculated as follows: a) the high pH conditions caused precipitation of some salts (e.g. $CaCO_3$) that coated the surface of the graphite electrodes, yielding a low efficiency of the electro-osmosis process; b) increasing the calcium concentration, the ionic strength of the electrolyte increases substantially causing a diminishing of the zeta potential (see **Figures 26 to 31**) and consequently reducing the amount of water flow.

For **test VI**, similar occurrence was observed. The only difference was that the pH could not be maintained at 10 by using $CaCO_3$ at the anode reservoir. Consequently smaller water flow than that for **Test V** was produced. Only 250 mL of water emerged at the cathode side in 31 days of experiment.

III.4.2. Coefficient of electro-osmotic permeability (k_e):

Figures 74 a, b show the coefficient of electro-osmotic permeability as a function of time for all the tests conducted. **Tests I and III** produced similar values of k_e (1-3 x 10^{-6} $cm^2/(V.s)$) , while **Test II** gave electro-osmotic permeability values around 5 x 10^{-6} $cm^2/(V.s)$, as can be seen in **Figure 74a.** Among the tests under pH control, **Tests IV** and **V** presented values of k_e up to 3-4 x 10^{-5} $cm^2/(V.s)$ while **Test VI** produced electro-osmotic permeability values on the order of 10^{-6} $cm^2/(V.s)$.

III.4.3. Current density:

With the exception of **Test IV,** all other tests presented the same trend of current density as a function of time **(Figure 75).** Values up to 0.5 mA/cm^2 were recorded at the beginning of the experiments with gradual decrease as the tests proceeded. **Test IV** produced current densities up to 2.3 mA/cm^2 with gradual increase the first 12 days of the test.

III.4.4. Influent pH:

In **Tests I, II,** and **III,** the pH of the influent (anode reservoir) dropped to values around 2 and remained constant afterward **(Figure 76a).** The build up of acid conditions at the anode was due to the oxidation of water represented by the equation (Acar, Y., etc., 1990) :

$$2H_2O \longrightarrow O_2 + 4H^+ + 4e^-$$

To conduct the experiments under pH control, it was necessary to add base to the anode reservoir. The pH for **Tests IV** and **V** were maintained at 10 with NaOH and $Ca(OH)_2$, respectively. For **Test VI,** $CaCO_3$ was used as the base and the pH could not

be controlled at 10; instead the pH was maintained at 6. **Figure 76b** shows the pH of the influent solution as a function of time for the tests under controlled pH conditions.

III.4.5. Effluent pH:

Figure 77a show the pH of the effluent solution as a function of time for the **Tests I, II and III.** The effluent pH of the **Tests I and III** rose to values around 12 and then dropped gradually due to the acid front generated at the anode. **Test II** presented a fairly constant pH (around 12) throughout the experiment, indicating that the electrolysis rate overcame the acid front at the anode. The basic condition at the cathode was caused by the reduction of water as follows:

$$2H_2O + 2e^- \longrightarrow H_2 + 2OH^-$$

Hydrochloric acid was used to adjust the pH at the cathode (effluent) reservoir in all the three tests under pH control. **Figure 77b** presents the pH of the effluent as a function of time for **Tests IV, V, and VI.**

III.4.6. C8 concentration at the effluent:

C8 concentrations at the effluent for all the tests conducted are shown in **Figure 78.** From this figure it is noticed that **Tests I, III, V and VI** presented very low effluent C8 concentrations. In the **Test II,** values up to 10 ppm were detected at the effluent solutions. **Test IV** exhibited the highest C8 concentration at the effluent reaching a maximum at 10 days of experiment correspondent to 55 ppm. At 20 days, almost no C8 could be found in the effluent solution.

III.4.7. C8 concentration at the influent:

The acidic constant for the perfluoro-octanoic acid is 2.9, indicating that at pH values higher that 2.9, most of the C8 molecules are present in solution in an anionic form (perfluoro-octanoate ion). Therefore it is expected that C8 molecules migrate towards the anode during the electro-osmosis process. The graph of concentration of C8 at the influent

solution as a function of time for all the electro-osmosis tests (except Test I) is shown in **Figure 79.**

Tests II and III did not present notable amounts of C8 at the influent solution because of the low pH condition. The C8 molecules at pH values lower than 2.9 have neutral charge and do not migrate to the anode.

Test IV also did not show significant C8 concentration at the analyte due to the high amount of water flow towards the cathode that exceeded the electrical migration of the C8 molecules.

Low water flow and basic pH conditions were present in **Tests V and VI,** and high amounts of C8 were determined at the influent solutions. Concentrations up to 90 and 40 ppm were detected for **Tests V and VI,** respectively.

III.4.8. C8 removal:

Figures 80 and 81 show the cumulative C8 removed at the cathode (in milligrams) and the percentage of total C8 displaced from the soil at the effluent as a function of time, respectively. It is observed that **Test IV** presented the highest removal while the other tests did not show significant amounts of C8 at the effluent solution. About 28 mg (88 %) of the ammonium perfluoro-octanoate was withdrawn from the contaminated soil by the electro-osmosis process in **Test IV. For Tests I, V, and VI,** low removal was achieved and values up to 1.7 mg of cumulative C8 were removed (2.5 %). **In Test II,** around 4.5 mg (18 %) of the surfactant present in the contaminated soil was removed. It is observed that in **Test III,** only 1.2 mg of C8 was recovered at the cathode which corresponded to 50 % of the total perfluoro-octanoate present in the soil. The amount of C8 removed at the cathode (effluent) was related to the velocity of the water flowing through the soil core due to the electro-osmosis process. **Test IV** had the highest water flow velocity and produced the highest C8 removal at the cathode.

Among all tests performed, **Test V** and **VI** presented the highest C8 removal at the anode. Around **78 %** and **63 %** of C8 were recovered at the anode in **Tests V** and **VI**, respectively. The explanation of these observations was already discussed in section IV.4.7.

III.4.9. Water content:

The water content profile across the soil sample after the completion of the tests is shown in **Figure 82.** From the graph it is noticed that generally, the water content is high at the anode side and gradually decreases toward the cathode. This observation is an indication that water has been withdrawn at the cathode side by the electro-osmosis process, yielding the build up of the water content profile across the soil core.

III.4.10. The pH profile:

Figure 83 presents the pH distribution across all the soil samples tested as a function of distance from the anode. **Tests I, II,** and **III** produced similar pH trends with increasing values toward the cathode. The build up of acidic conditions at the anode and alkaline conditions at the cathode were previously discussed in sections IV.4.4 and IV.4.5.

No significant changes in pH were observed over the soil core in other tests performed under pH control. Fixed values of pH around 10.5, 9.0 and 6.0 were recorded for **Tests IV, V,** and **VI,** respectively.

III.4.11. C8 distribution:

The relative C8 concentration across the soil samples as a function of distance from the anode after the tests were completed is shown in **Figure 84.** The horizontal solid line at value 1 corresponds to the original surfactant concentration at the beginning of the experiments. **Tests I, V** and **VI** produced an accumulation of the contaminant at the middle section between the cathode and anode while in **Tests III** and **IV** almost no C8

was found in the entire soil core. For **Test II**, an agglomeration of about 5 times the initial concentration was observed at the region near the anode and very low concentrations were detected at other sections of the soil sample.

The formation of concentration profiles is caused by three major components affecting the C8 movement through the soil - the electrical, the convective and the sorptive. The electrical factor is related to the migration of the anionic form of the surfactant towards the anode; the convective component is attributed to the transport of the contaminant simply by the water flow; and the sorptive influence (also called retardation factor) is caused by the adsorption of the C8 onto the soil.

It is noticed that **Test I** had low water flow rate and low pH around the anode side. This indicated that the convective component and the electrical migration in the region close to the anode were not significant. Moreover, the retardation factor was prominent at the sections of low pH. Consequently, an accumulation of C8 was observed halfway between the electrodes.

The same explanation could be applied to **Test II** except that the agglomeration occurred at the region close to the anode. Higher potential gradient and longer test time than **Test I** possibly was the reason for the observed contrast.

Test III was the longest test and almost no C8 was detected in all sections of the soil sample.

The convective component was the major factor that contributed to the removal of the C8 in **Test IV**. This test presented the best removal rate and it is estimated that almost no C8 was left in the soil.

Test V and VI also showed an accumulation of C8 at the middle section of the soil core. This was caused by the reasons cited above for **Test II**, except that the sorptive factor was less significant.

III.4.12. Mass balance:

The following **Table V** exhibits the results of the C8 mass balance obtained for the electro-osmosis tests executed.

Table V. Mass balance of C8 for the electro-osmosis tests.

Test #	C8 removed at the cathode (mg)	C8 removed at the anode (mg)	C8 remained in the soil (mg)	Total (mg)	Original C8 in the soil	
					(ppm)	(mg)*
I	0.6	9.1	18.8	28.5	33±10	15.6~29.2
II	4.5	0.4	20.1	25.0	33±10	13.7~25.6
III	1.24	1.17	0.07	2.48	16±5	3.96~7.57
IV	28.3	3.3	0.8	32.4	33±10	14.7~27.5
V	1.7	54.1	13.4	69.2	33±10	14.4~26.9
VI	0.2	25.7	15.3	41.2	67±11	35.9~50.0

* range of C8 mass originally in the soil.

III.4.13. Moisture content effect on electro-osmotic flow:

Two tests with different moisture content (1% and 12%) and one test without electricity were compared to evaluate the the effect of moisture content on the electro-osmotic flow. The time required to saturate the soil column, indicated by the presence of effluent at the cathode reservoir was recorded. The plot of cumulative effluent volume as a function of time is shown in **Figure 85.** From the graph it is noticed that there is no significant difference on the soil saturation time among the three tests performed. However, after the saturation time, higher water flow rate was observed for the test with 12 % of initial moisture content.

IV. Conclusions and Recommendations

Based on the laboratory experimental results obtained, the following conclusions can be deduced:

1. Chemical analysis demonstrated that Ca^{2+}, Na^{+}, HCO_3^{-}, SO_4^{2-} and Cl^{-} are the major ionic species present in the plant groundwater sampled. Other properties such as alkalinity, pH, conductivity and total dissolved solids are in accordance with typical groundwater characteristics.
2. Low concentration of C8 (113±2 ppb) was detected in the groundwater sample.
3. The soil composition analysis from below the anaerobic digestion ponds showed that high percentage of clay is present at the top soil zone (depth < 10 feet), a region where the electro-osmosis process can be successfully applied.
4. High concentrations of C8 were found in the soil samples in the top 10 feet at ADPS-1 and ADPS-2, at around 16 and 33 ppm, respectively. This is the area where the electro-osmosis process needs to and can be applied.
5. As expected, specific surface area, organic matter content, and cation exchange capacity influence the composition analysis, i.e., higher percentage of clay results in higher specific surface area, organic matter content, cation exchange capacity, C8 concentration, and lower hydraulic permeability.
6. Adsorption studies indicate that the pH greatly affects C8 soil adsorption. The lower the pH, the more C8 adsorbed. There is almost no adsorption when pH is greater than 8.0. The acidity constant of C8 is $10^{-2.9}$ and the pH_{zpc} is in the range of 2.0 to 2.5. An electrostatic repulsion between anionic C8 and negatively charged soil surfaces occurs at pH values higher than 3.0. As a result, the extent of C8 adsorption decreases with increasing pH. The same reasons can be used to explain the extent of desorption increases with the increasing pH.

8. Temperature is an important factor on the adsorption and desorption. The higher the temperature, the more C8 dissoluted from the soil, making it difficult to retain C8 on the soil surface.

9. The initial C8 concentration in the aqueous phase affects adsorption substantially. While the C8 concentration is less than 50 ppm, the extent of C8 adsorption is diminished significantly at pH greater than 5.0. However, when the C8 concentration is greater than 50 ppm, the percentage of C8 adsorbed is higher within the pH range of 5.0 to 8.0. The possible reason is the hydrophobic effect that makes the C8 easier to be retained on the soil surface.

10. The results of the adsorption experiments under electrical field indicated that the Type C (where the cathode is at the influent side and the anode at the effluent side) exhibits the most C8 retaining capacity and effluent pH is the lowest. Inversely, Type B adsorption system (where the anode is at the influent side and the cathode at the effluent side) gave the highest effluent pH and showed the lowest C8 adsorption affinity. The reasons for effluent pH changes were found to be caused by the redox reactions of the water at the electrode surface.

11. Electro-osmosis experiments performed without pH conditioning showed little C8 removal. In these tests, significant amounts of surfactant remained in the soil presumably caused by the low fluid velocity and the build up of high pH gradients across the soil core.

12. The build up of acidic conditions at the anode during the application of the electro-osmosis process is due to the oxidation of water. The products of the oxidation are oxygen gas (O_2) and hydrogen ions (H^+). Inversely, the basic condition at the cathode is attributed to the reduction of water. This electrochemical reaction decomposes the water producing hydrogen gas (H_2) and hydroxyl ions (OH^-).

13. The results demonstrated that it will be practical to remove the C8 by electro-osmosis process under pH controlled conditions at the influent and effluent zone. A 97 %

removal of the C8 in the effluent at the cathode was achieved in the test under pH control at the anode (pH = 10) with NaOH/HCl.

14. The best practice to obtain high degree C8 removal is to promote high water velocity through the soil core. This can be achieved by maintaining alkaline pH conditions at the electrolyte region. However, it is necessary that the water flow velocity overcomes the electrical migration of the anionic C8 which moves in an opposite direction to water flow.
15. The most important physical-chemical property of the soil to affect the electro-osmosis process is the pH_{ZPC}. The electro-osmotic water flow rate is directly proportional to the pH_{ZPC} of the soil particles.
16. Lower efficiency of the electro-osmosis process was observed when $Ca(OH)_2$ or $CaCO_3$ instead of NaOH was used in the pH conditioning at the anode. This observation can be attributed to the following reasons: a) high pH conditions caused precipitation of some salts, e.g., $CaCO_3$ that coated the surface of the electrodes, yielding low efficiency of the electro-osmosis process; b) By introducing calcium ions (instead of sodium ions) into the system, the ionic strength increases substantially, causing a diminishing of the zeta potential (ζ) and consequently the fluid velocity through the soil towards the cathode.
17. Tests in which $Ca(OH)_2$ and $CaCO_3$ were used to control pH showed high C8 concentrations at the anodic solution. In these experiments, the high pH conditions and low water flow velocity through the soil core contributed to the electrical migration of the anionic C8 towards the anode.
18. The moisture content effect on the electro-osmotic flow was evaluated. The results indicate that the moisture content does not significantly affect the time required for the soil column saturation, but does affect the electro-osmotic flow.

V. References

Acar, Y., Gale, R., Putnam, G., Hamed, J. and Wong, R., Electrochemical Processing of Soils: Theory of pH Gradient Development by Diffusion, Migration, and Linear Convection, J. Env. Sci. Health. A25(6), 687-714, 1990

Arpad K., Handbook of Soil Mechanism, Volume II., Soil Testing, Oxford, NY, 1980.

Brunaouer, S. L., Emmet, P. H., and Teller, E, Adsorption of Gases in Multimolecular Layers, J. Amer. Chem. Soc., 60, 309, 1938.

Casagrande, L., Electro-osmosis in Soils, Geotechnique, Vol. 1, p. 1959-1977, 1949.

Chappell, B., and Burton, P., Electro-Osmosis Applied to Unstable Embarkment, J.Geotech. Eng. Div., ASCE, 101(8), 733-740, 1975.

Esrig, M. and Majteni, S. , A New Equation for Electro-Osmosis flow and Its Implication for Porous Media, Highway Research Record, No.11, HRB Publicatiion 1331, 31-45, 1965.

Fetter, C. W., Applied Hydrogeology, Charles E., Merill Publishing Co., 1980.

Helmholtz, H. von. ann. Physik Wiedemanm, 7, 337, 1879.

Pojasek, J. W., Membrane Ultrafiltration Disposing of Hazardous Chemical Waste, Environ. Sci. Tech., 13 (7), 810, 1979.

Schmid, G., Z. Electrochem, 56, 35-81, 1952

Shuckrow, A. J., Pajak, A. P., and Touhil, C. J., Concentration Technology for Hazardous Aqueous Waste Treatment, EPA-600/2-81-019, 1981.

Sims, J. T. , and Heckendorn, S. E., Methods of Soil Analysis, U. of Delaware, College of Agricultural Sciences, Agricultural Experimental Station, Cooperative Ex-tension, Newark, DE, 1991.

Staas, E. B., Waste Disposal Practices. A Threat to Health and the Nation's Water Supply, Report to the U.S. Congress, CED-28-120, GAO, June 16, 1978.

Standard Methods for the Examination of Water and Wastewater, 16th edition, American Public Health Association, Washington DC, 1985.

Appendix B

Electro-osmosis test II

Physical properties of the soil core

Soil sample: ADPS-2 (0-5')

Amount of the specimen placed in the cell: 646.1 g
C8 concentration: 33 μg/g dry soil
Amount of dry soil: 595.1 g
Water content: 7.9 %
Cell volume : 363.2 cm^3 (length: 10.0 cm; cross sec. area: 36.32 cm^2)
Bulk density: 1.64 g/cm^3
Particle density: 2.64 g/cm^3
Porosity: 0.38
Pore volume: 138.0 cm^3

Electrodes: graphite
Electrolyte solution: process water (pH = 7.1)
Potential applied: 15.0 V
Potential gradient: 1.5 V/cm

Appendix C

Electro-osmosis test III

Physical properties of the soil core

Soil sample: ADPS-2 (5-10')
- Amount of the specimen placed in the cell: 681.1g
- C8 concentration: 16 µg/g dry soil
- Amount of dry soil*: 576.9 g
- Water content: 15.3 %
- Cell volume : 363.2 cm^3 (length: 10.0 cm; cross sec. area: 36.32 cm^2)
- Bulk density: 1.59 g/cm^3
- Particle density: 2.64 g/cm^3
- Porosity: 0.40
- Pore volume: 144.4 cm^3

Electrodes: graphite
Electrolyte solution: process water (pH = 7.1)
Potential applied: 15.0 V
Potential gradient: 1.5 V/cm

*Considerable amount of wax - around 215 g - was present in this sample. The paraffin was used to seal the bore column at the moment of the sample collection.

Appendix D

Electro-osmosis test IV

Physical properties of the soil core

Soil sample: ADPS-2 (0-5')

Amount of the specimen placed in the cell: 693.1g
C8 concentration: 33 μg/g dry soil
Amount of dry soil: 638.4 g
Water content: 7.9 %
Cell volume : 363.2 cm^3 (length: 10.0 cm; cross sec. area: 36.32 cm^2)
Bulk density: 1.76 g/cm^3
Particle density: 2.64 g/cm^3
Porosity: 0.33
Pore volume: 119.9 cm^3

Electrodes: graphite
Electrolyte solution: process water (pH = 7.1)
Potential applied: 15.0 V
Potential gradient: 1.5 V/cm
Controlled pH at the anode with HCl and Na(OH); pH = 10.
Controlled pH at the cathode with HCl and NaOH; pH = 10.

Appendix E

Electro-osmosis test V

Physical properties of the soil core

Soil sample: ADPS-2 (0-5')

- Amount of the specimen placed in the cell: 678.2 g
- C8 concentration: 33 μg/g dry soil
- Amount of dry soil: 624.6 g
- Water content: 7.9 %
- Cell volume : 363.2 cm^3 (length: 10.0 cm; cross sec. area: 36.32 cm^2)
- Bulk density: 1.72 g/cm^3
- Particle density: 2.64 g/cm^3
- Porosity: 0.35
- Pore volume: 127.1 cm^3

Electrodes: graphite
Electrolyte solution: process water
Potential applied: 15.0 V
Potential gradient: 1.5 V/cm
Controlled pH at the anode with HCl and $Ca(OH)_2$; pH = 10.
Controlled pH at the cathode with HCl and NaOH; pH = 10.

Appendix F

Electro-osmosis test VI

Physical properties of the soil core

Soil sample: mixture of ADPS-2 (0-17') and BGMW-6 (0-2')

Amount of the specimen placed in the cell: 647.7g
C8 concentration: 67 μg/g dry soil
Amount of dry soil: 641.2 g
Water content: 10.1 %
Cell volume : 363.2 cm^3 (length: 10.0 cm; cross sec. area: 36.32 cm^2)
Bulk density: 1.76 g/cm^3
Particle density: 2.64 g/cm^3
Porosity: 0.33
Pore volume: 121.1 cm^3

Electrodes: graphite
Electrolyte solution: process water
Potential applied: 15.0 V
Potential gradient: 1.5 V/cm
Controlled pH at the anode with HCl and $CaCO_3$; pH = 6.
Controlled pH at the cathode with HCl and NaOH; pH = 10.

Constant head permeameter apparatus

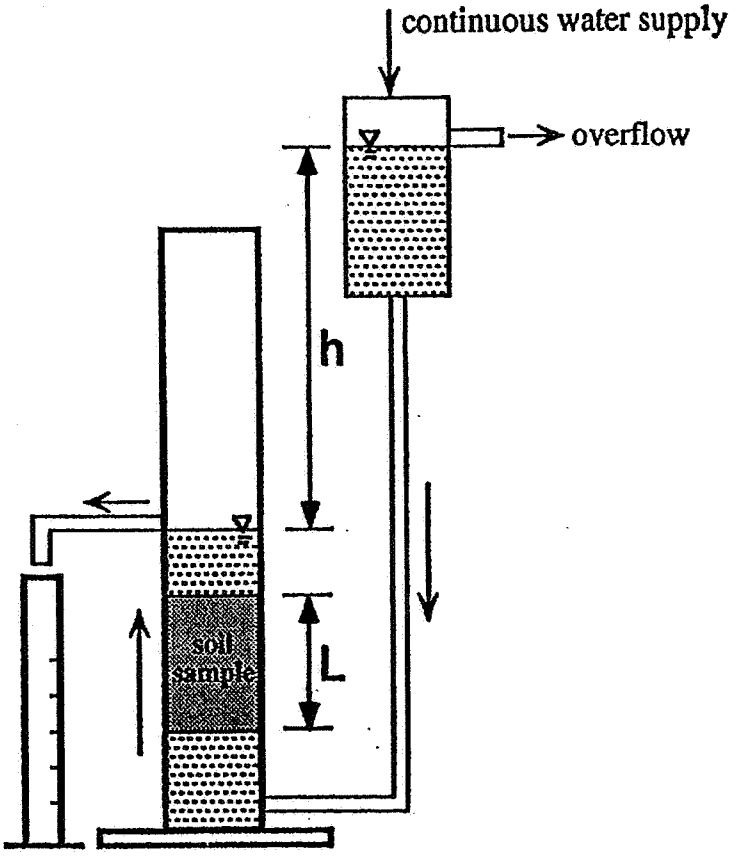

Figure 1. Constant head permeameter.
hydraulic head, h = 44 cm;
soil sample length, L = 11 cm;
Cross sectional area, A = 19.6 cm^2.
Ref: Fetter, C. W. (1980)

Adsorption System Type A

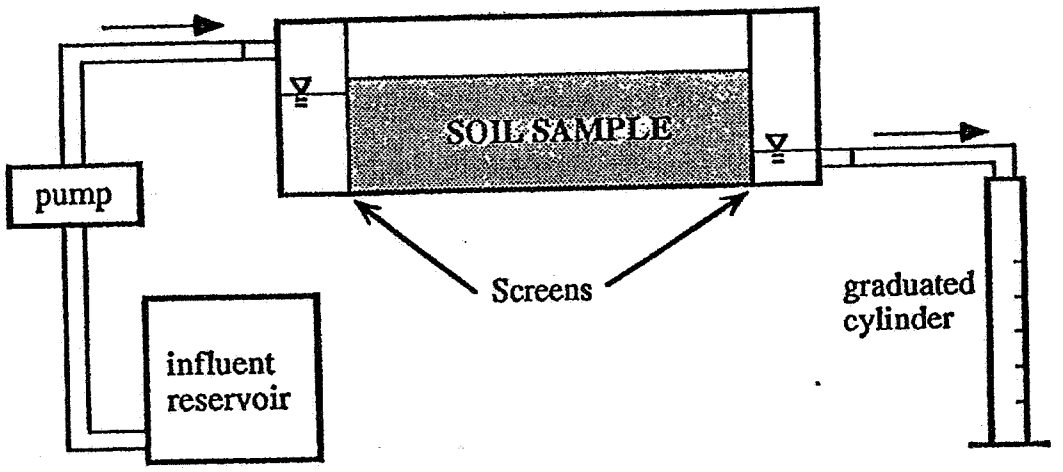

ASH010666

Figure 2a. Adsorption system type A for the adsorption study under no electrical field.

Adsorption System Type B

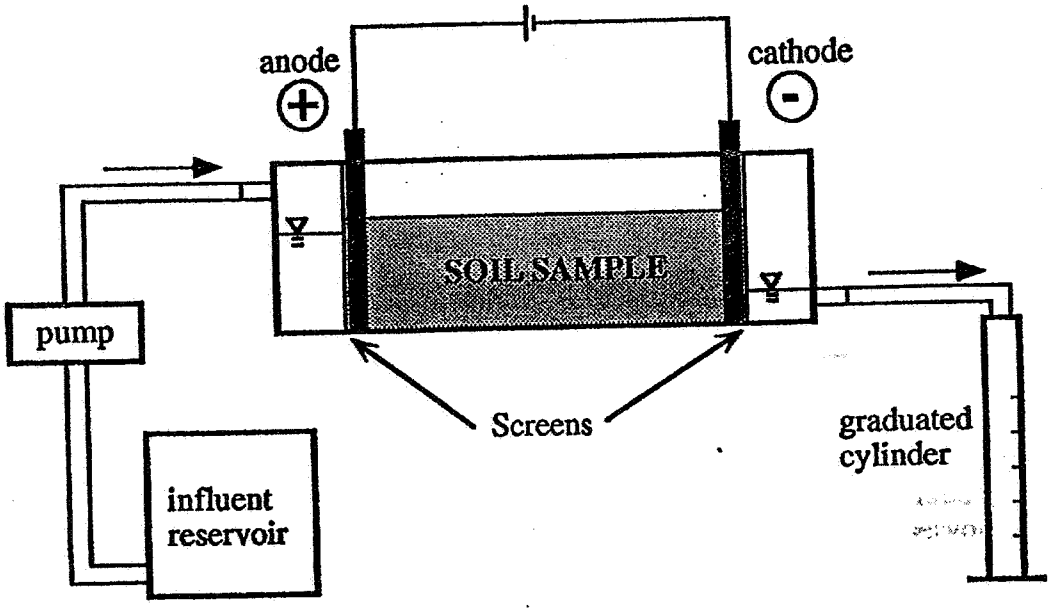

Figure 2b. Adsorption system type B for the adsorption study under electrical field.

Adsorption System Type C

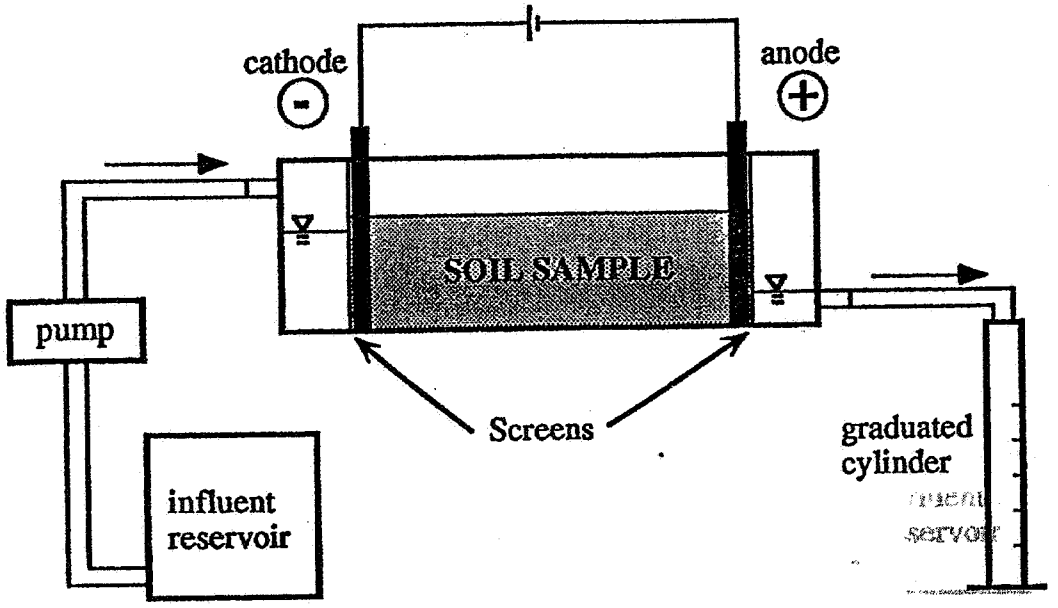

ASH010668

Figure 2c. Adsorption system type C for the adsorption study under electrical field.

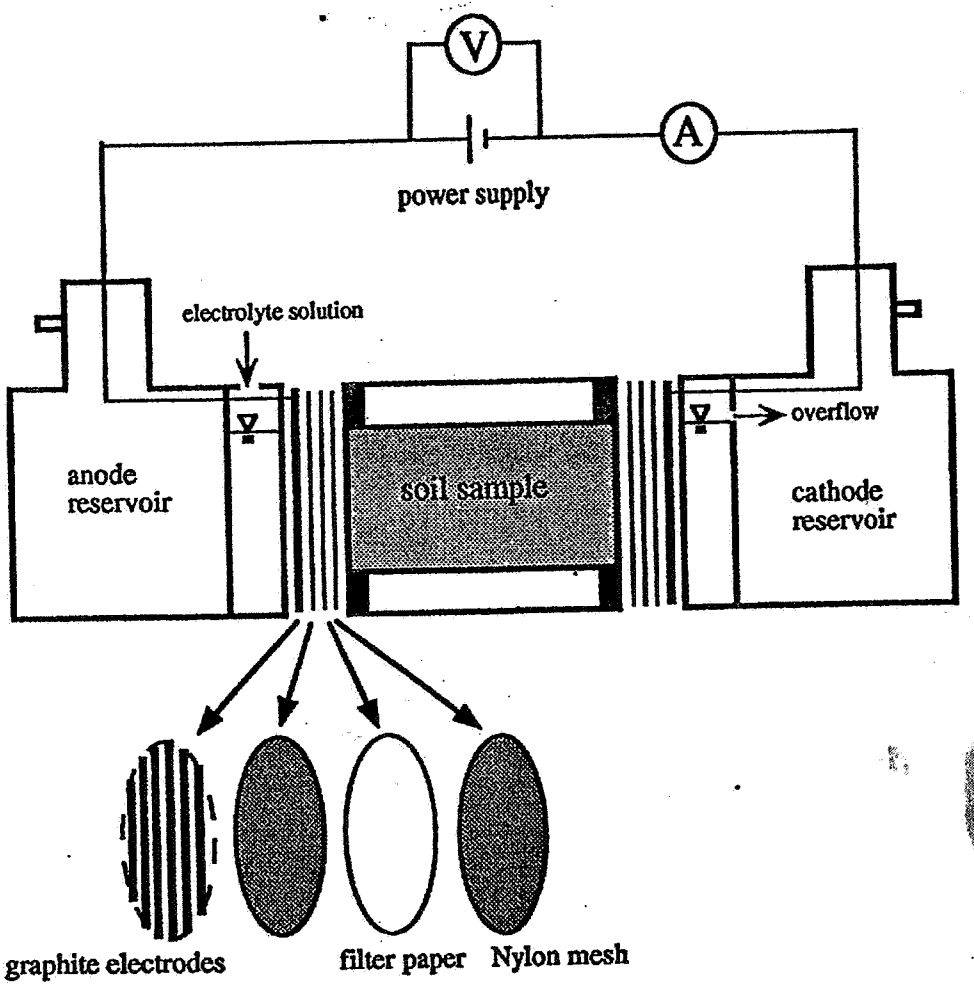

Figure 3. Typical electro-osmosis apparatus.

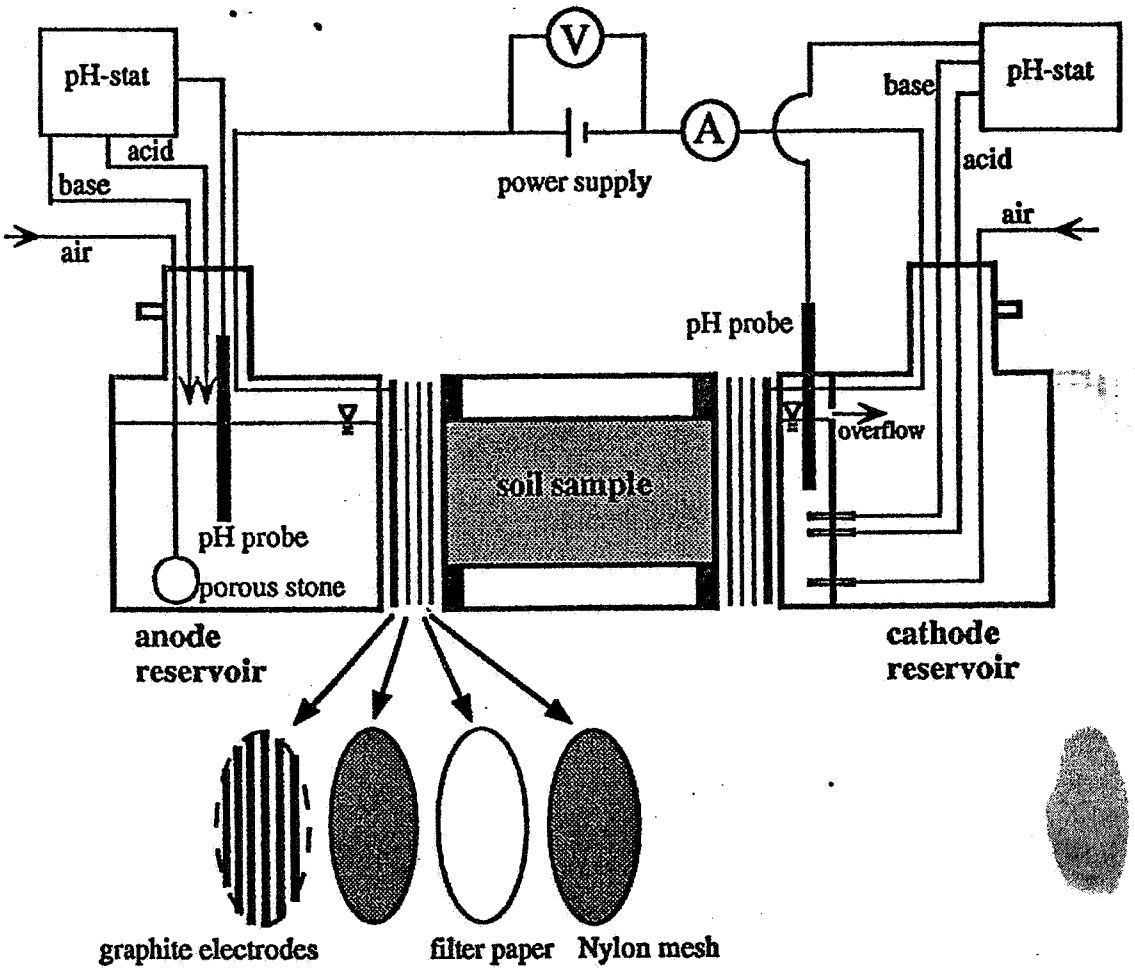

Figure 4. Electro-osmosis apparatus for tests under controlled pH conditions.

ASH010670

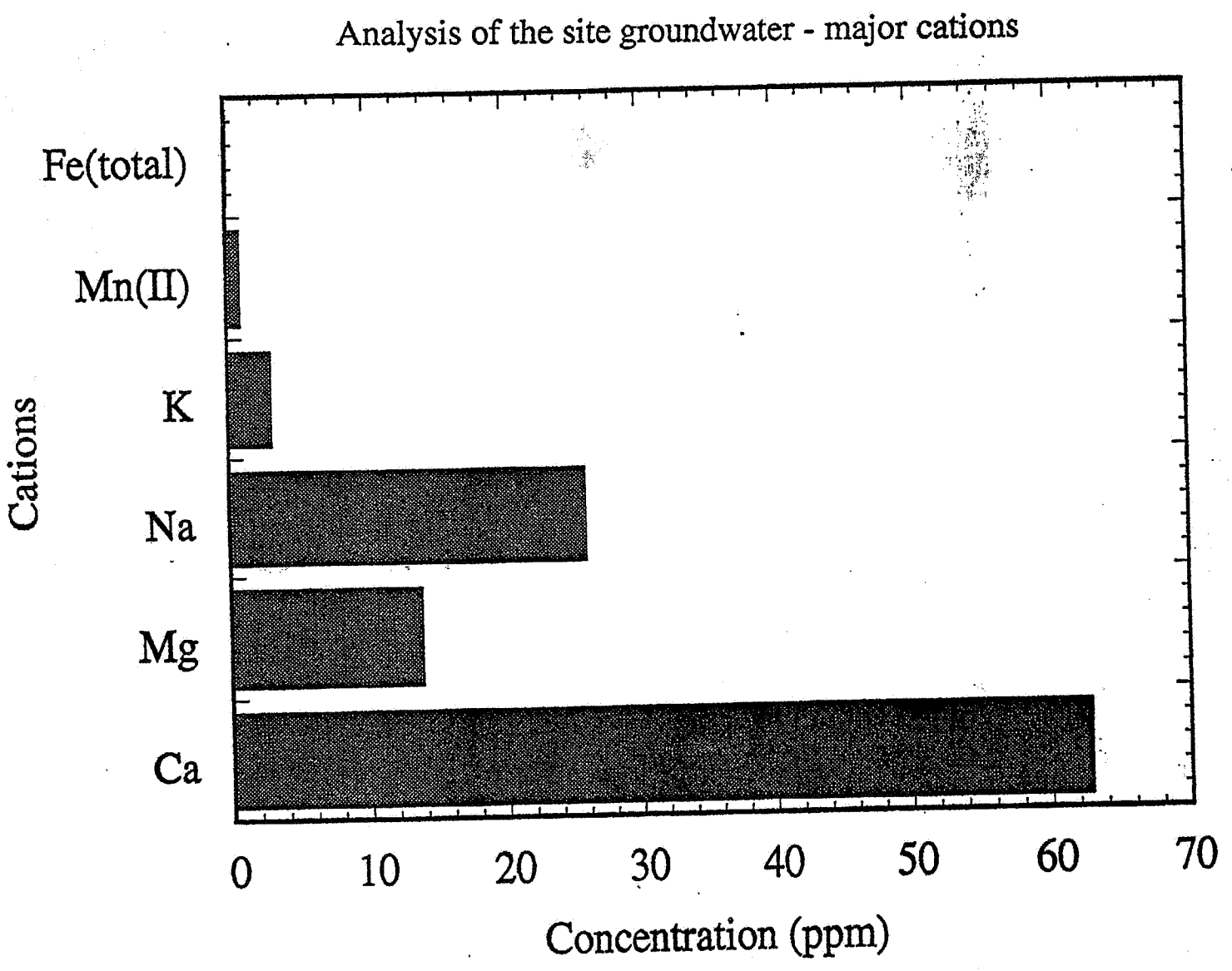

Figure 5. Characterization of the site fluid.
Major cations.

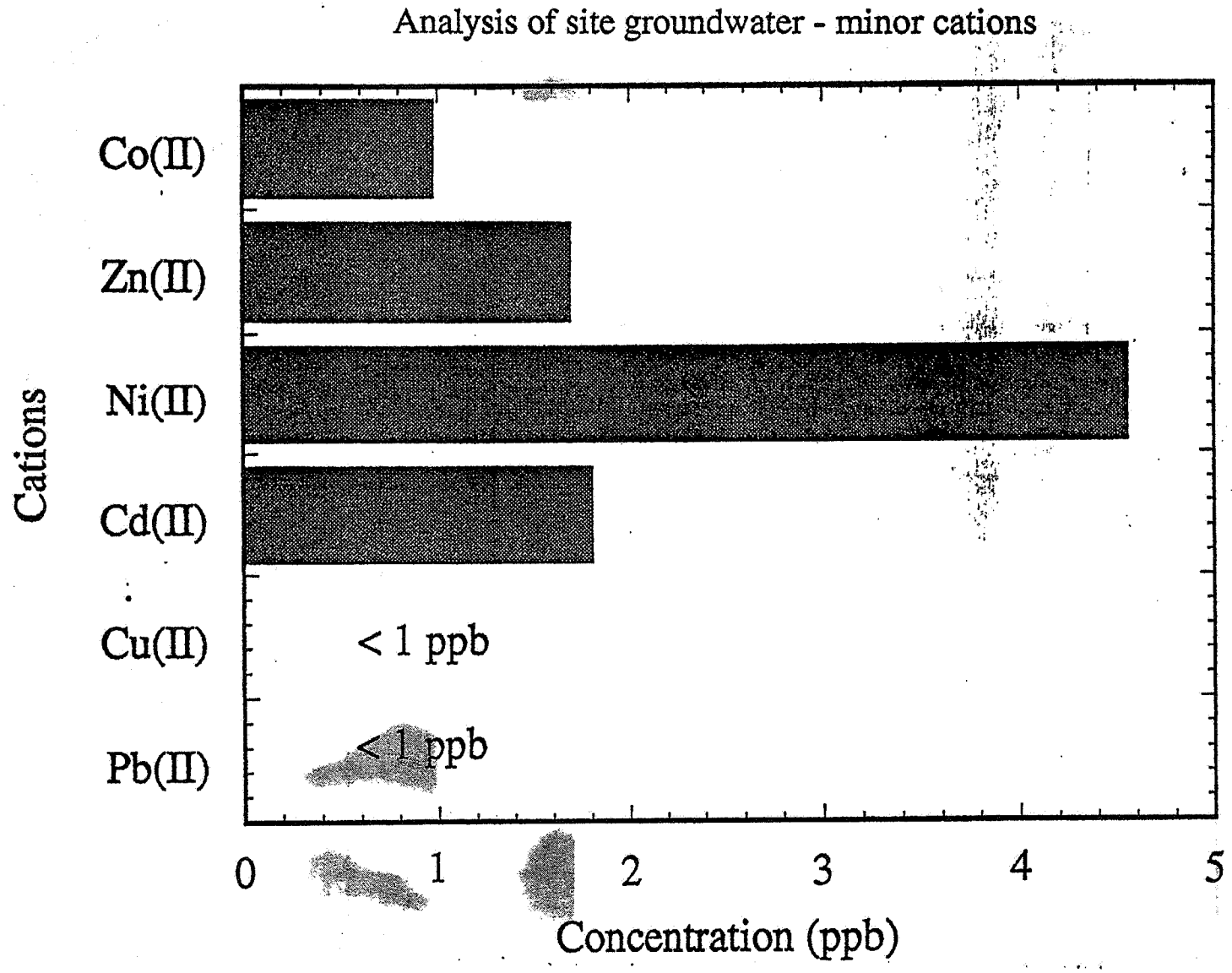

Figure 6. Characterization of the site groundwater. Minor cations.

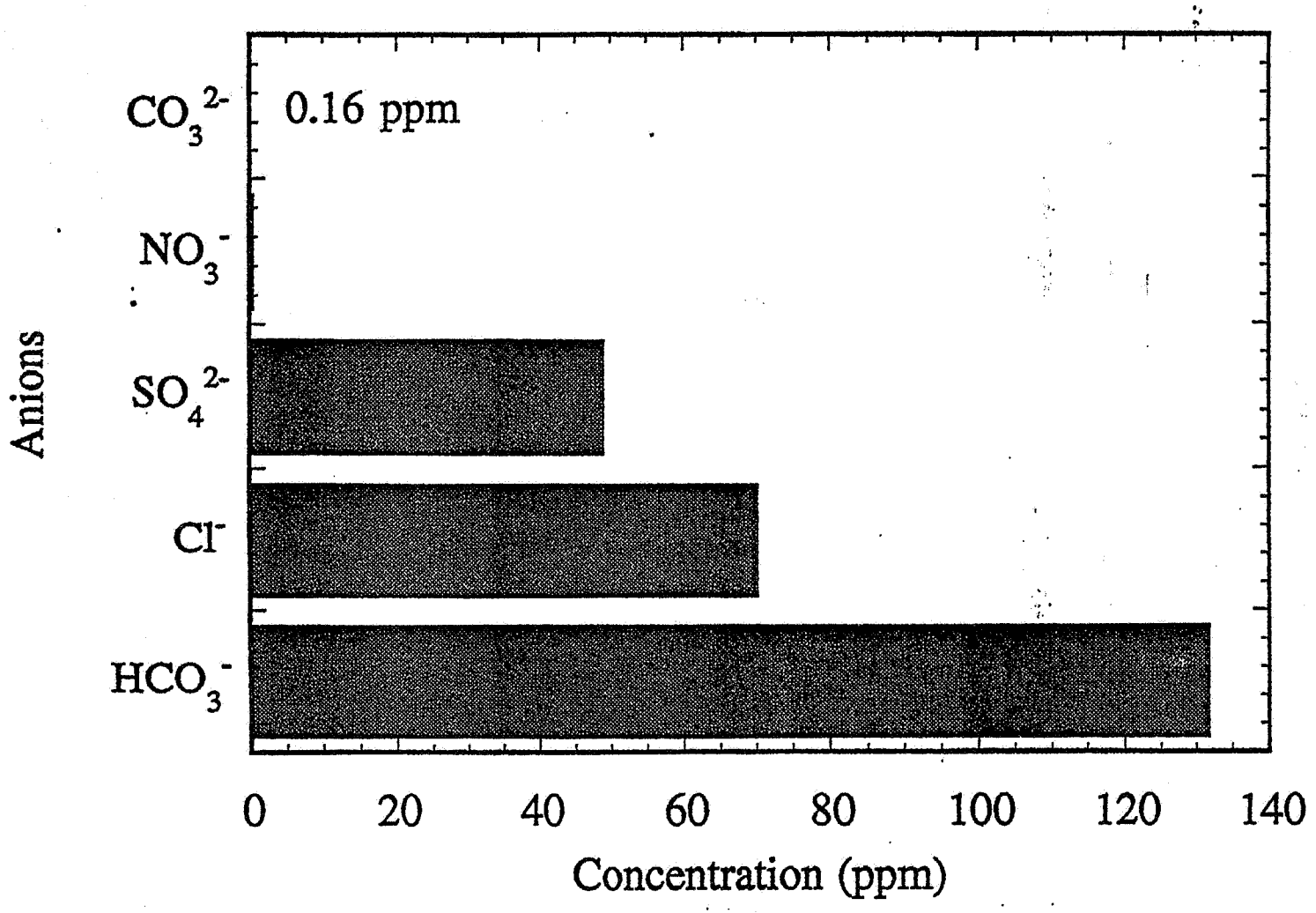

Figure 7. Characterization of the site groundwater. Anions.

Ionic distribution of the groundwater.

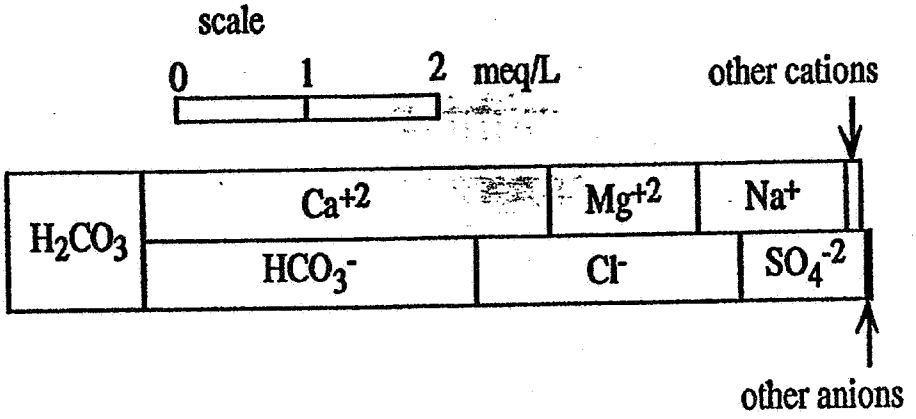

Cations (meq/L)	
Ca^{+2}	3.2
Mg^{+2}	1.1
Na^+	1.1
K^+	0.1
Mn^{+2}	3.6×10^{-2}
Fe (total)	5.8×10^{-3}
Cd(II)	3.2×10^{-5}
Ni(II)	1.6×10^{-5}
Zn(II)	5.2×10^{-5}
Co(II)	3.4×10^{-5}

Anions (meq/L)	
HCO_3^-	2.6
Cl^-	2.0
SO_4^{-2}	1.0
NO_3^-	9.6×10^{-3}
CO_3^{-2}	4.0×10^{-3}

ASH010674

Figure 8. Ionic distribution of the site groundwater .

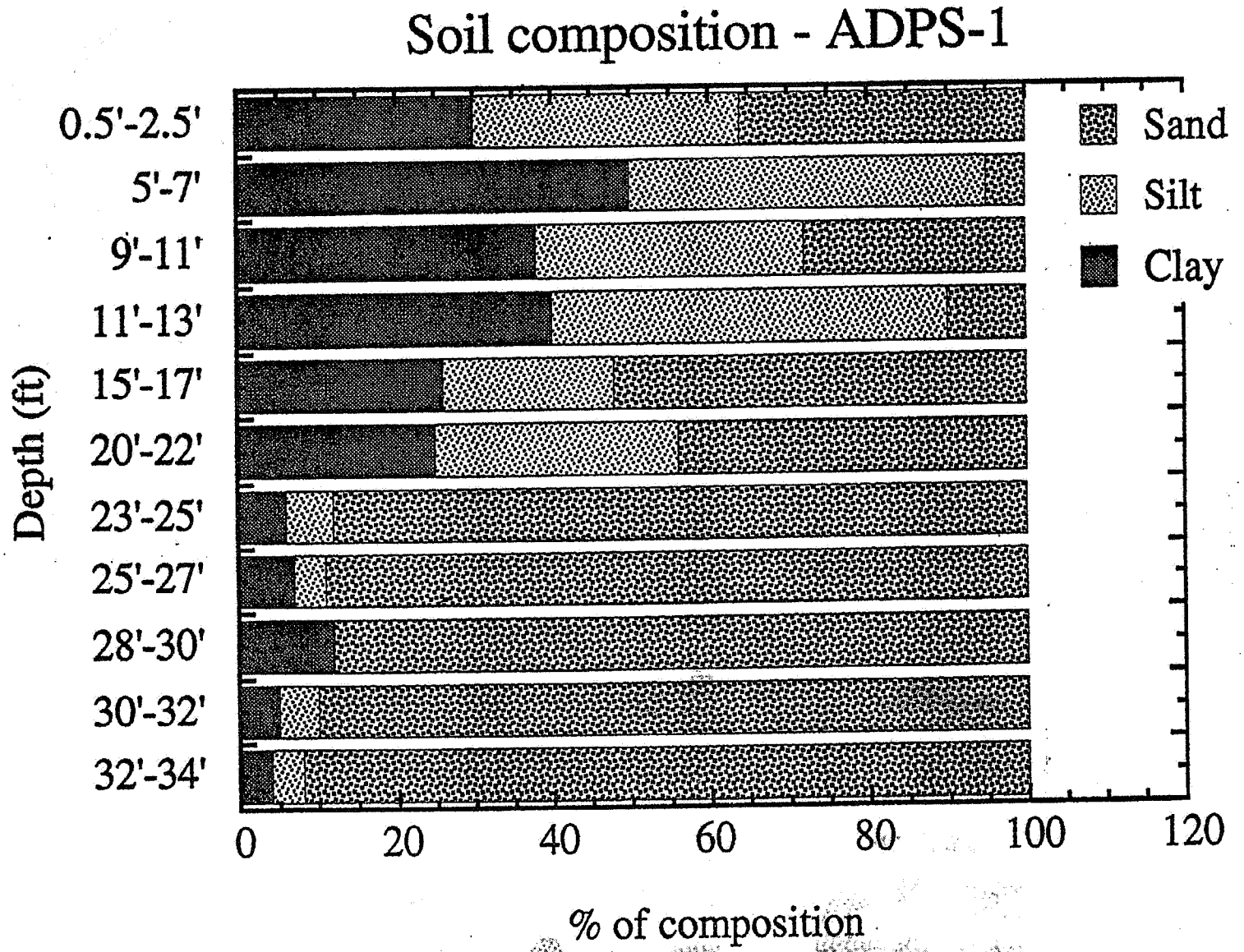

Figure 9a. Characterization of the soil samples.
Soil composition analysis of ADPS-1 soil samples (stack bars).

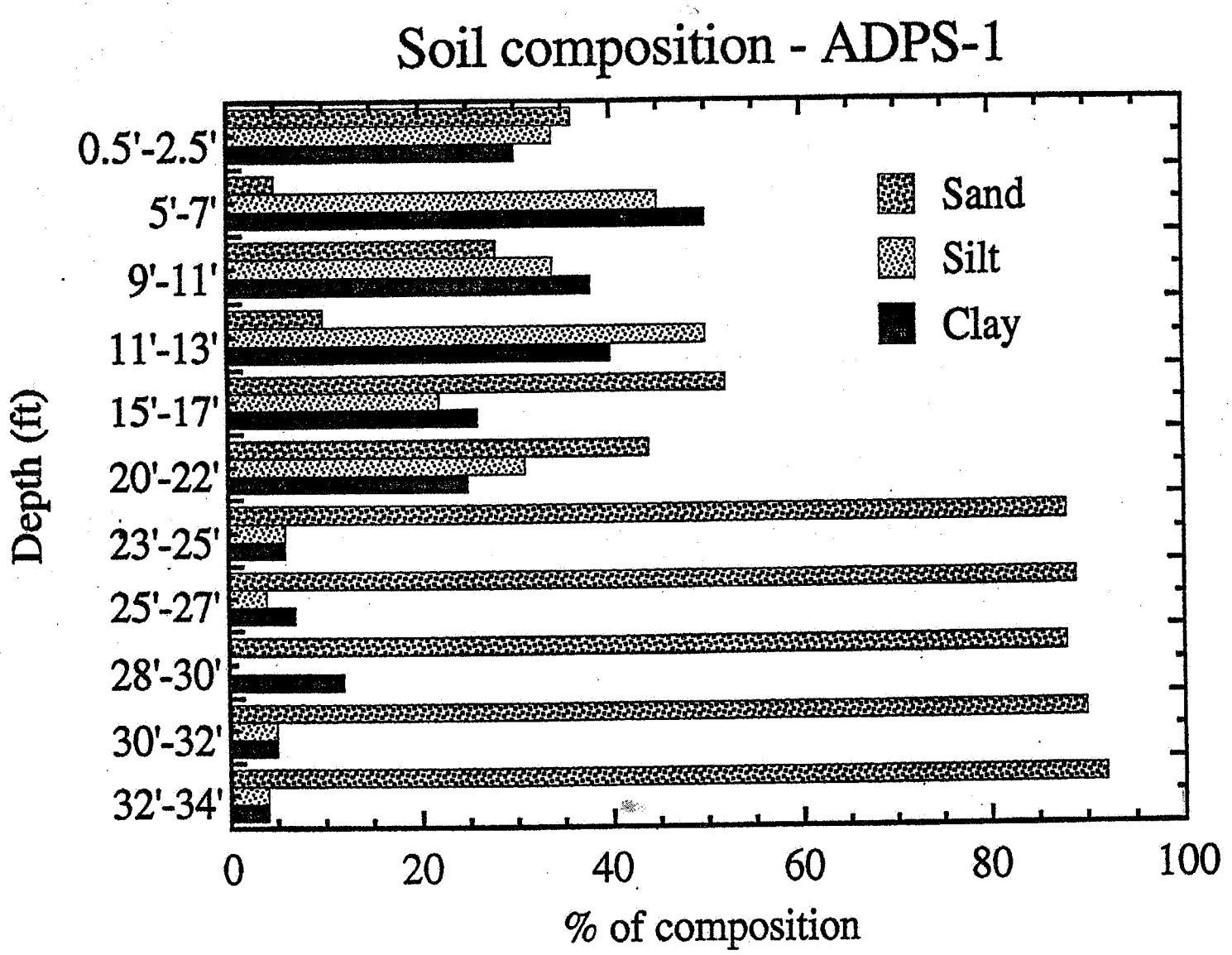

Figure 9b. Characterization of the soil samples.
Soil composition analysis of ADPS-1 soil samples.

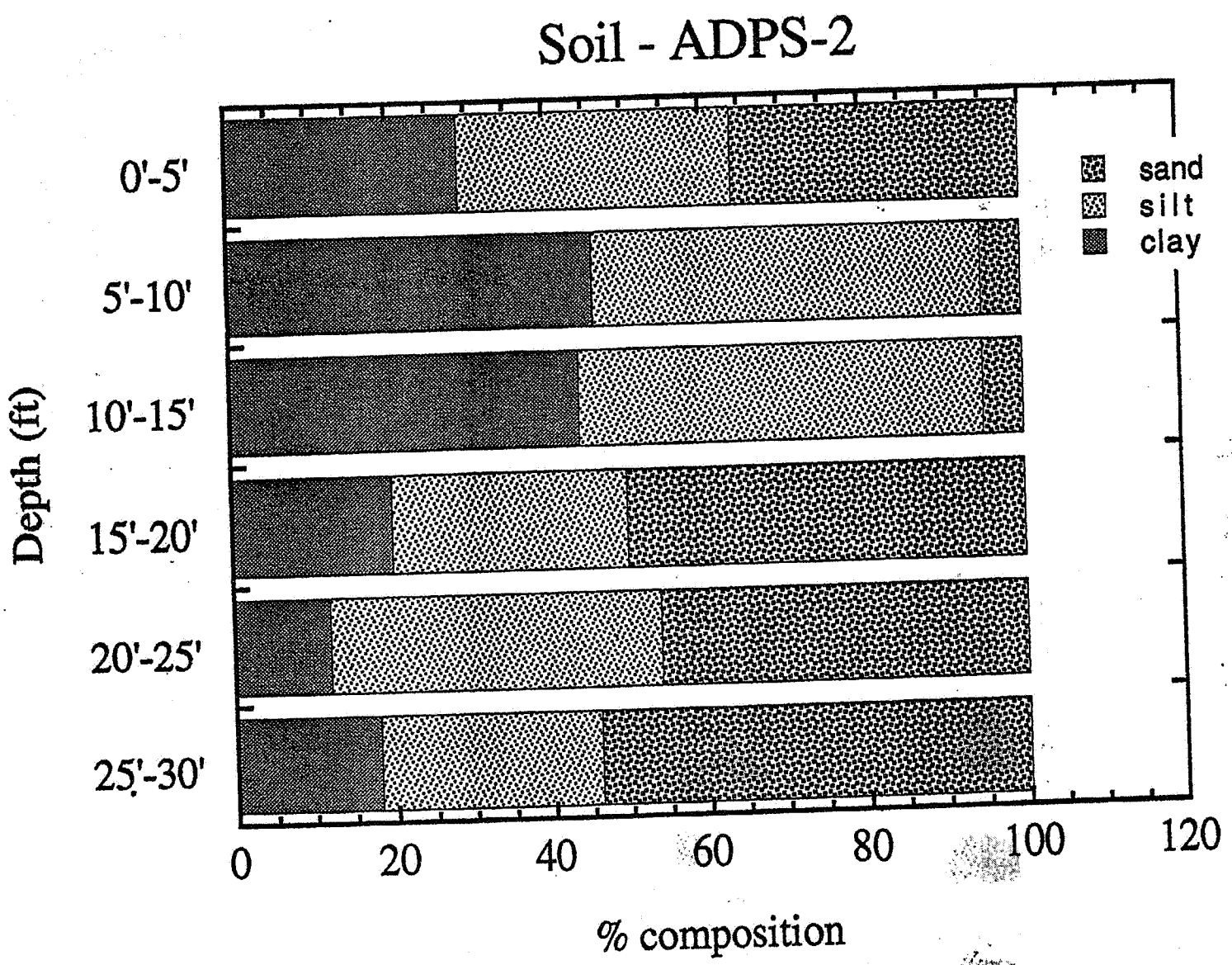

Figure 10a. Characterization of the soil samples.
Soil composition analysis of ADPS-2 soil samples (stack bars).

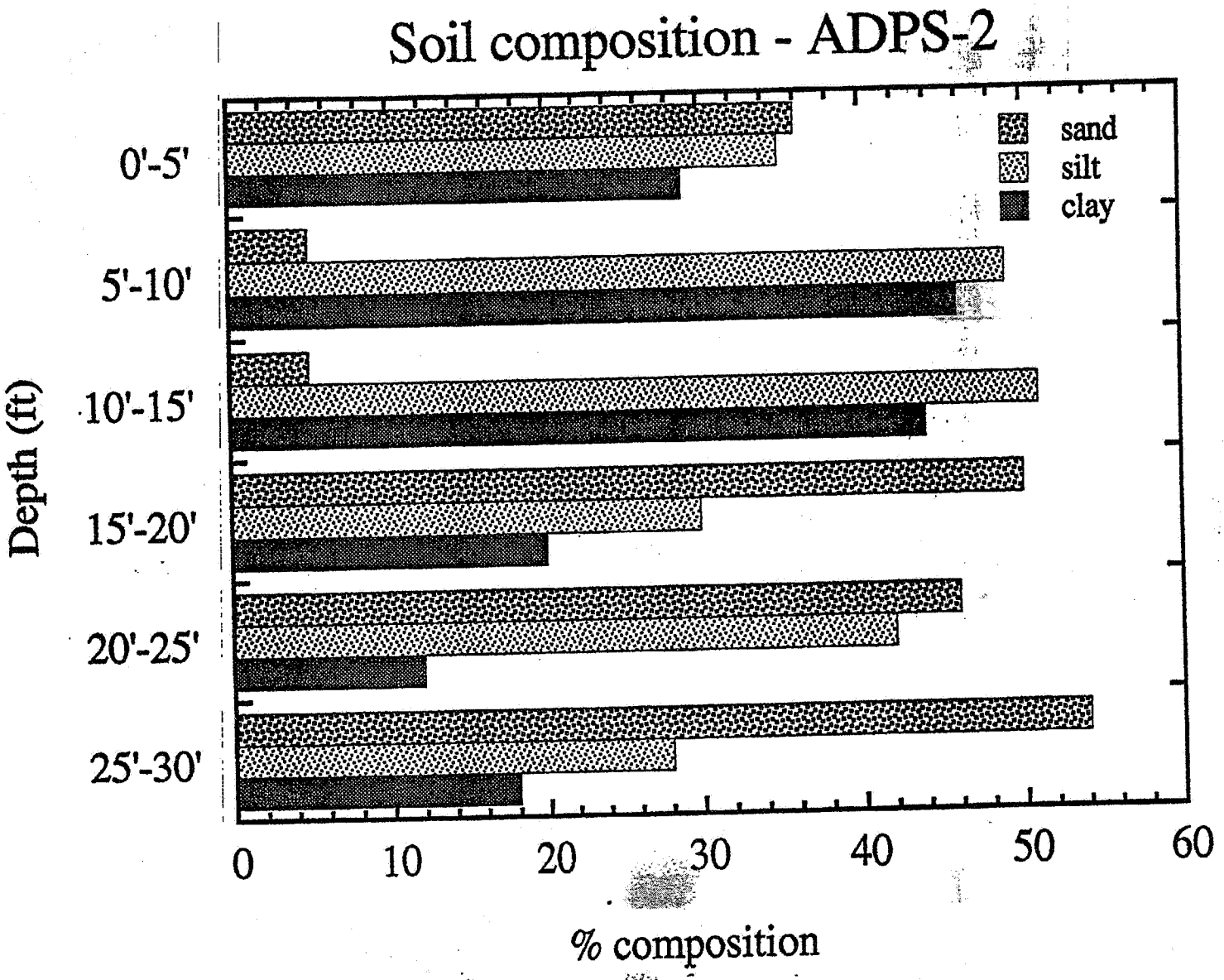

Figure 10b. Characterization of the soil samples.
Soil composition analysis of ADPS-2 soil samples.

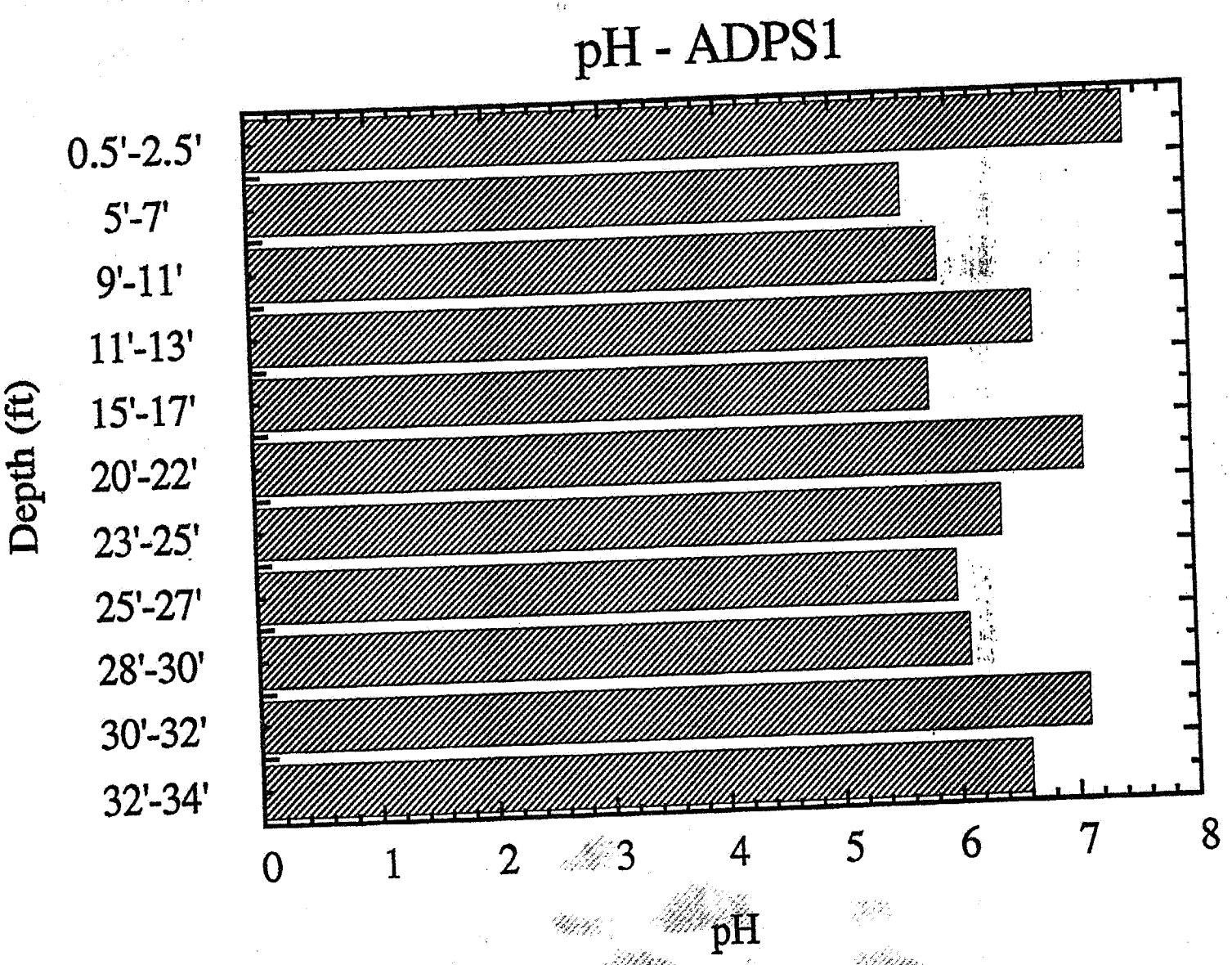

Figure 11. Characterization of the soil samples.
Soil pH of ADPS-1 soil samples.

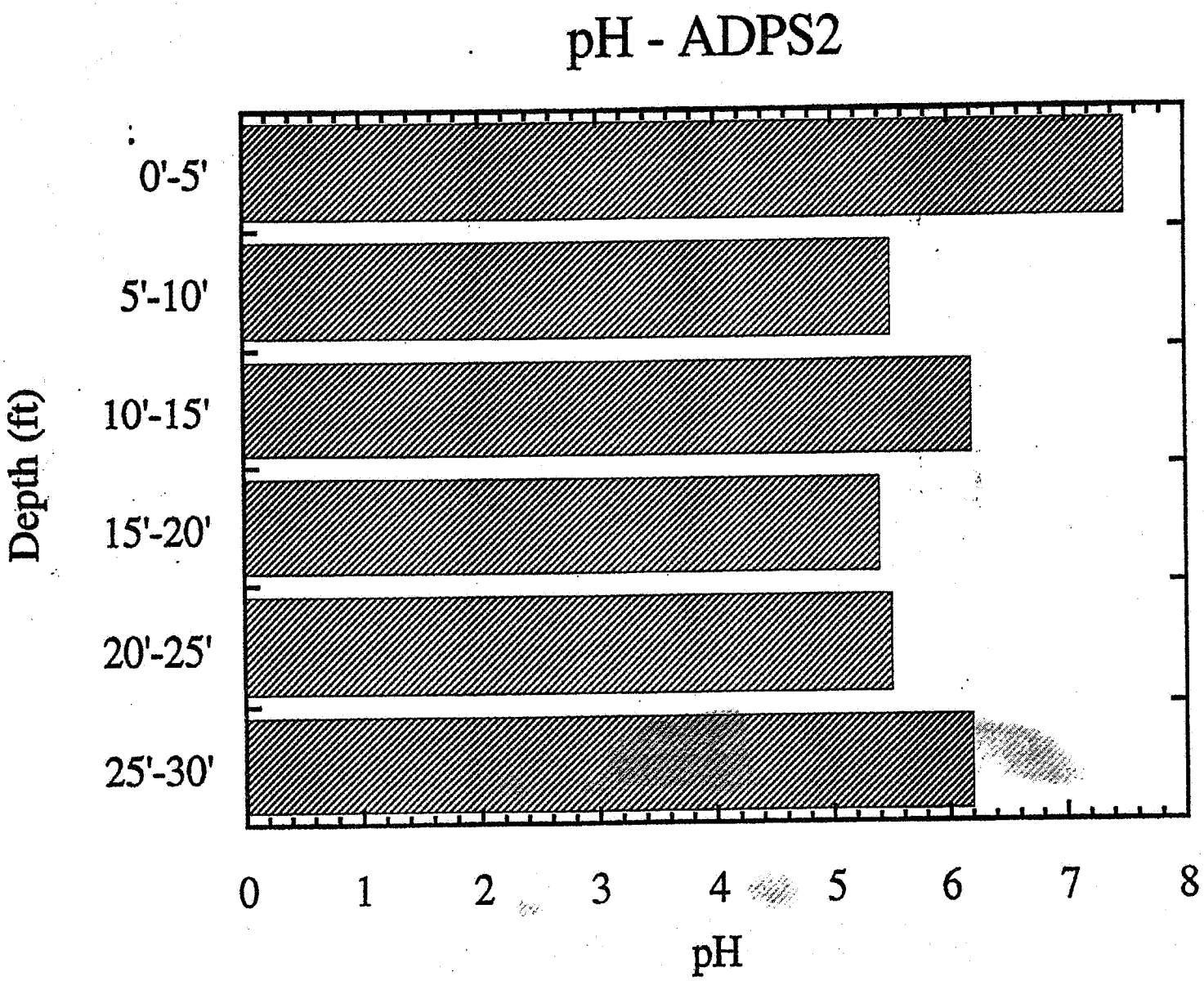

Figure 12. Characterization of the soil samples.
Soil pH of ADPS-2 soil samples.

089010HSV

EID103262

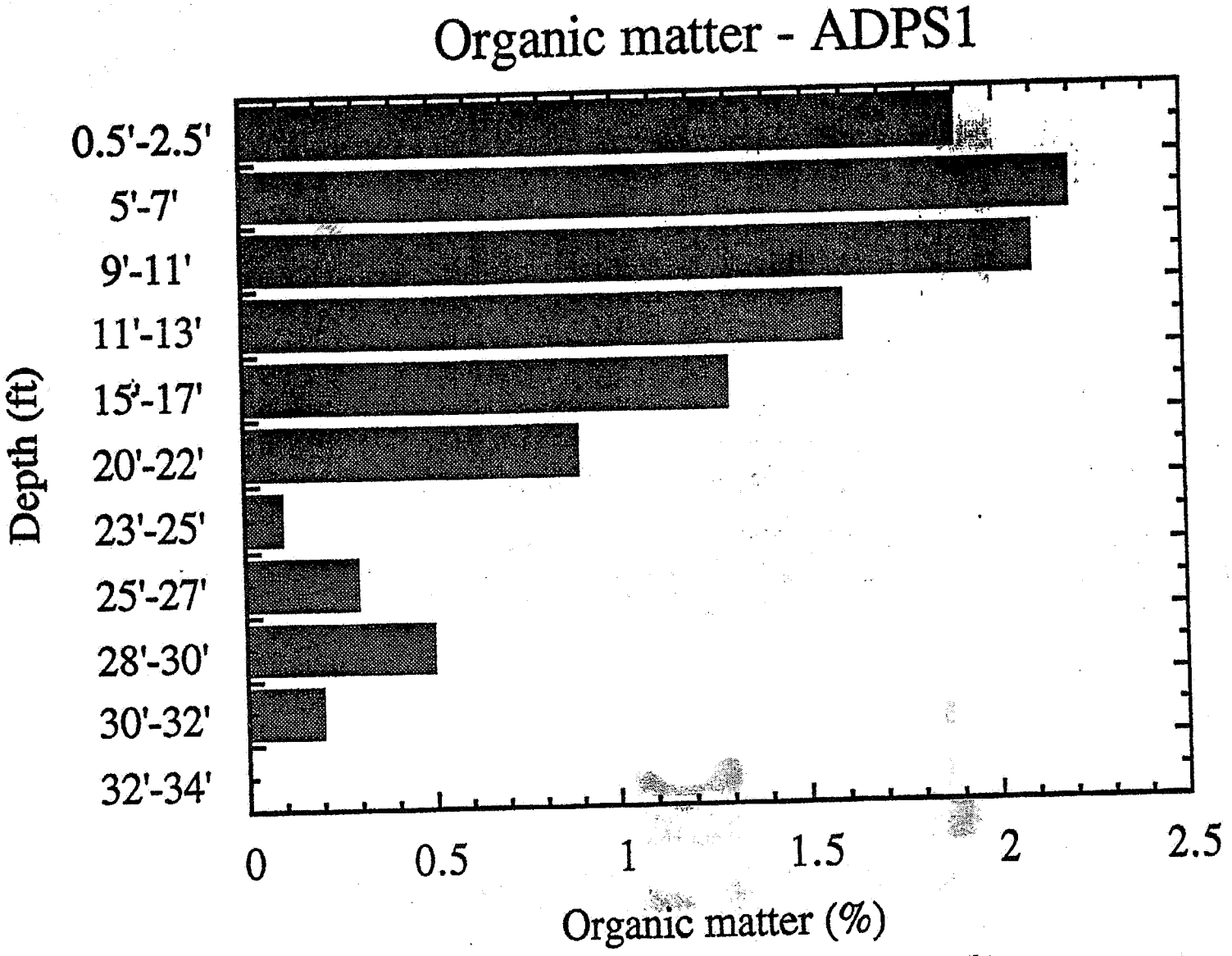

Figure 13. Characterization of the soil samples.
Organic matter percentage of ADPS-1 soil samples.

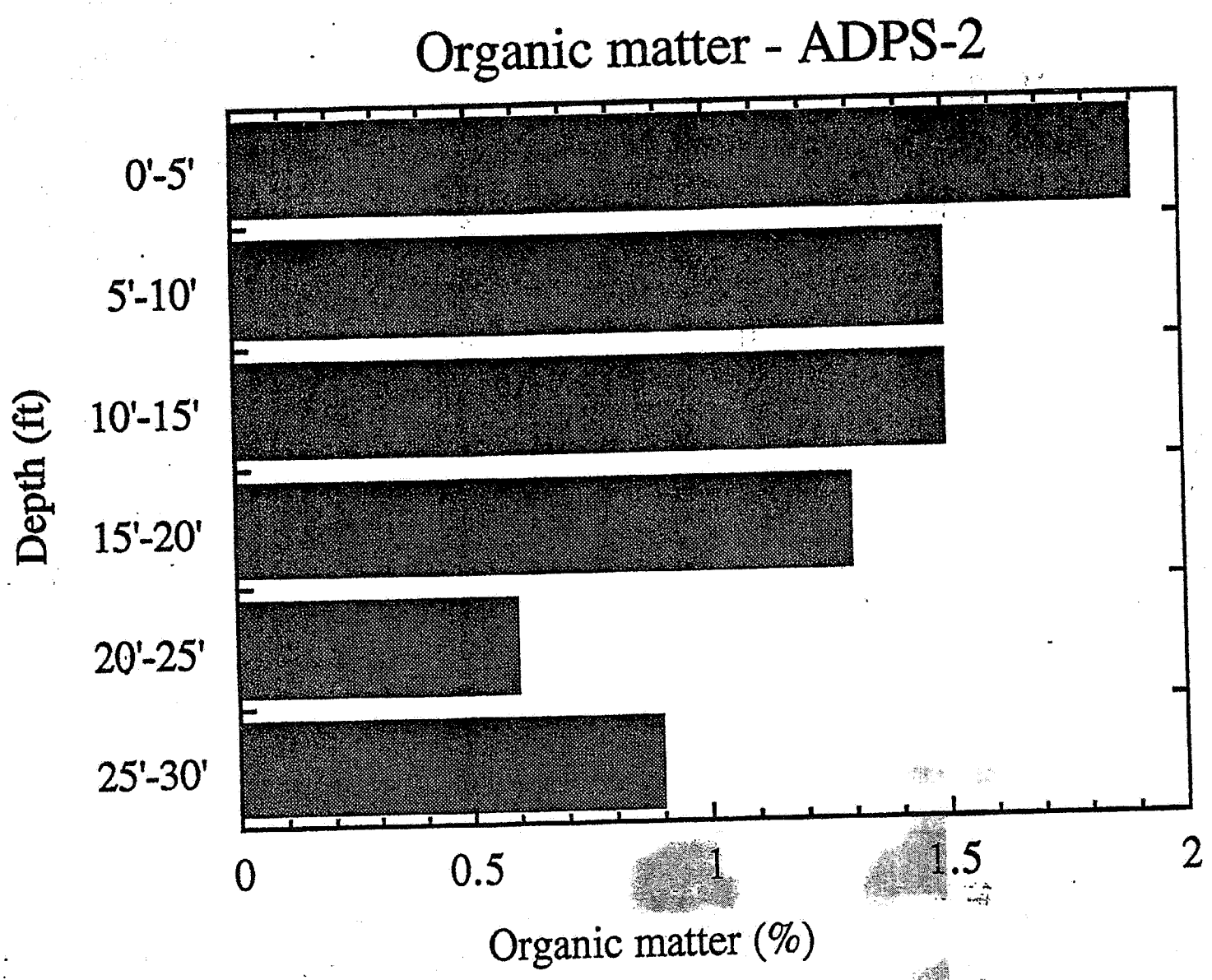

Figure 14. Characterization of the soil samples.
Organic matter percentage of ADPS-2 soil samples.

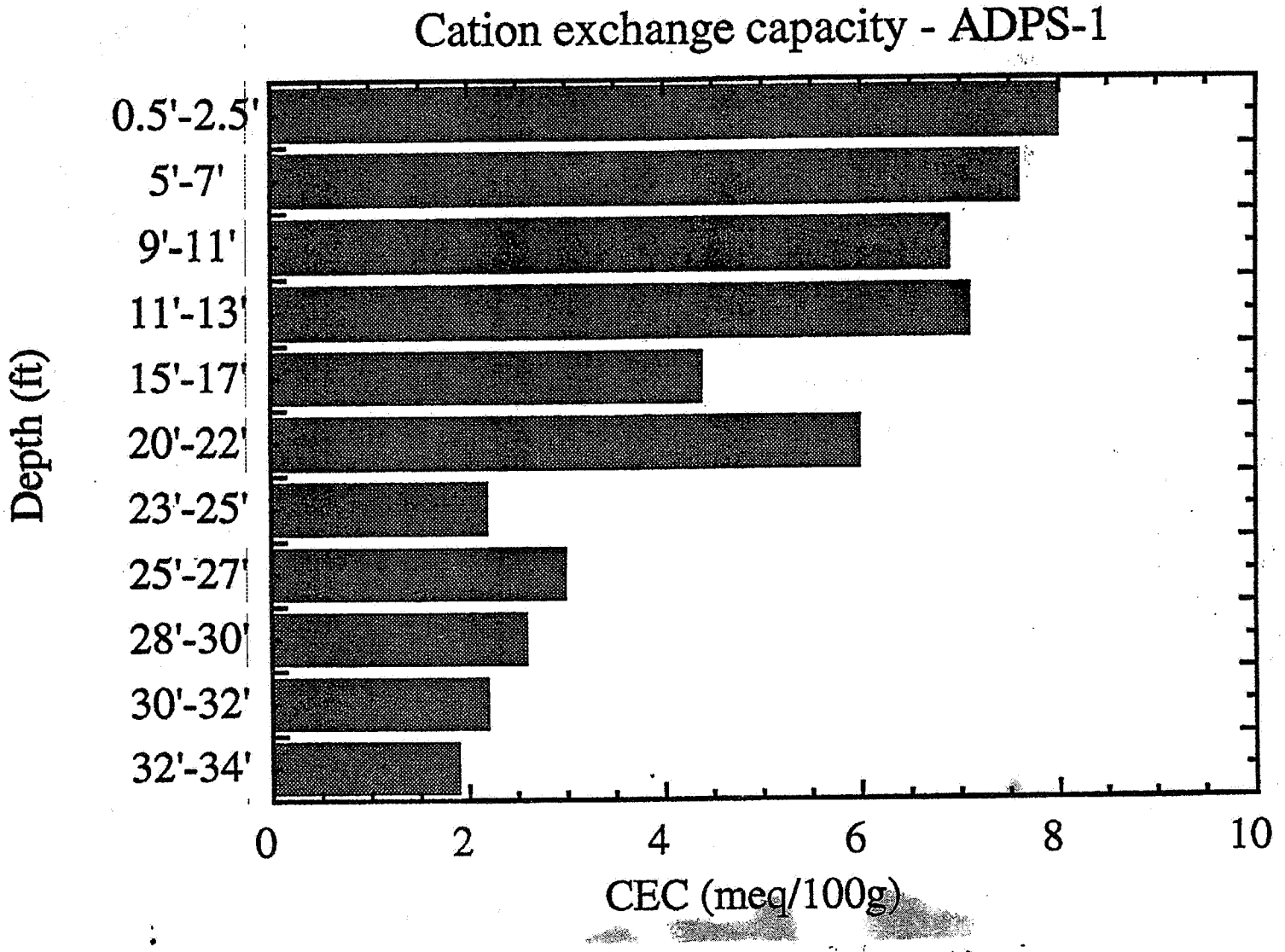

Figure 15a. Characterization of the soil samples.
Effective cation exchange capacity of ADPS-1 soil samples.

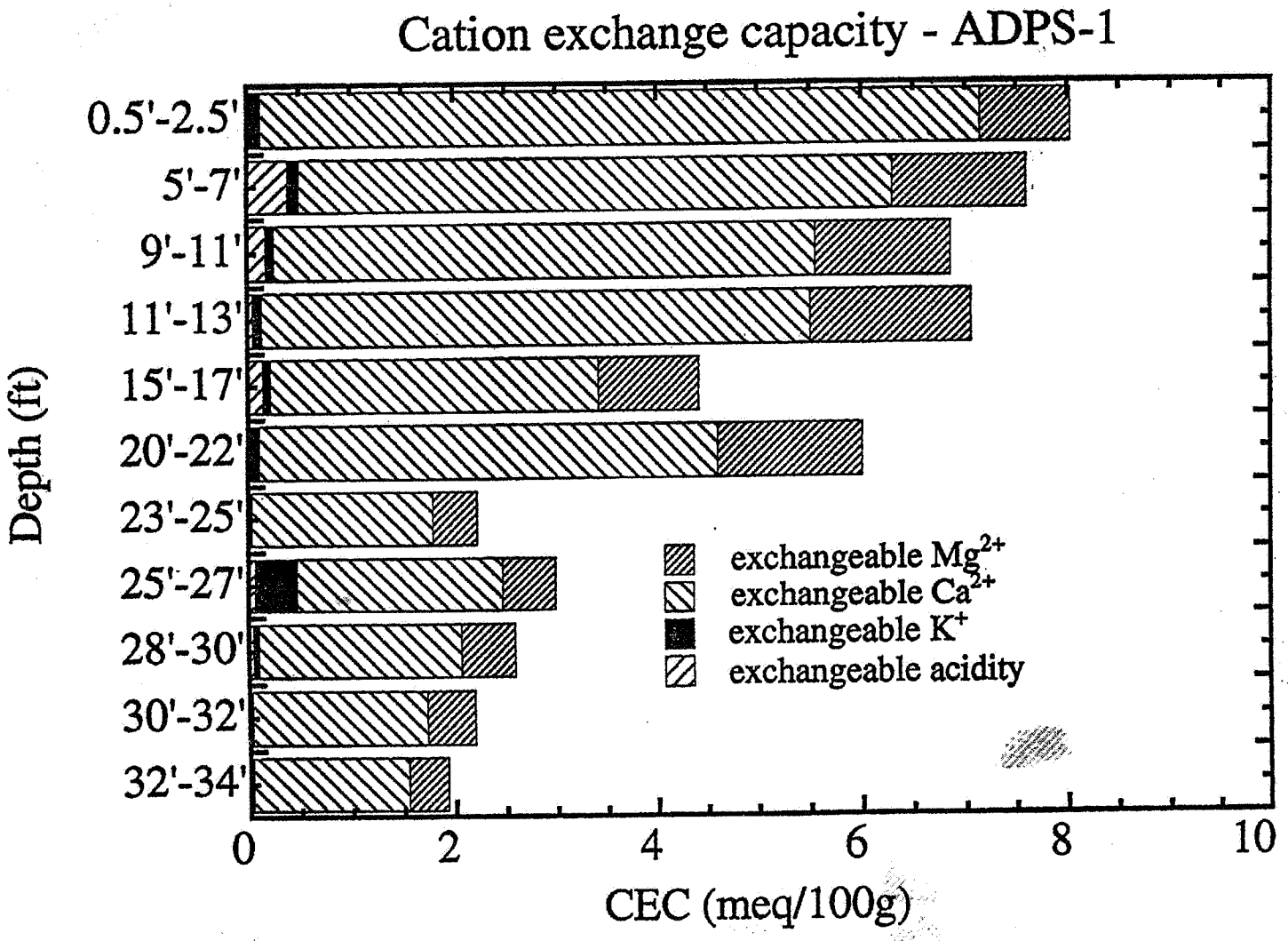

Figure 15b. Characterization of the soil samples.
Exchangeable ions of ADPS-1 soil samples (stack bars).

ASH010684

EID103266

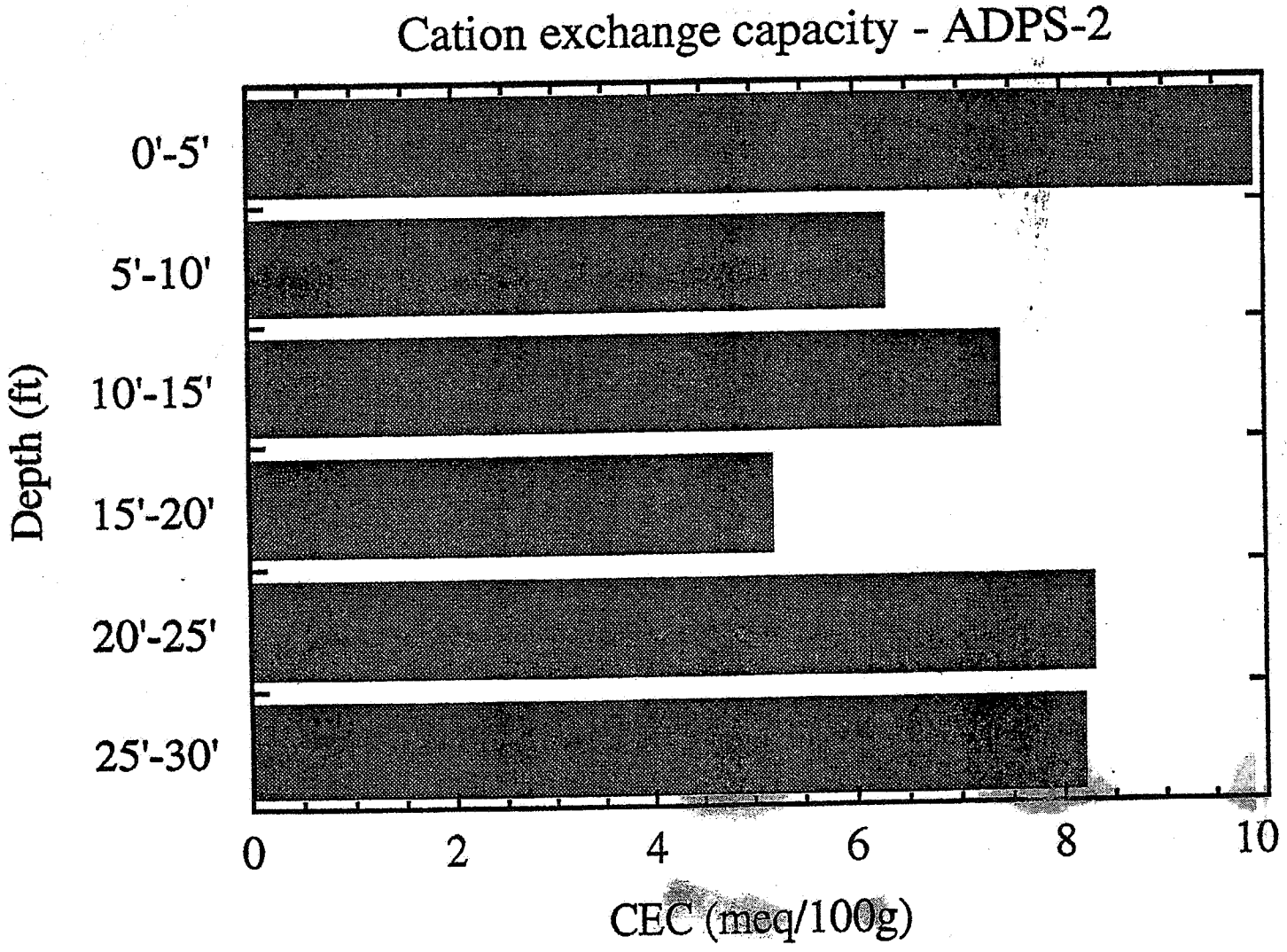

Figure 16a. Characterization of the soil samples.
Effective cation exchange capacity of ADPS-2 soil samples.

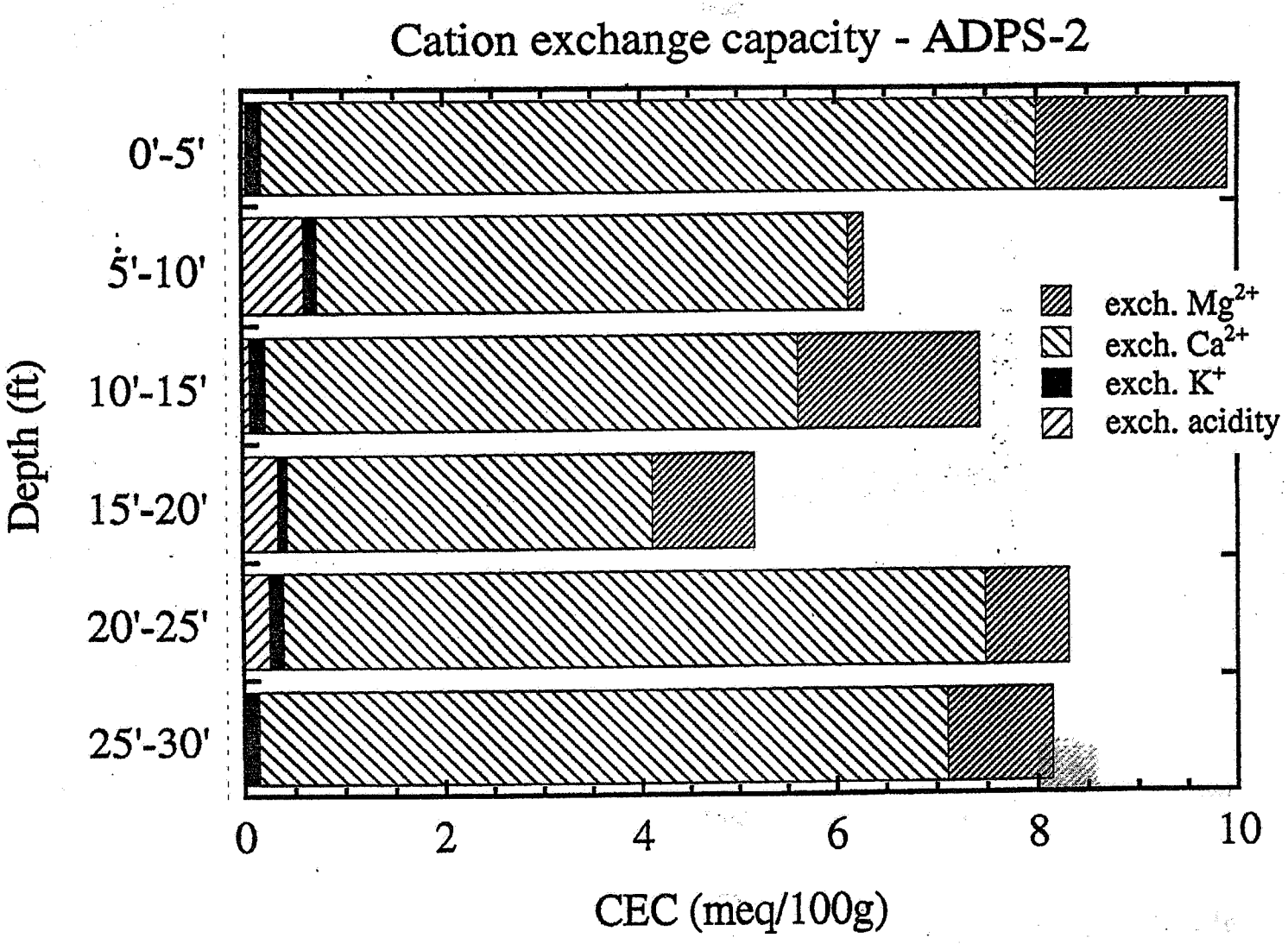

Figure 16b. Characterization of the soil samples.
Exchangeable ions of ADPS-2 soil samples (stack bars).

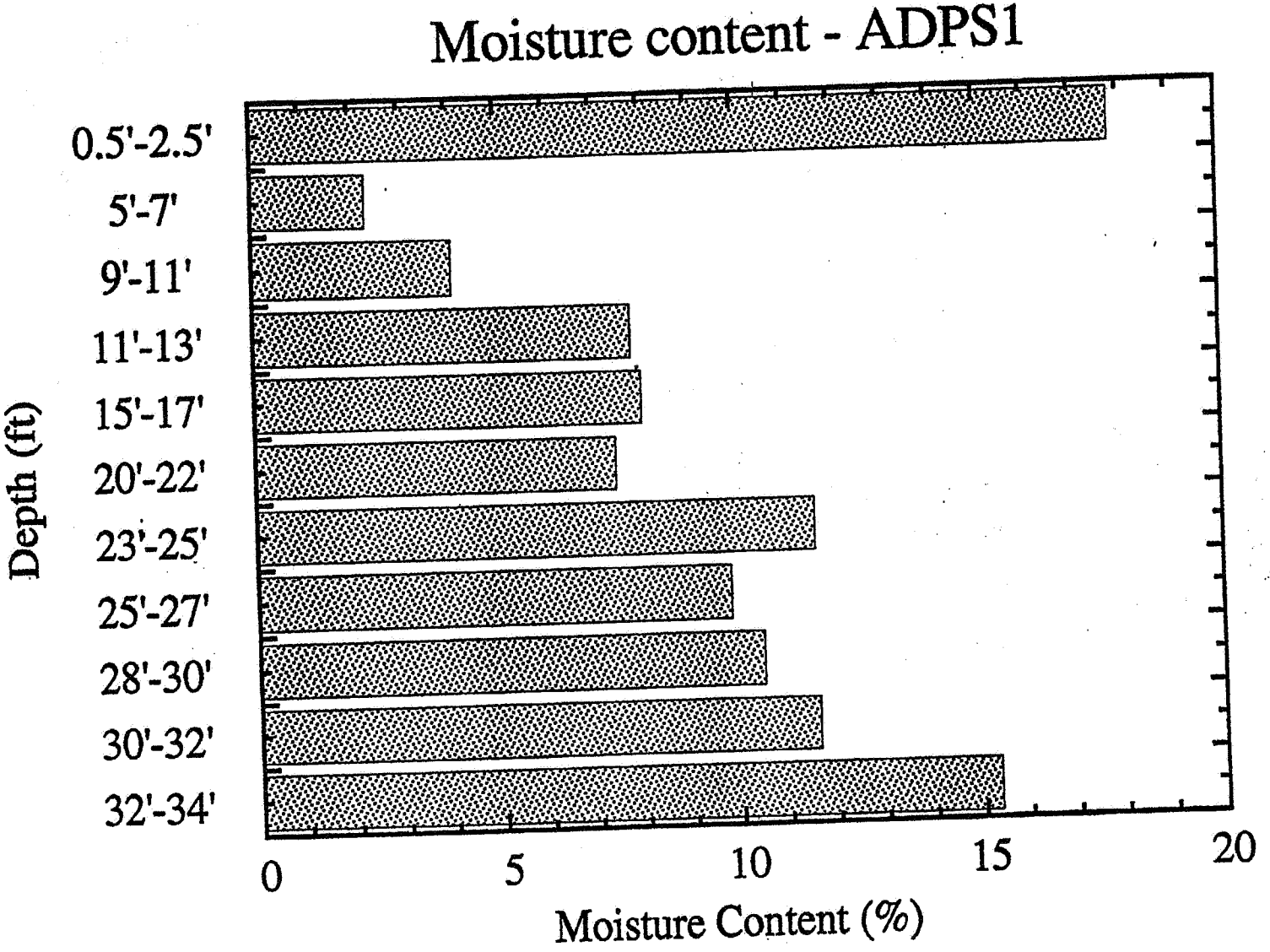

Figure 17. Characterization of the soil samples.
Moisture content of ADPS-1 soil samples.

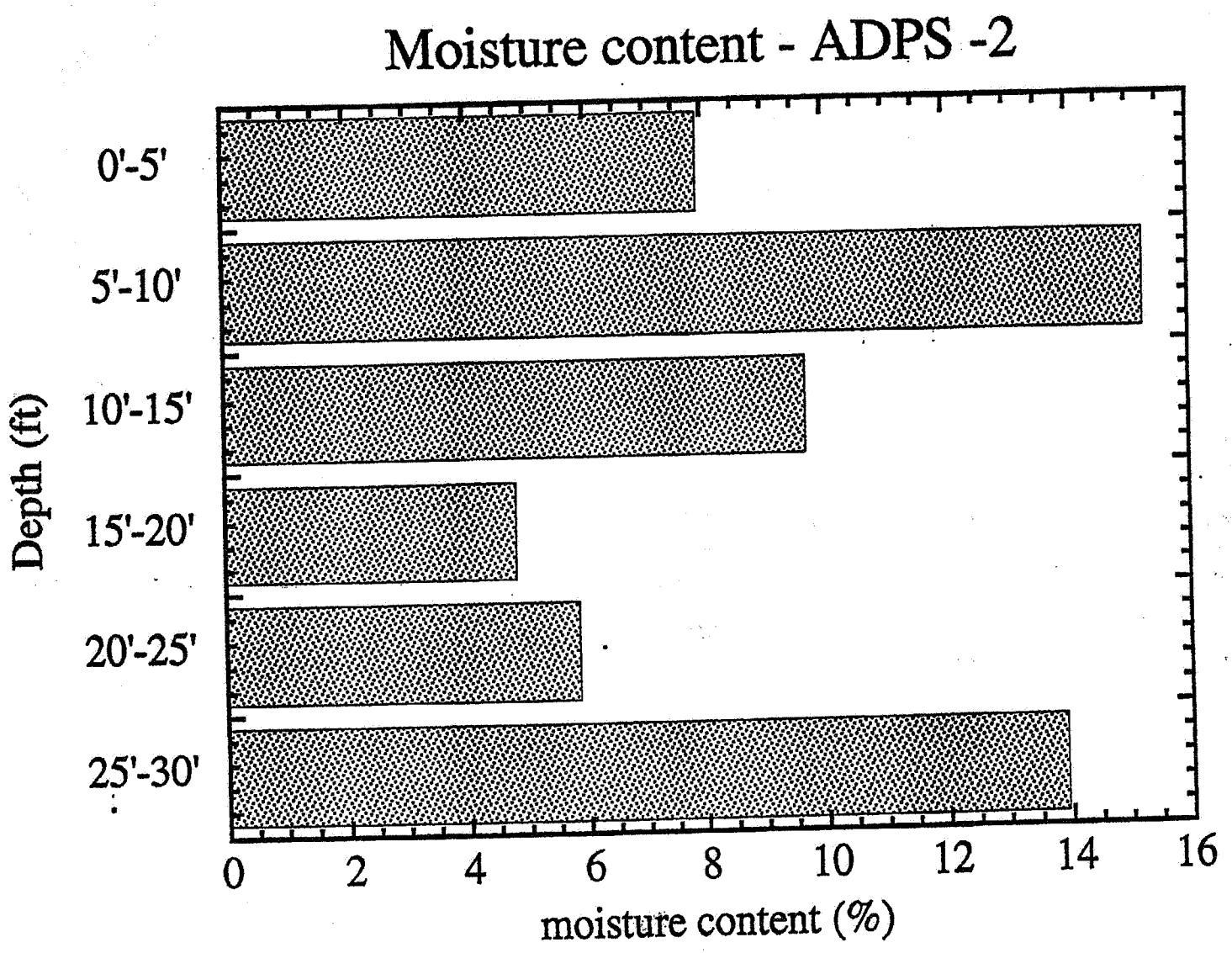

Figure 18. Characterization of the soil samples.
Moisture content of ADPS-2 soil samples.

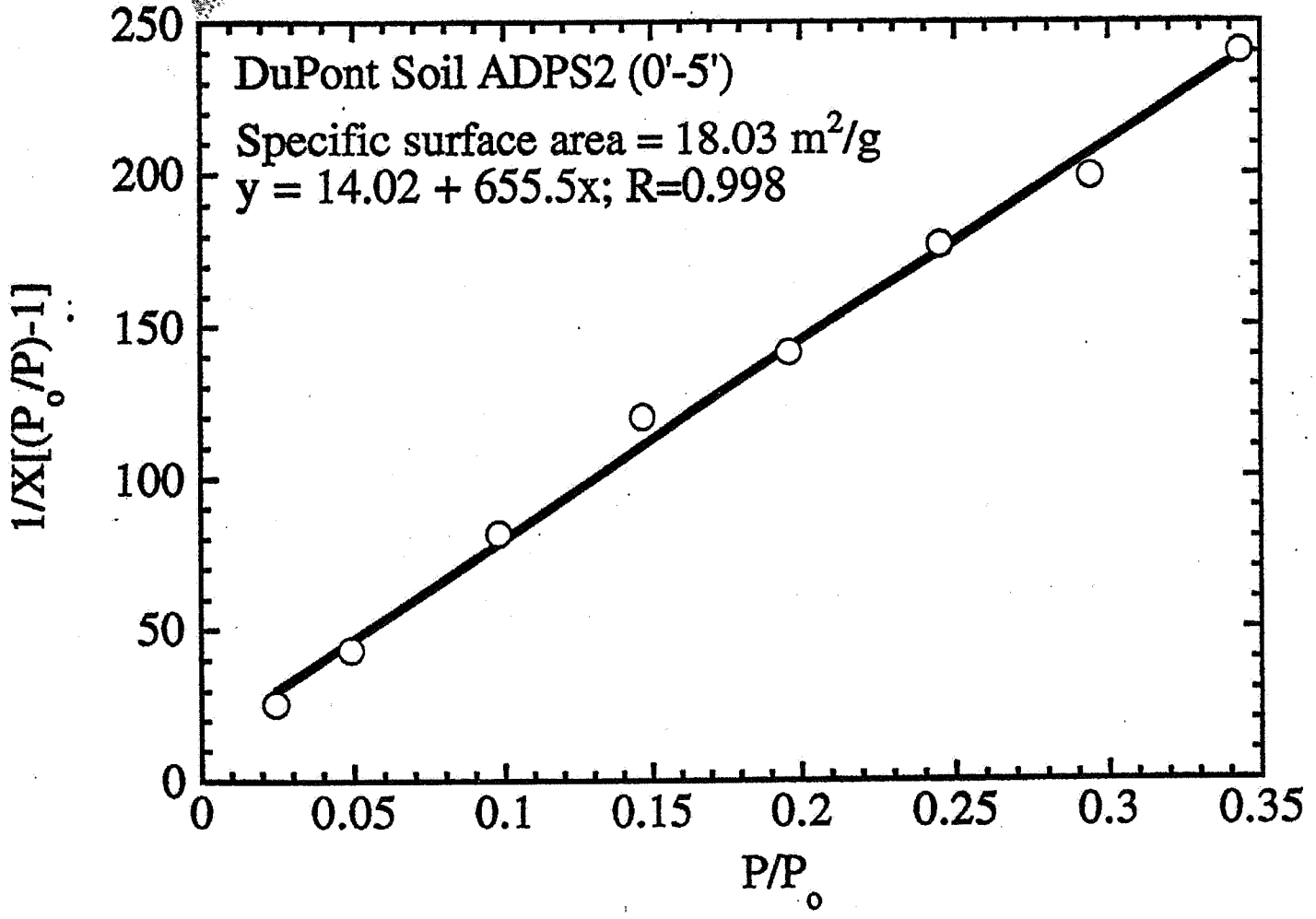

Figure 19. Characterization of the soil samples.
BET plot of ADPS-2 soil sample (depth range of 0 to 5 feet).

689010HSV

EID103271

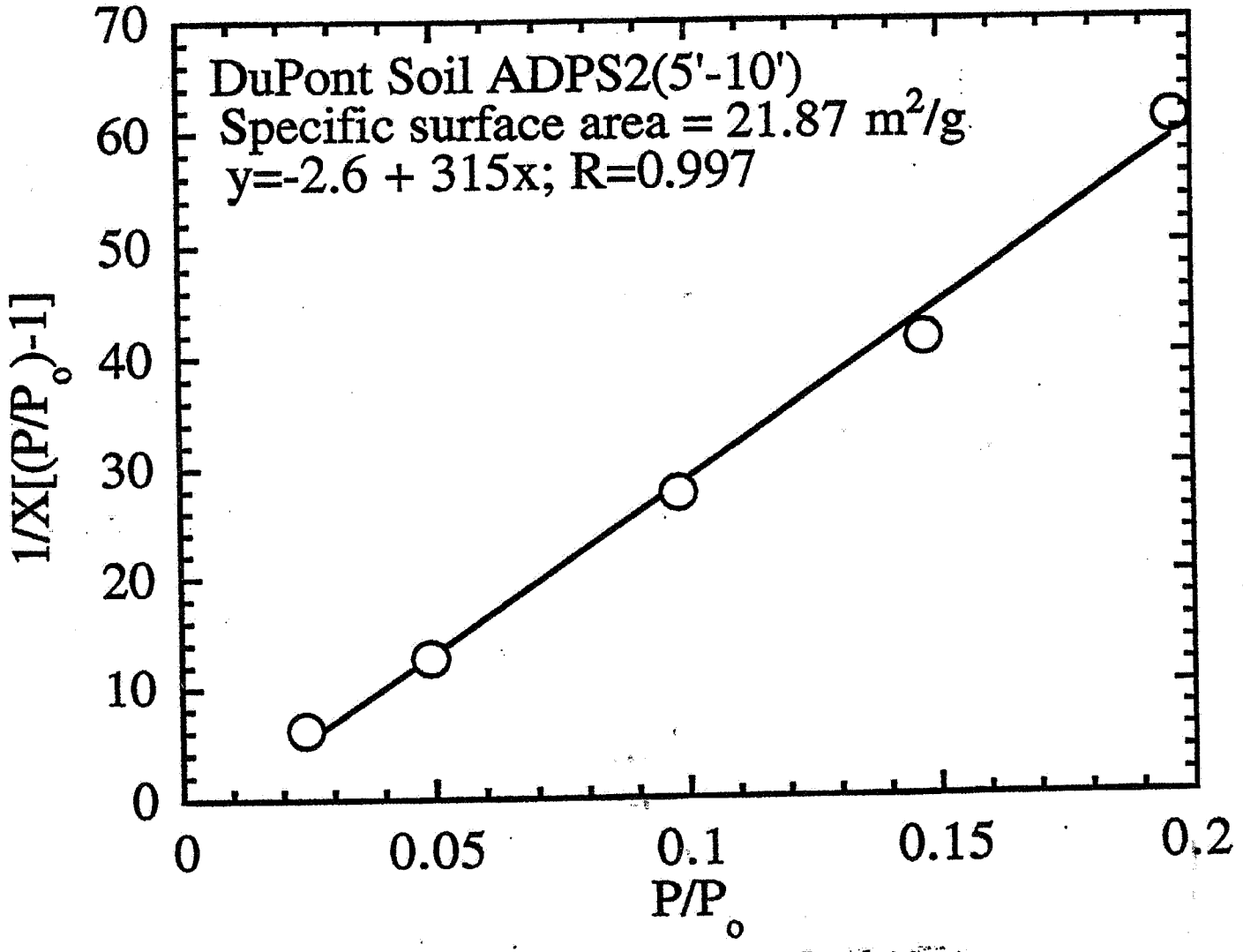

Figure 20. Characterization of the soil samples.
BET plot of ADPS-2 soil sample (depth range of 5 to 10 feet).

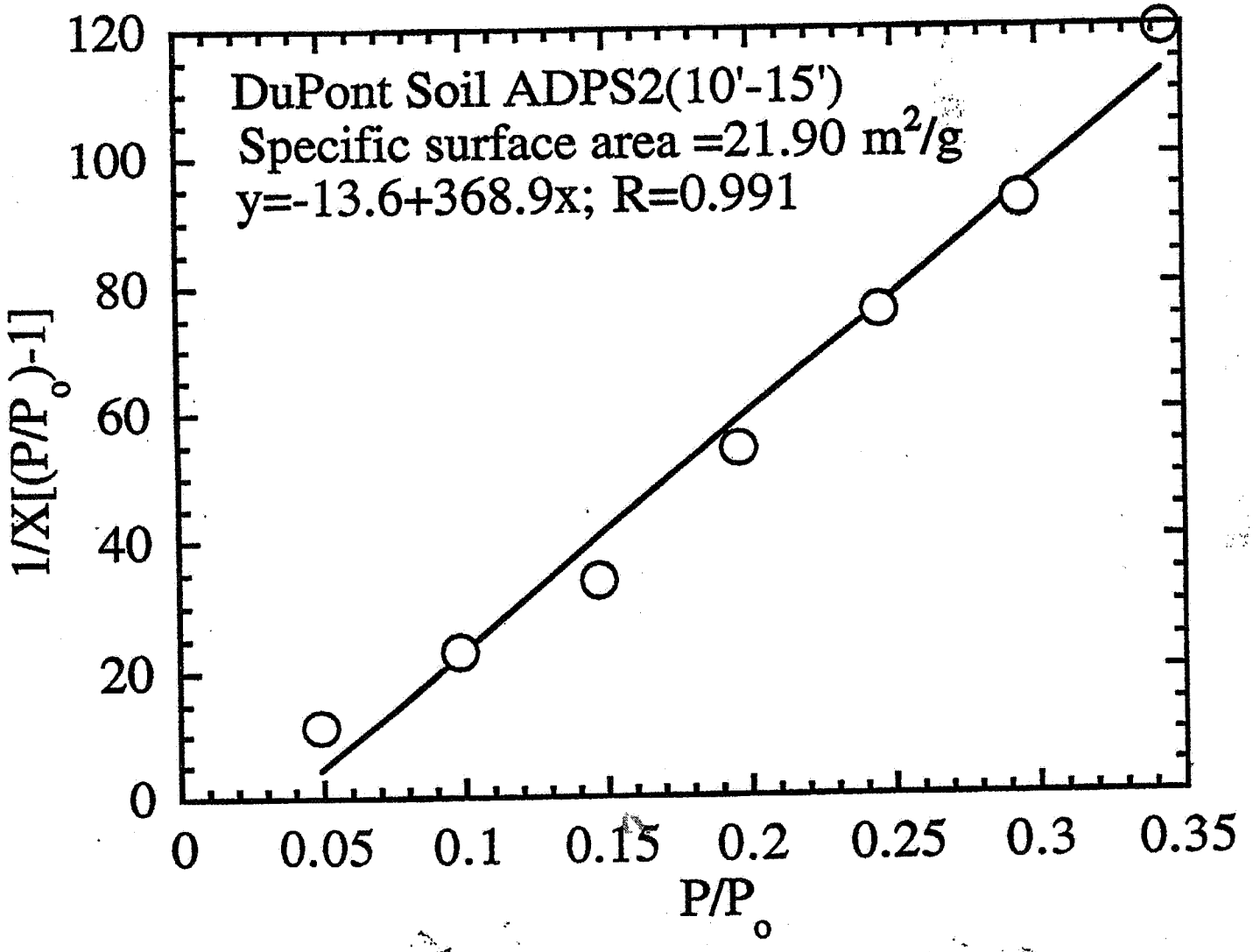

Figure 21. Characterization of the soil samples.
BET plot of ADPS-2 soil sample (depth range of 10 to 15 feet).

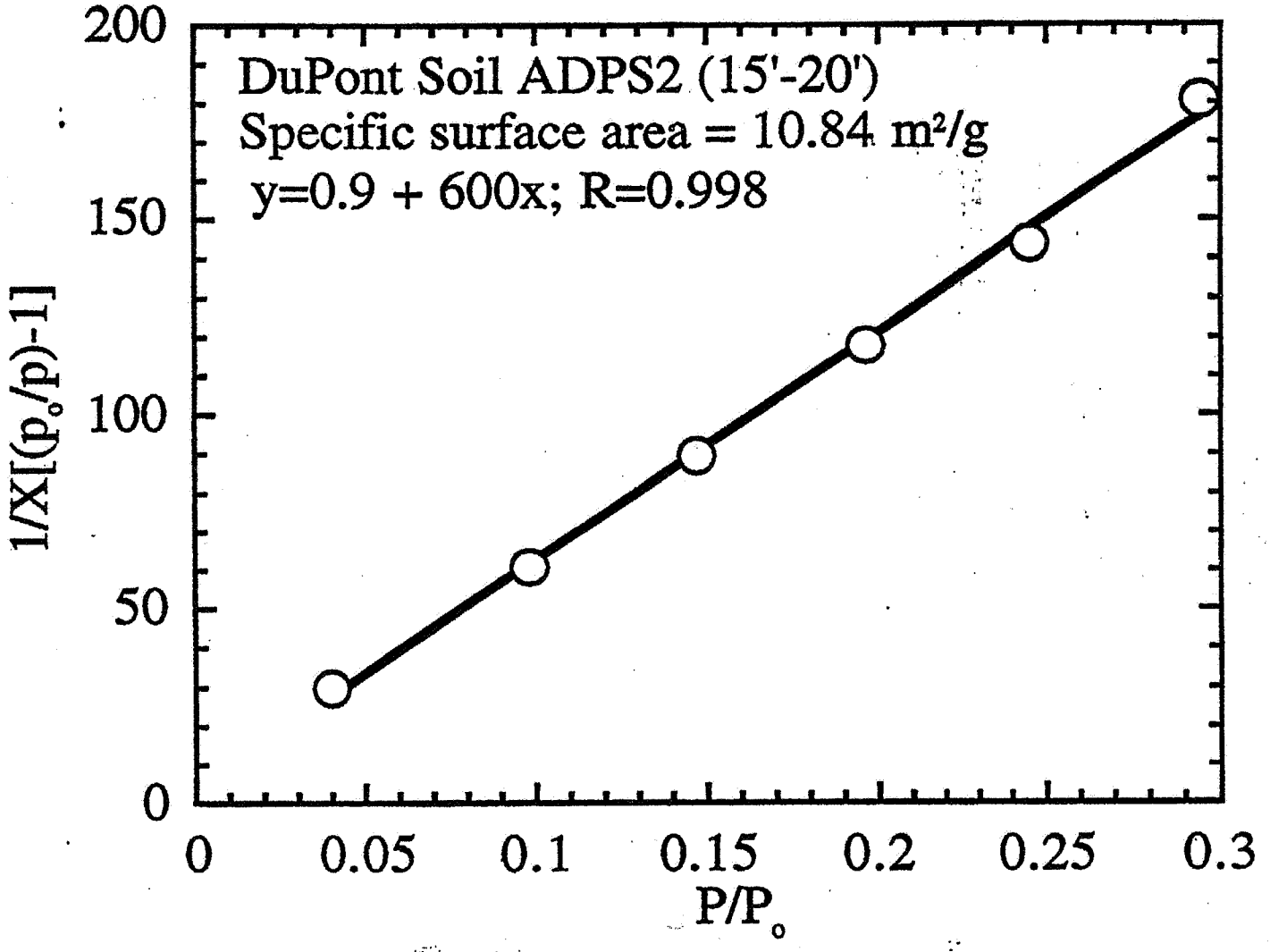

Figure 22. Characterization of the soil samples.
BET plot of ADPS-2 soil sample (depth range of 15 to 20 feet).

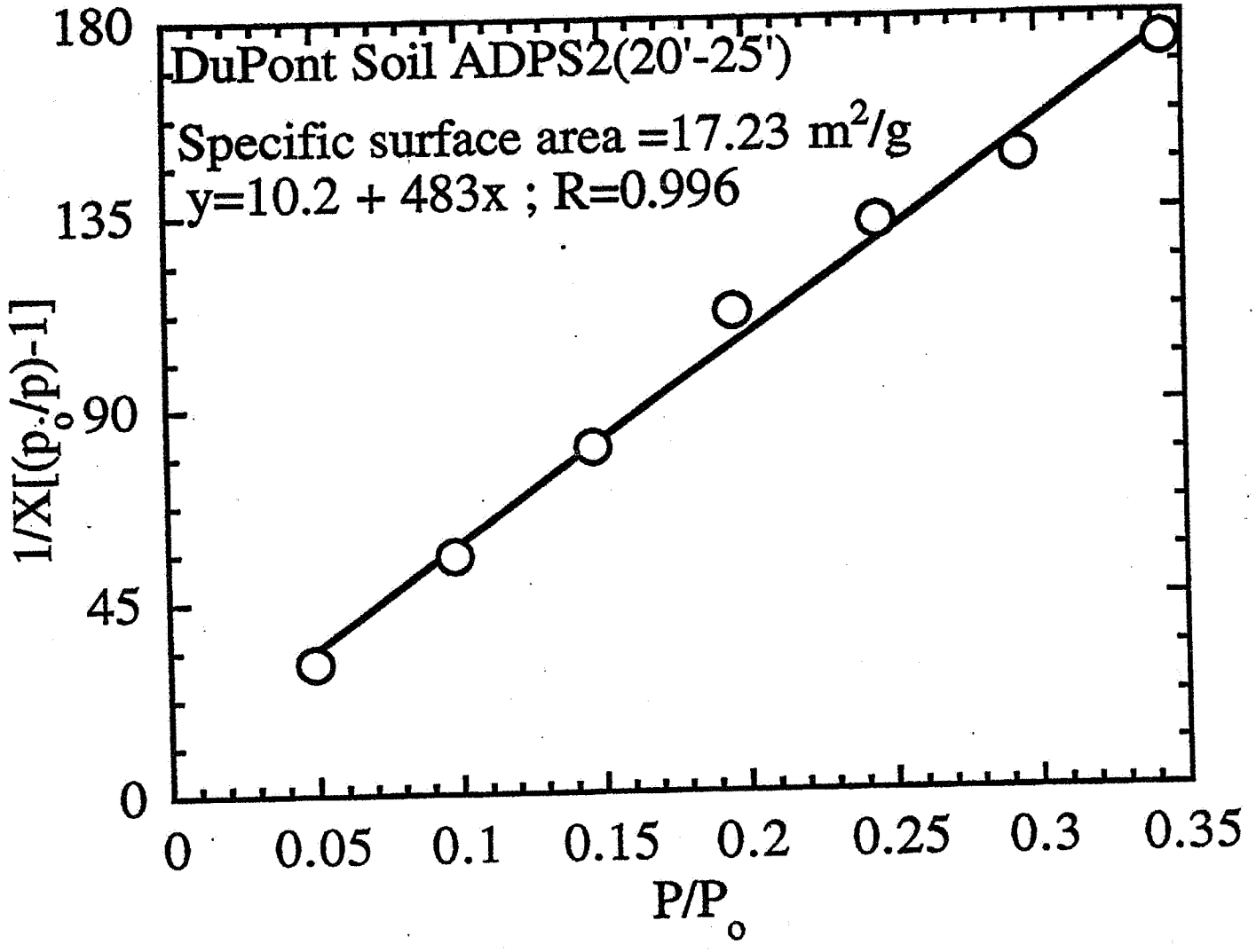

Figure 23. Characterization of the soil samples.
BET plot of ADPS-2 soil sample (depth range of 20 to 25 feet).

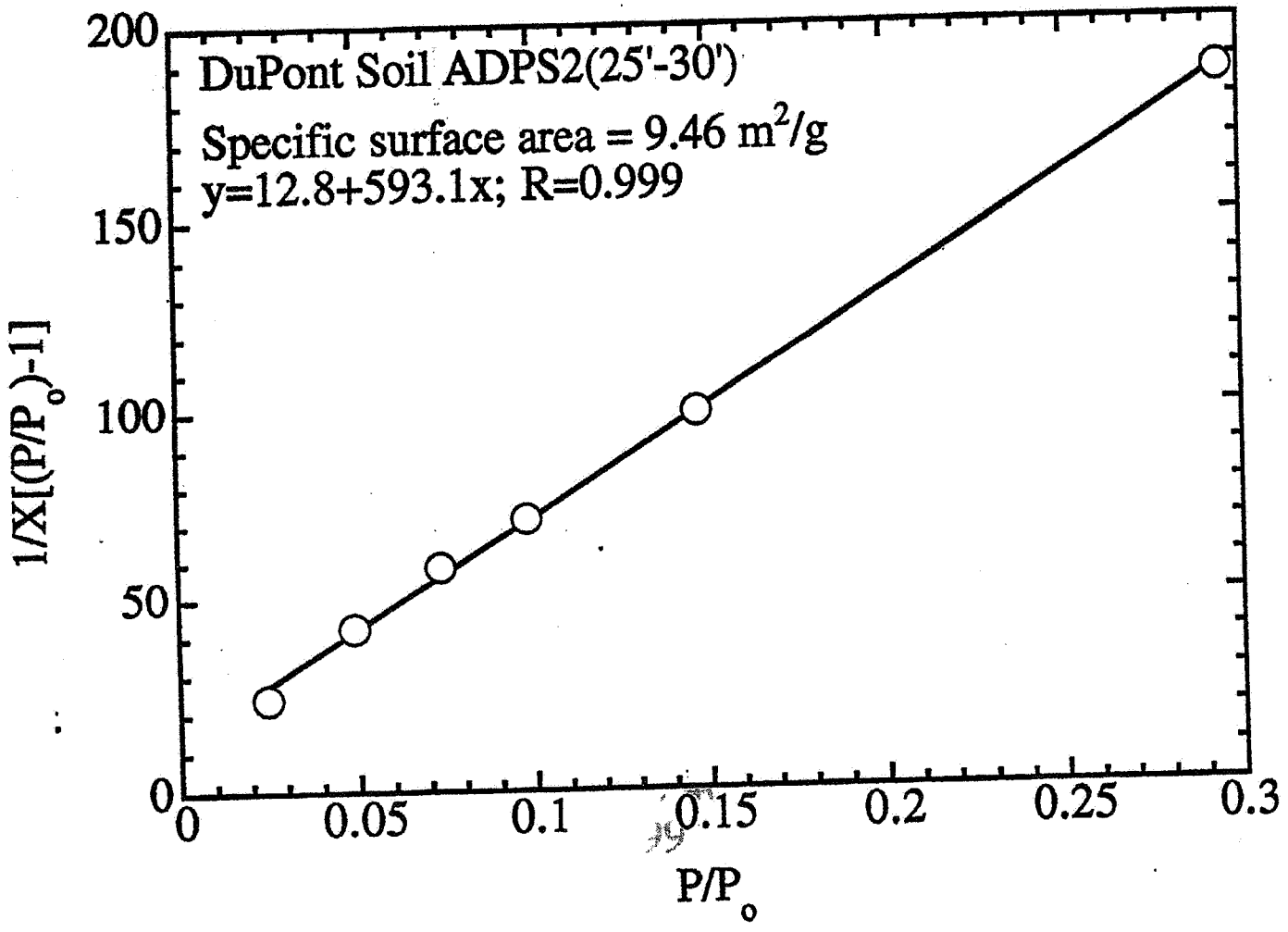

Figure 24. Characterization of the soil samples.
BET plot of ADPS-2 soil sample (depth range of 25 to 30 feet).

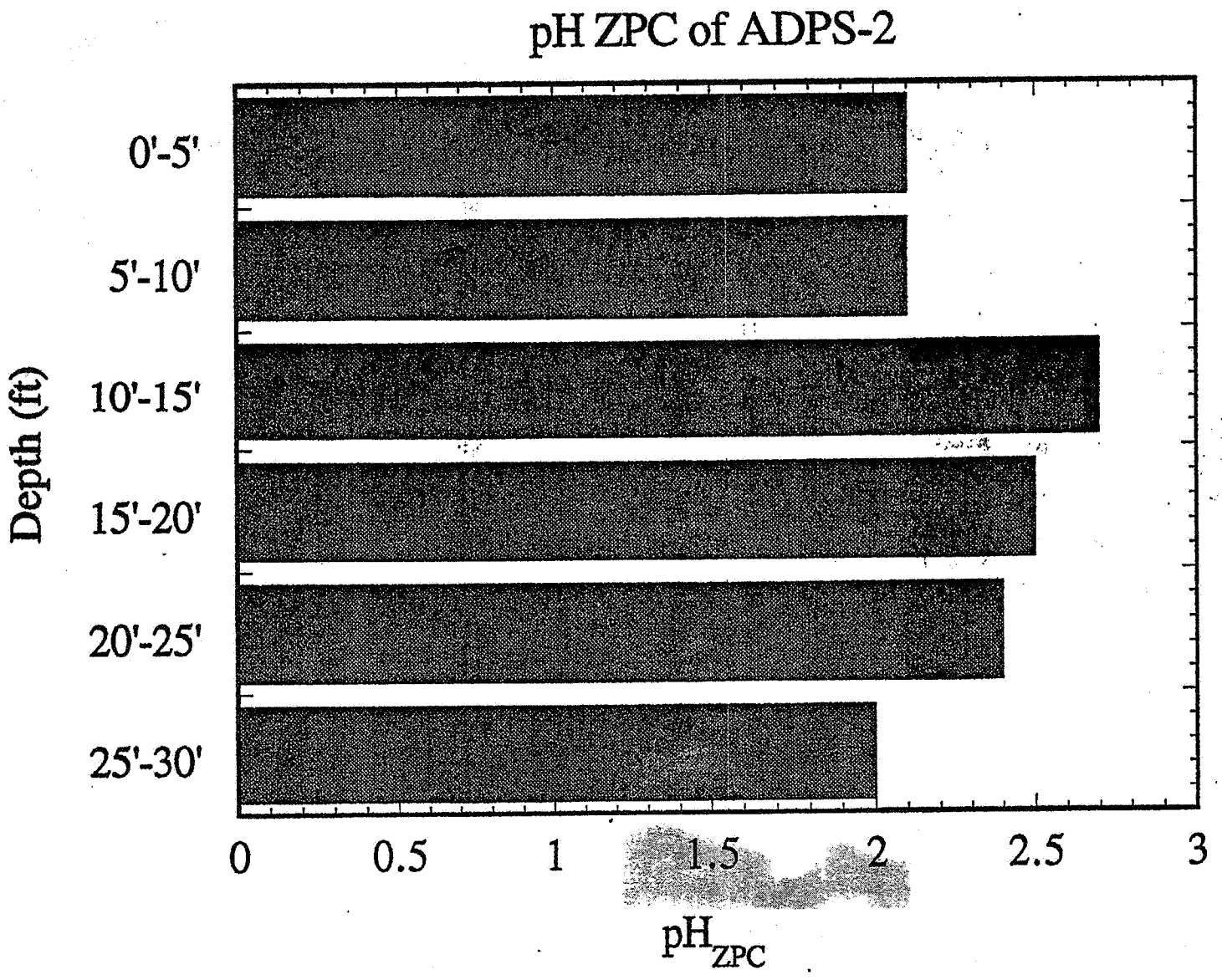

Figure 25. Characterization of the soil samples.
The pH_{ZPC} of ADPS-2 soil samples.

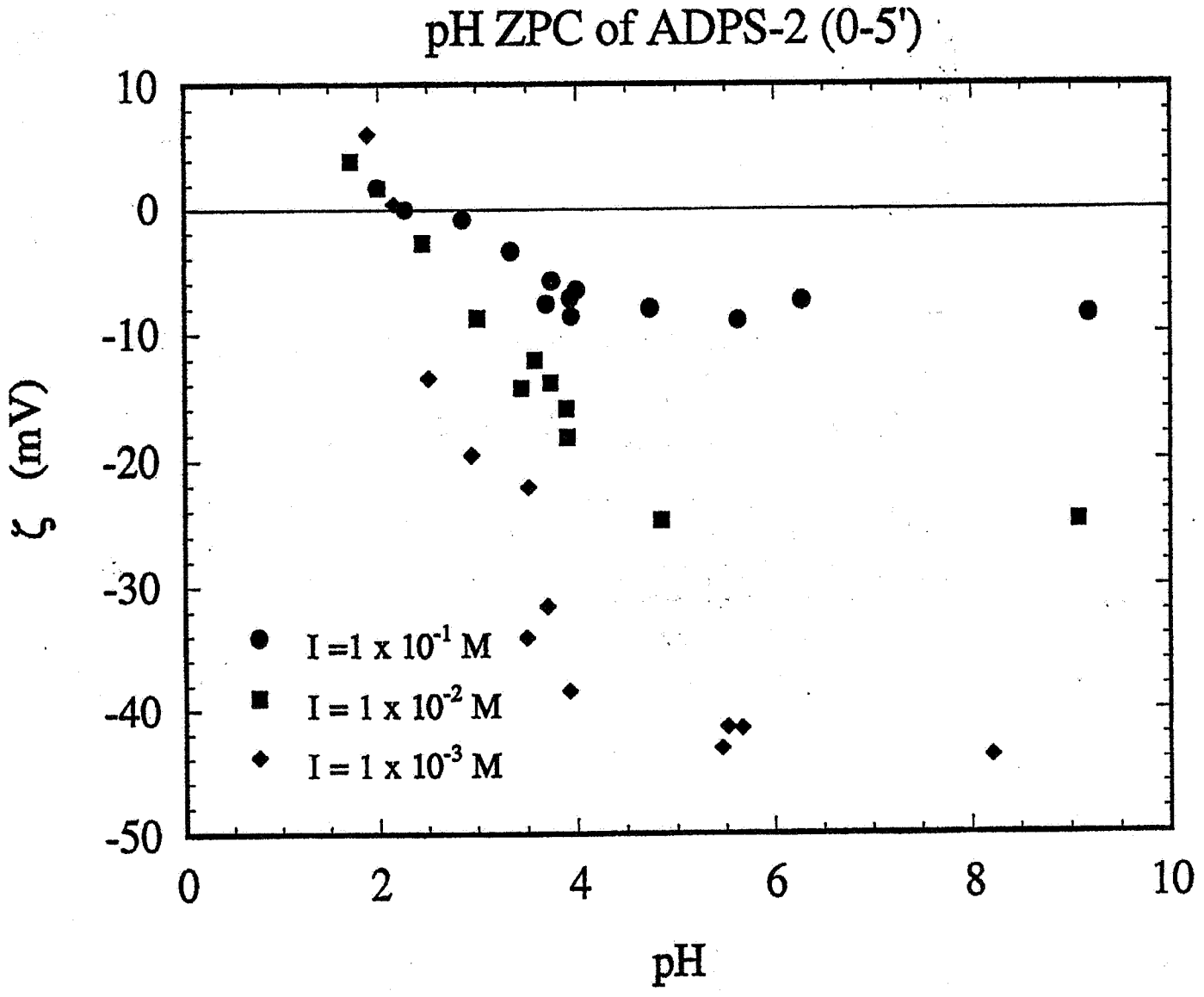

Figure 26. Characterization of the soil samples.
Determination of the pH_{ZPC} of ADPS-2 soil sample (depth range of 0 to 5 feet).

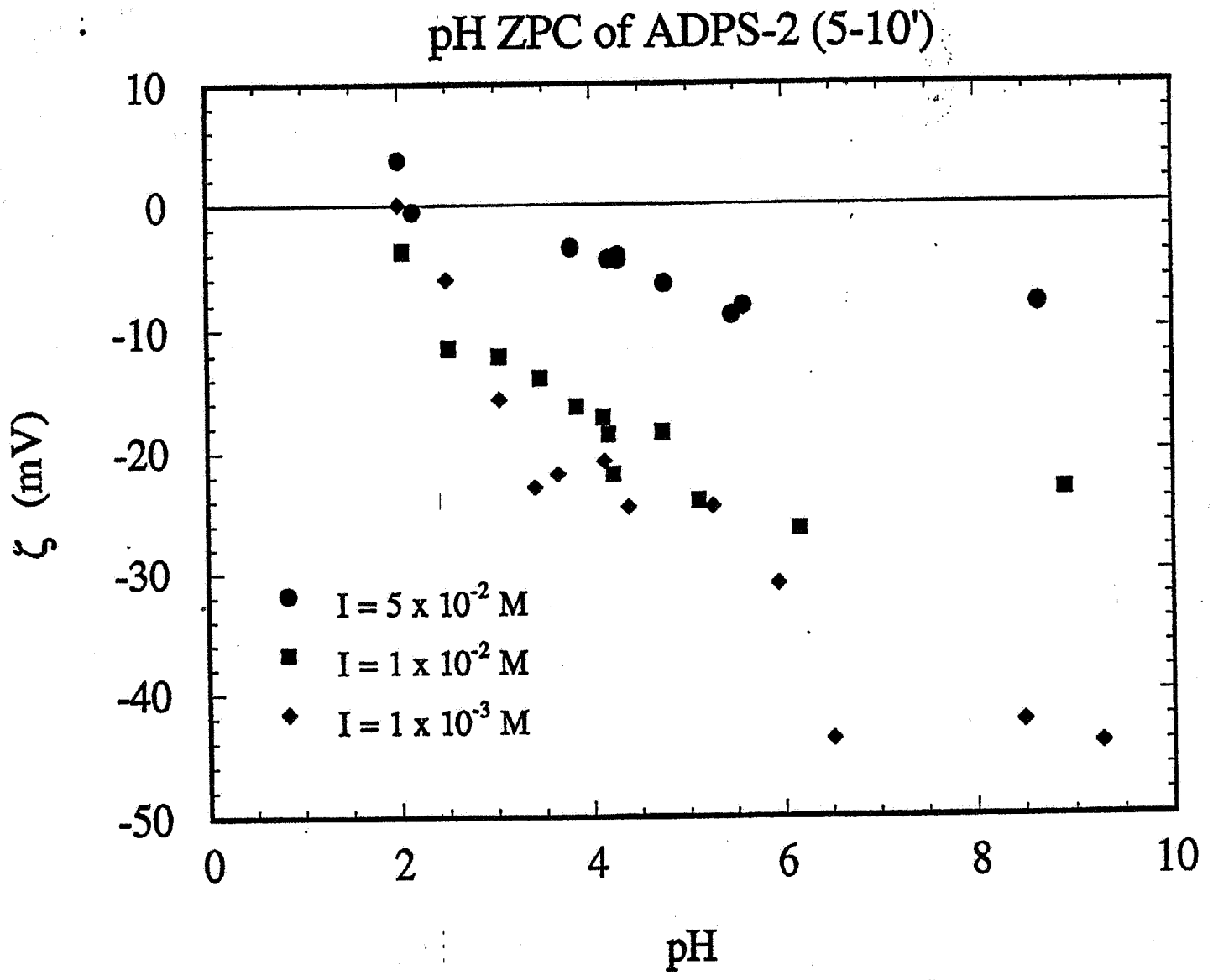

Figure 27. Characterization of the soil samples.
Determination of the pH_{ZPC} of ADPS-2 soil sample (depth range of 5 to 10 feet).

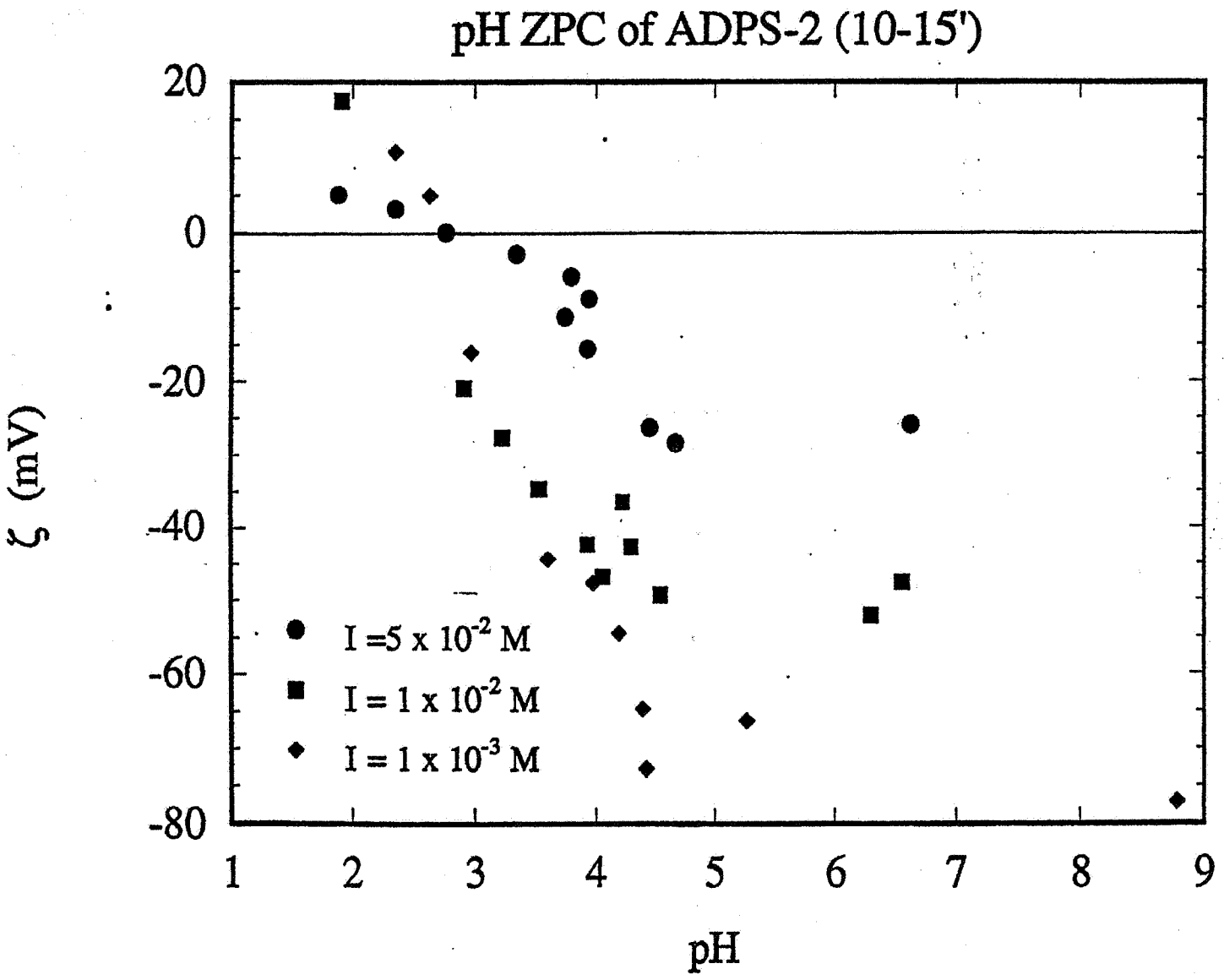

Figure 28. Characterization of the soil samples.
Determination of the pH_{ZPC} of ADPS-2 soil sample (depth range of 10 to 15 feet).

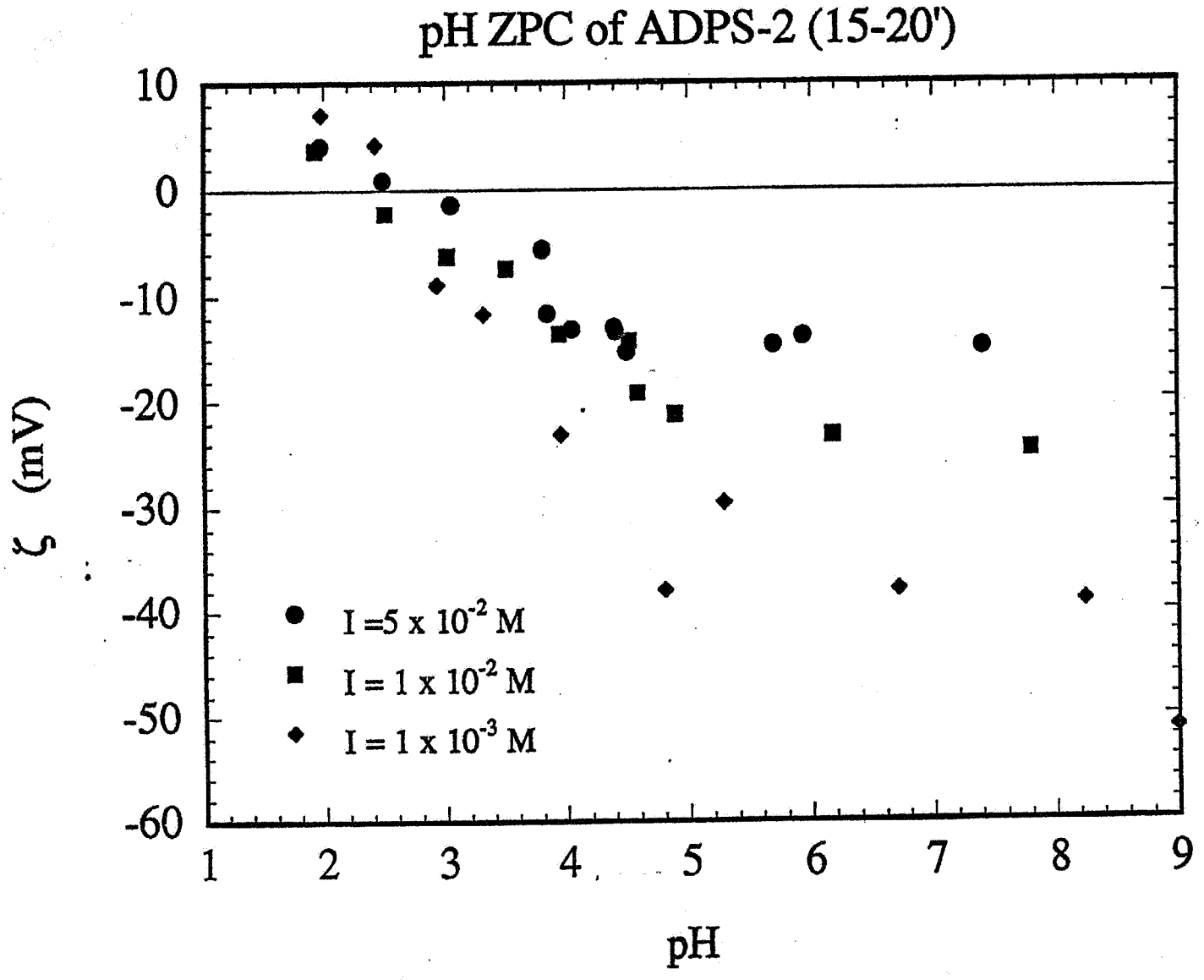

Figure 29. Characterization of the soil samples.
Determination of the pH_{ZPC} of ADPS-2 soil sample (depth range of 15 to 20 feet).

669010HSV

EID103281

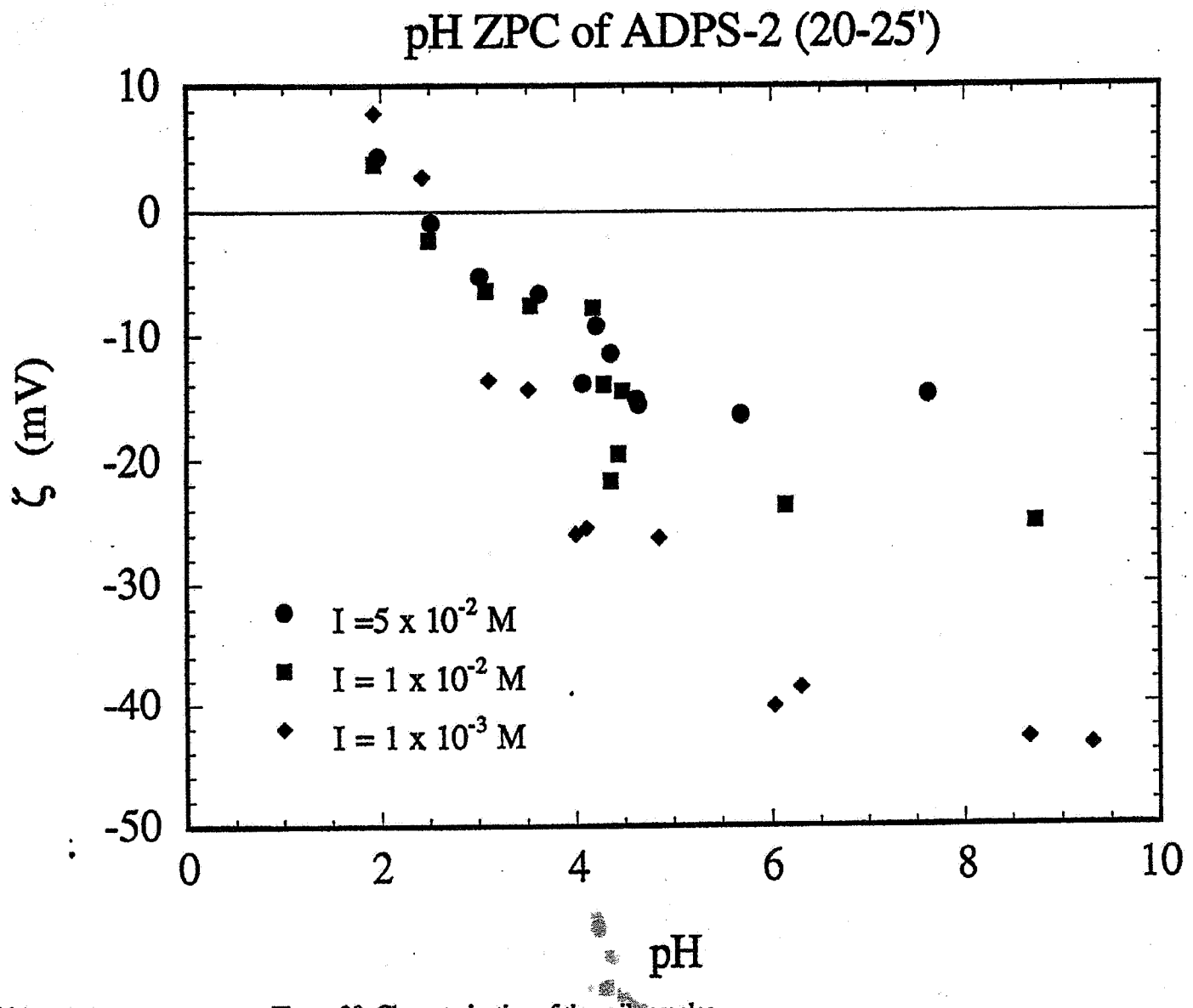

Figure 30. Characterization of the soil samples.
Determination of the pH_{ZPC} of ADPS-2 soil sample (depth range of 20 to 25 feet).

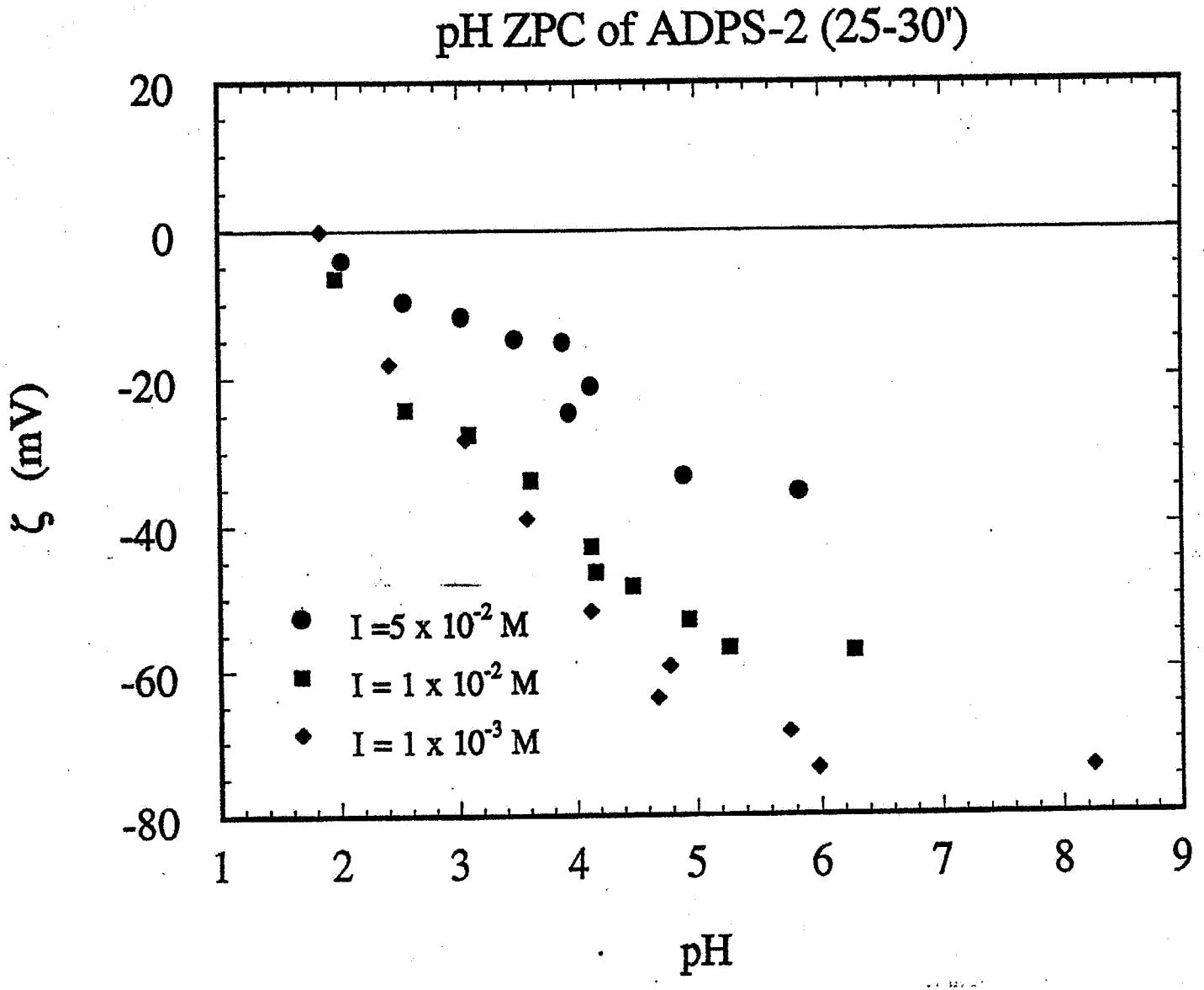

Figure 31. Characterization of the soil samples.
Determination of the pH_{ZPC} of ADPS-2 soil sample (depth range of 25 to 30 feet).

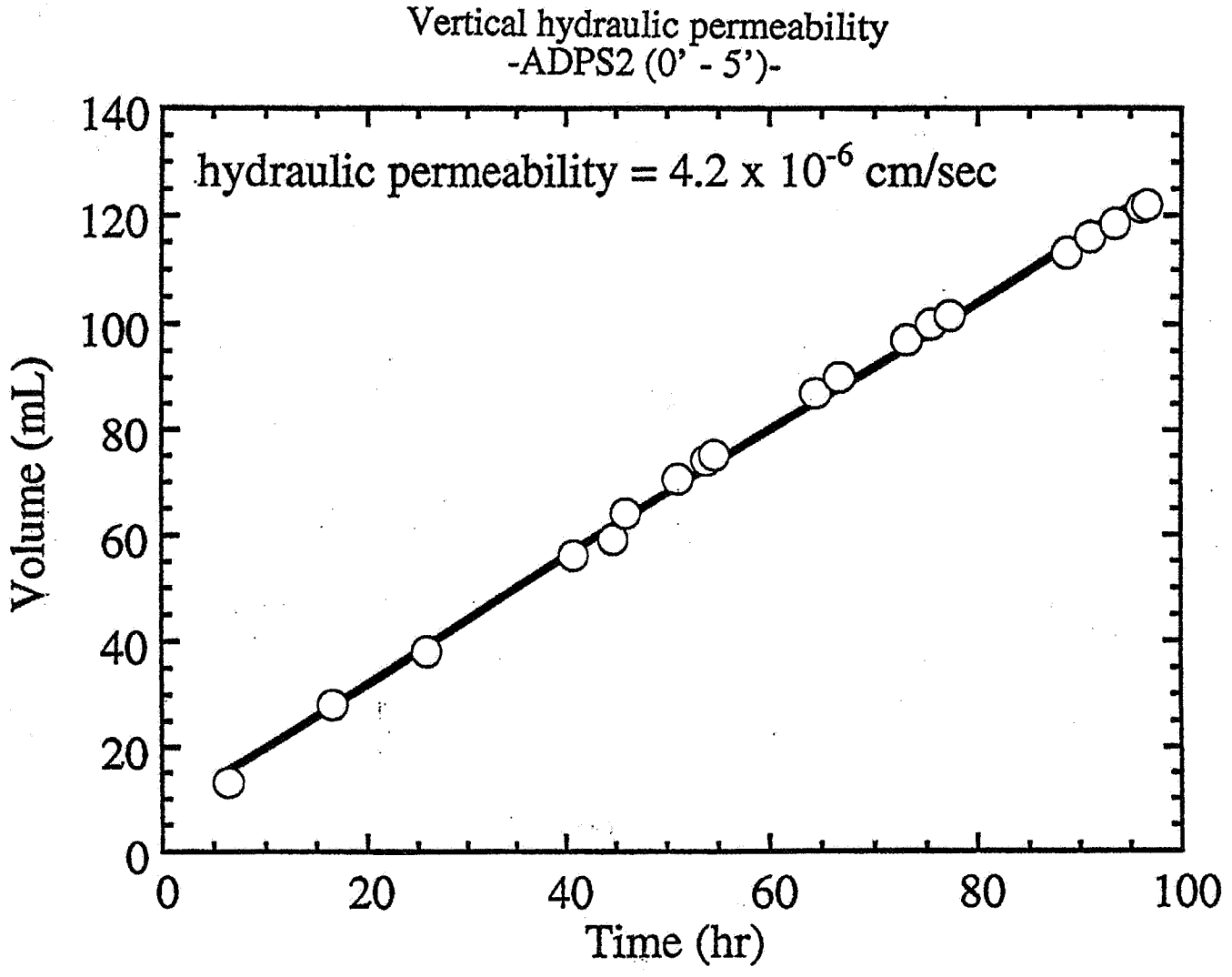

Figure 32. Soil permeability measurement by constant head permeameter.
Soil sample: ADSP2 (0' - 5').

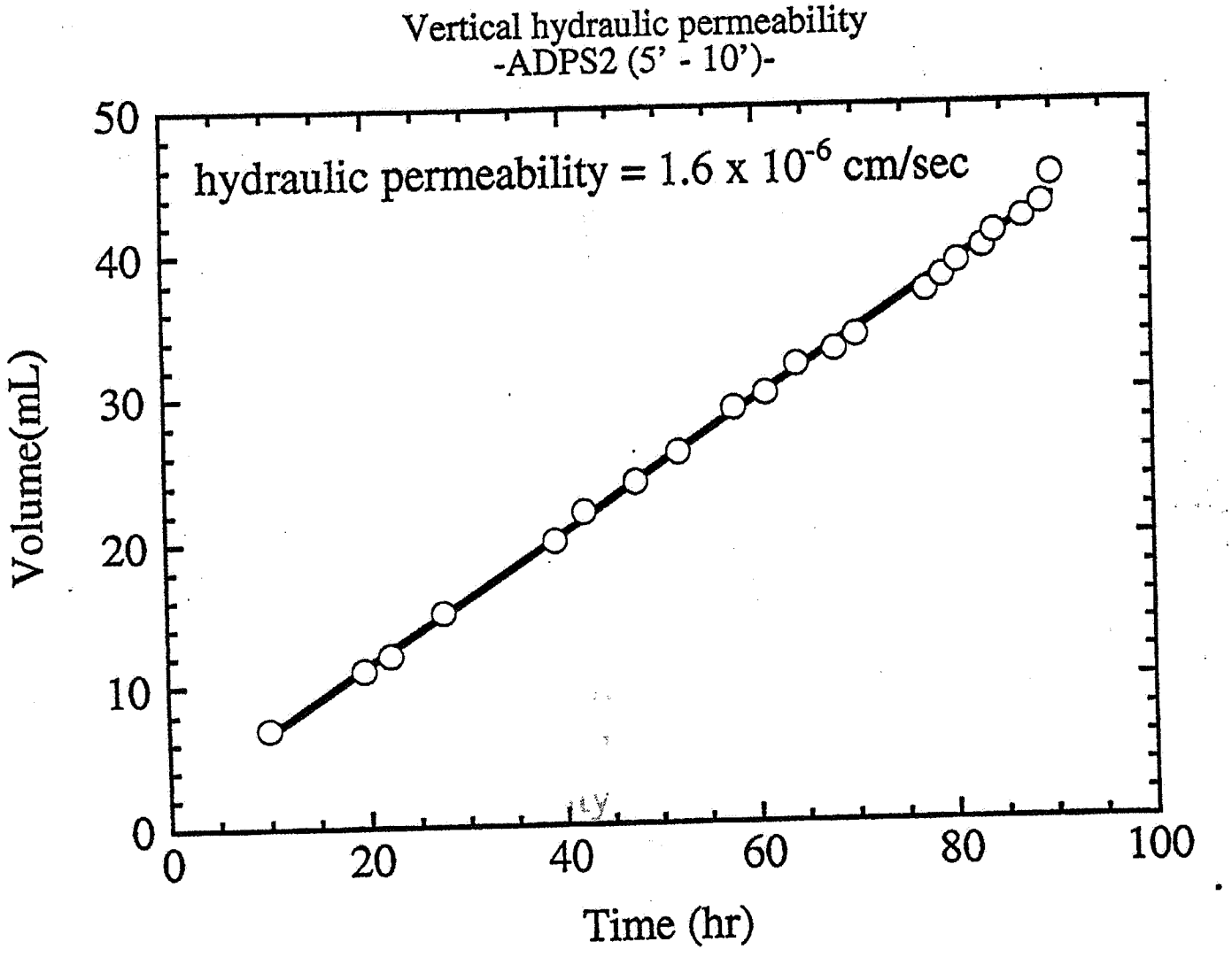

Figure 33. Soil permeability measurement by constant head permeameter.
Soil sample: ADSP2 (5' - 10').

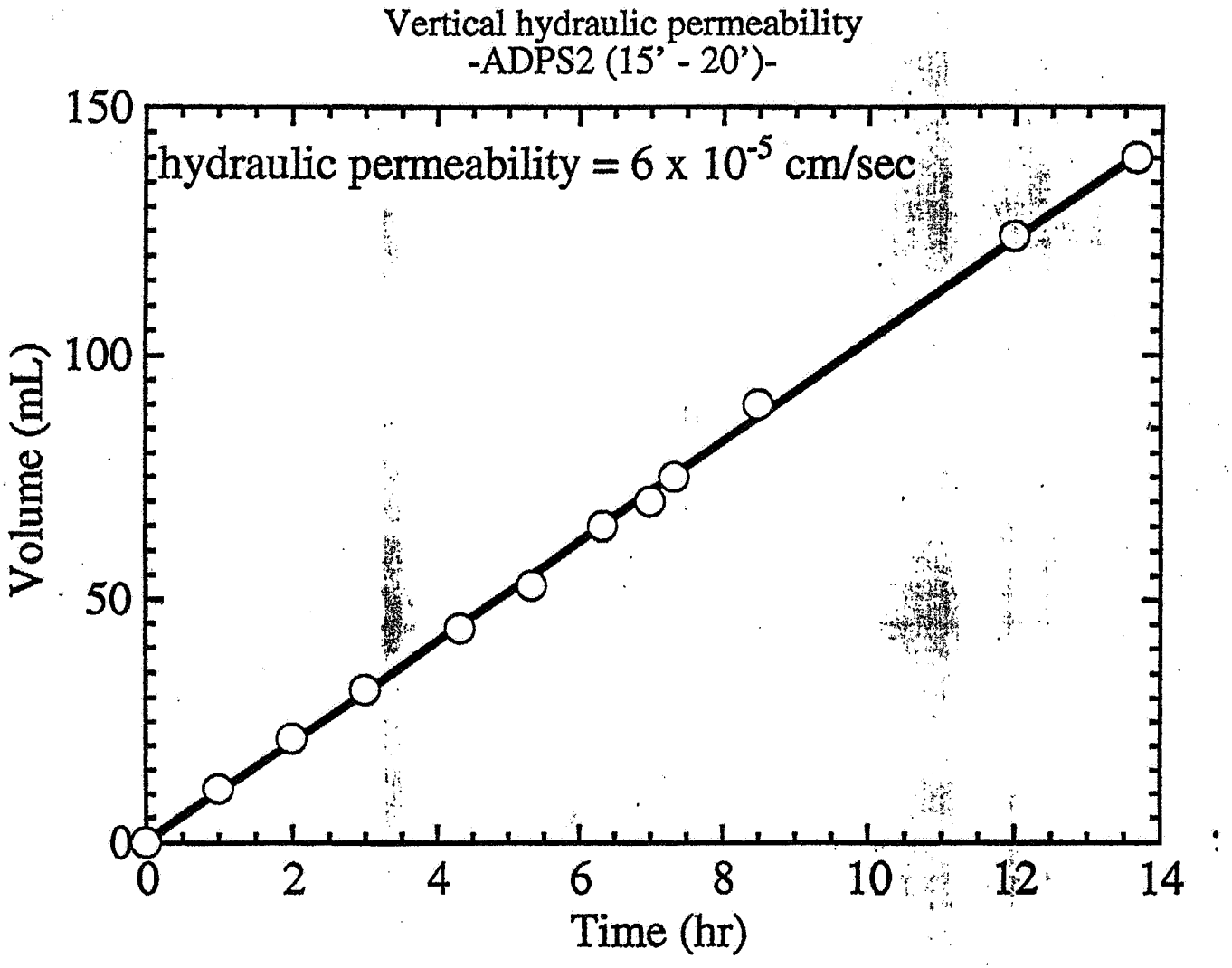

Figure 34. Soil permeability measurement by constant head permeameter.
Soil sample: ADSP2 (15' - 20').

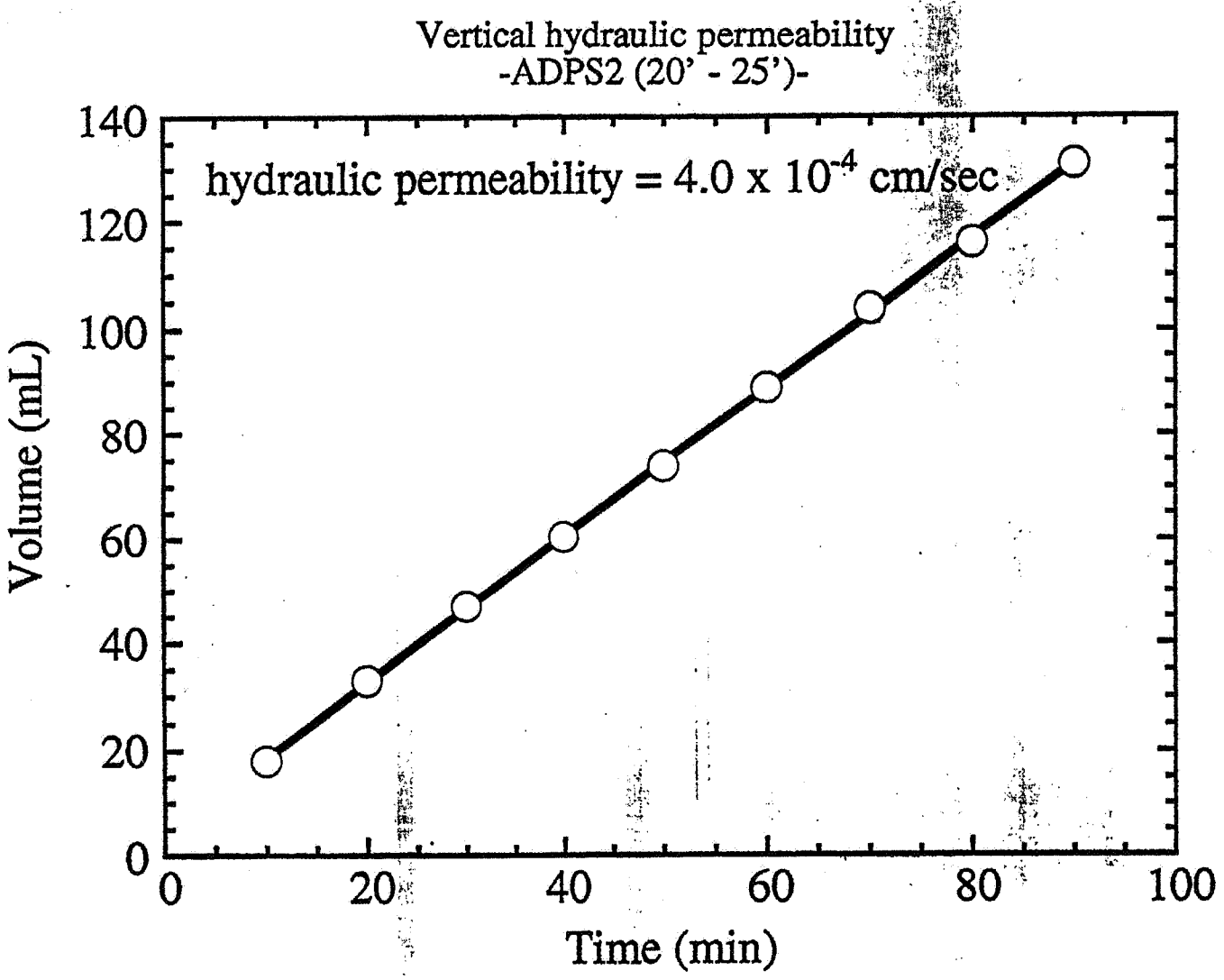

Figure 35. Soil permeability measurement by constant head permeameter.
Soil sample: ADSP2 (20' - 25').

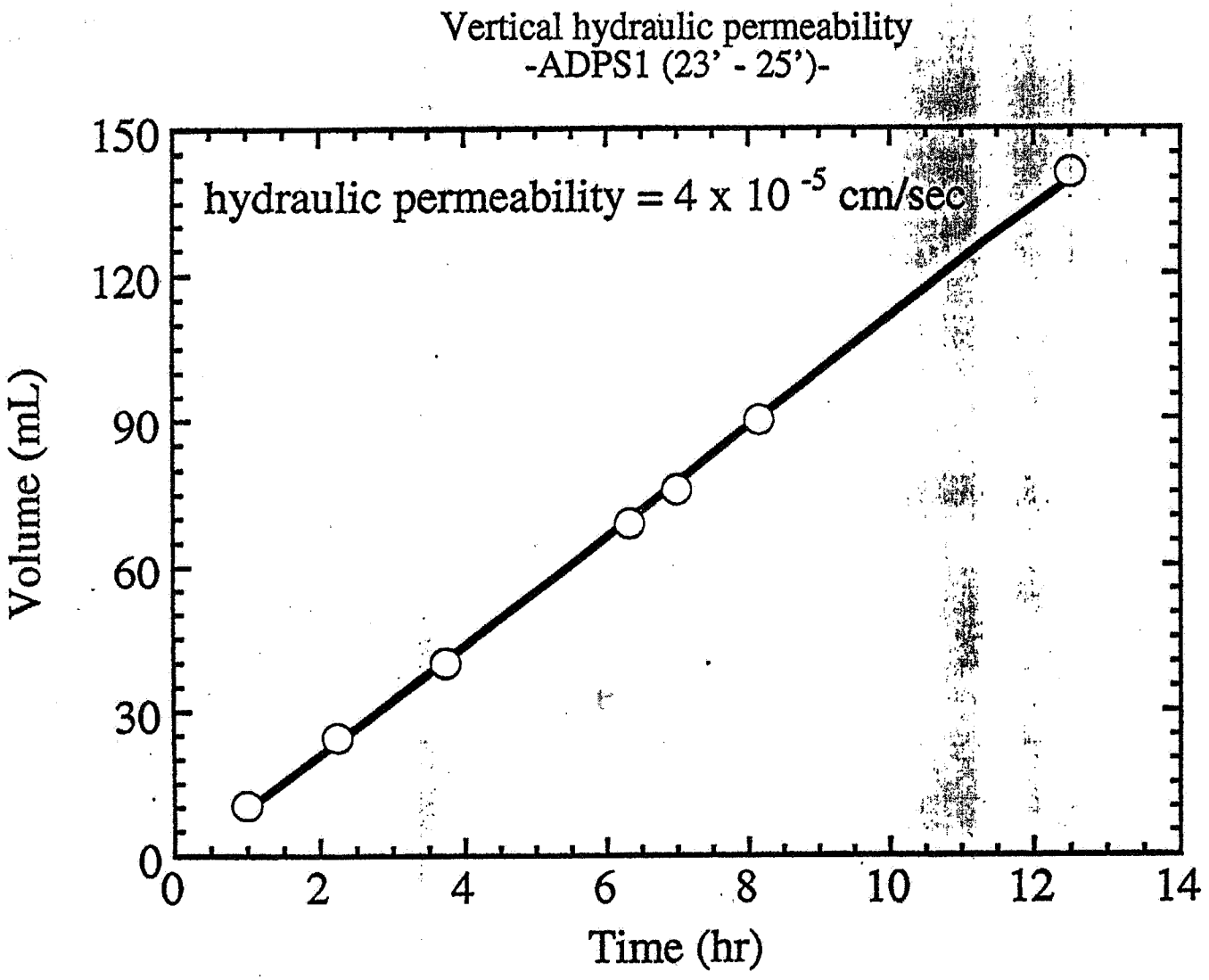

Figure 36. Soil permeability measurement by constant head permeameter.
Soil sample: ADSP1 (23' - 25').

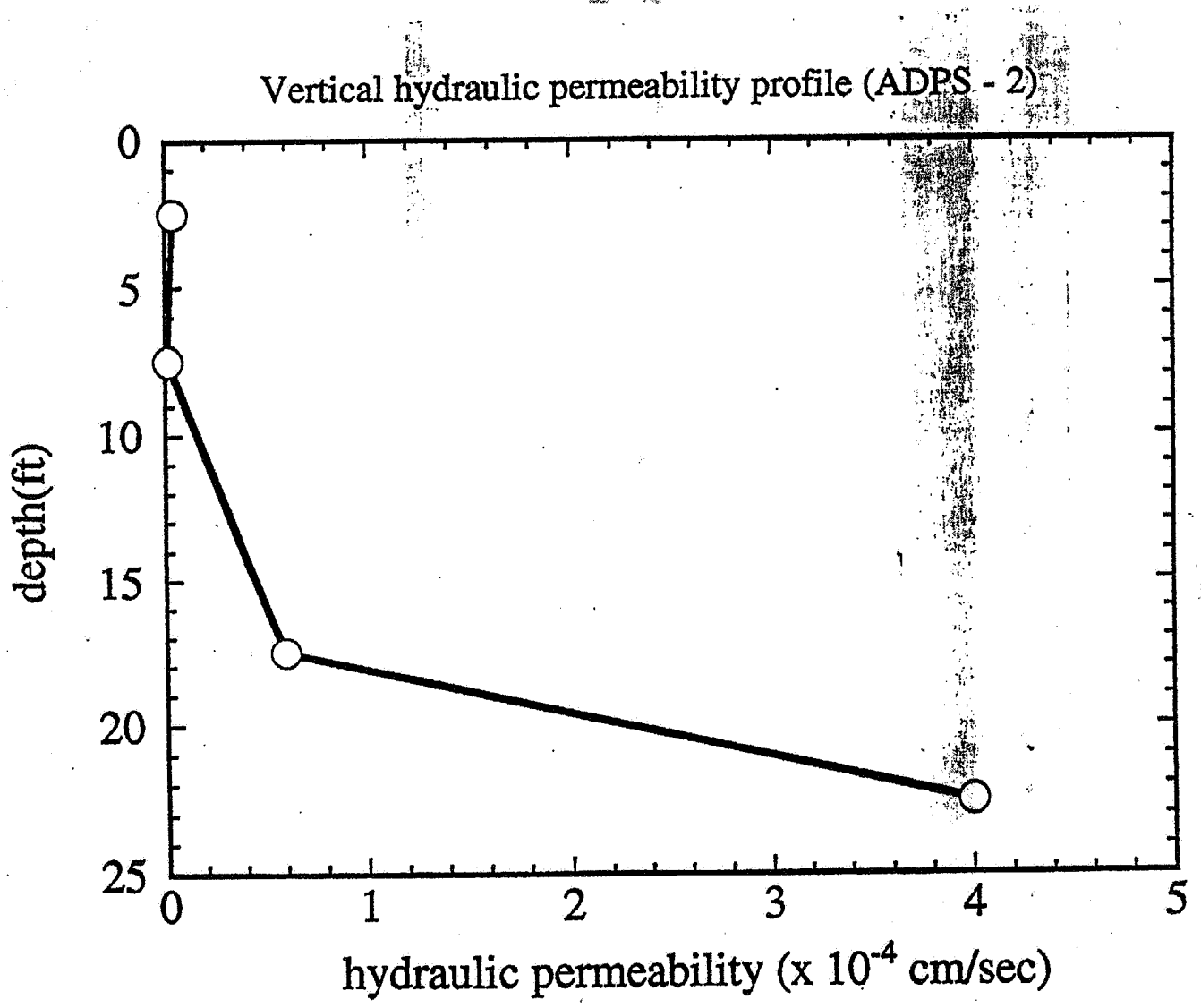

Figure 37. The hydraulic permeability profile for ADPS-2. The permeability is measured by constant head permeameter.

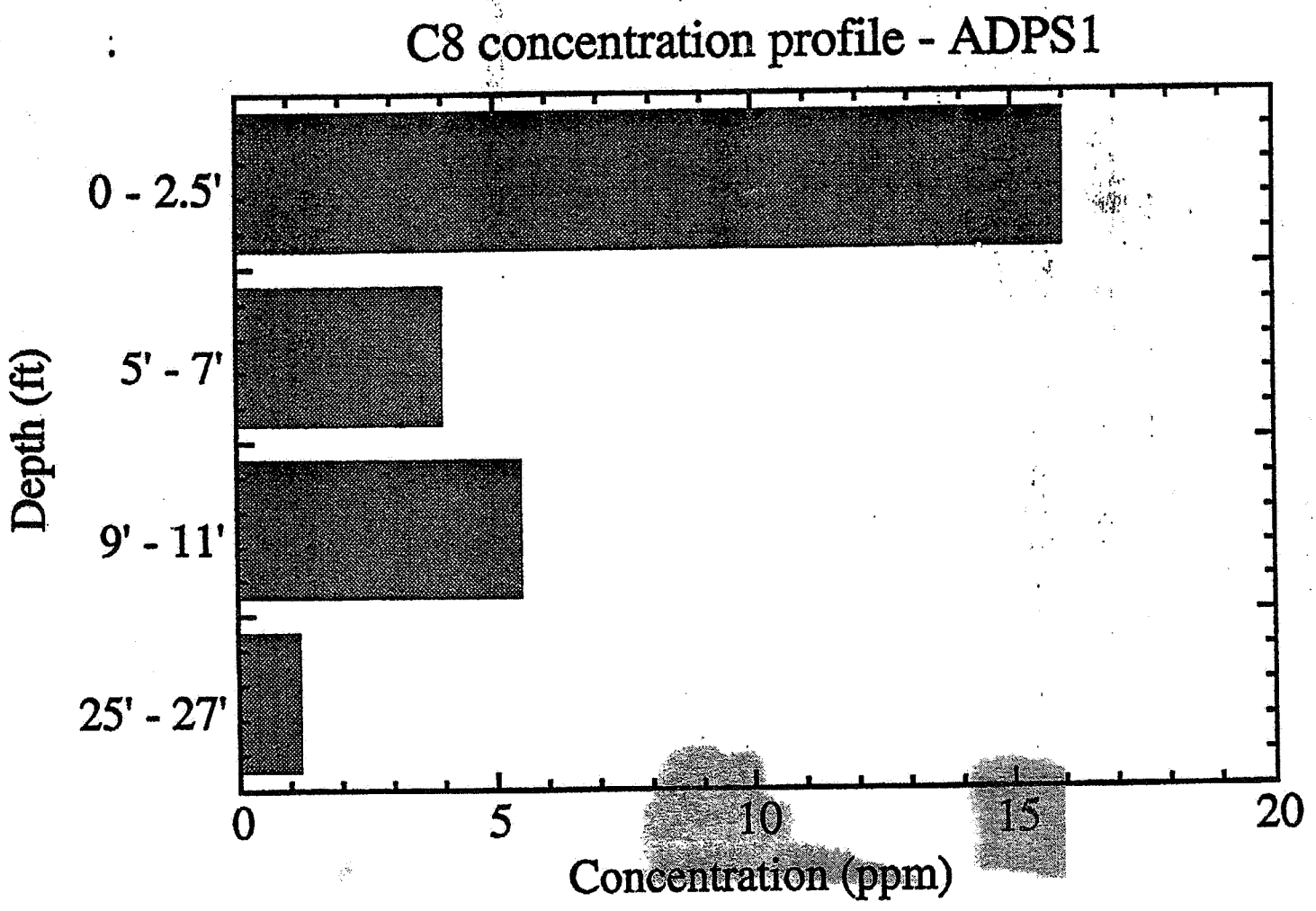

Figure 38. C8 concentration profile in ADPS-1 site.
Each data point is the average of triplicate.

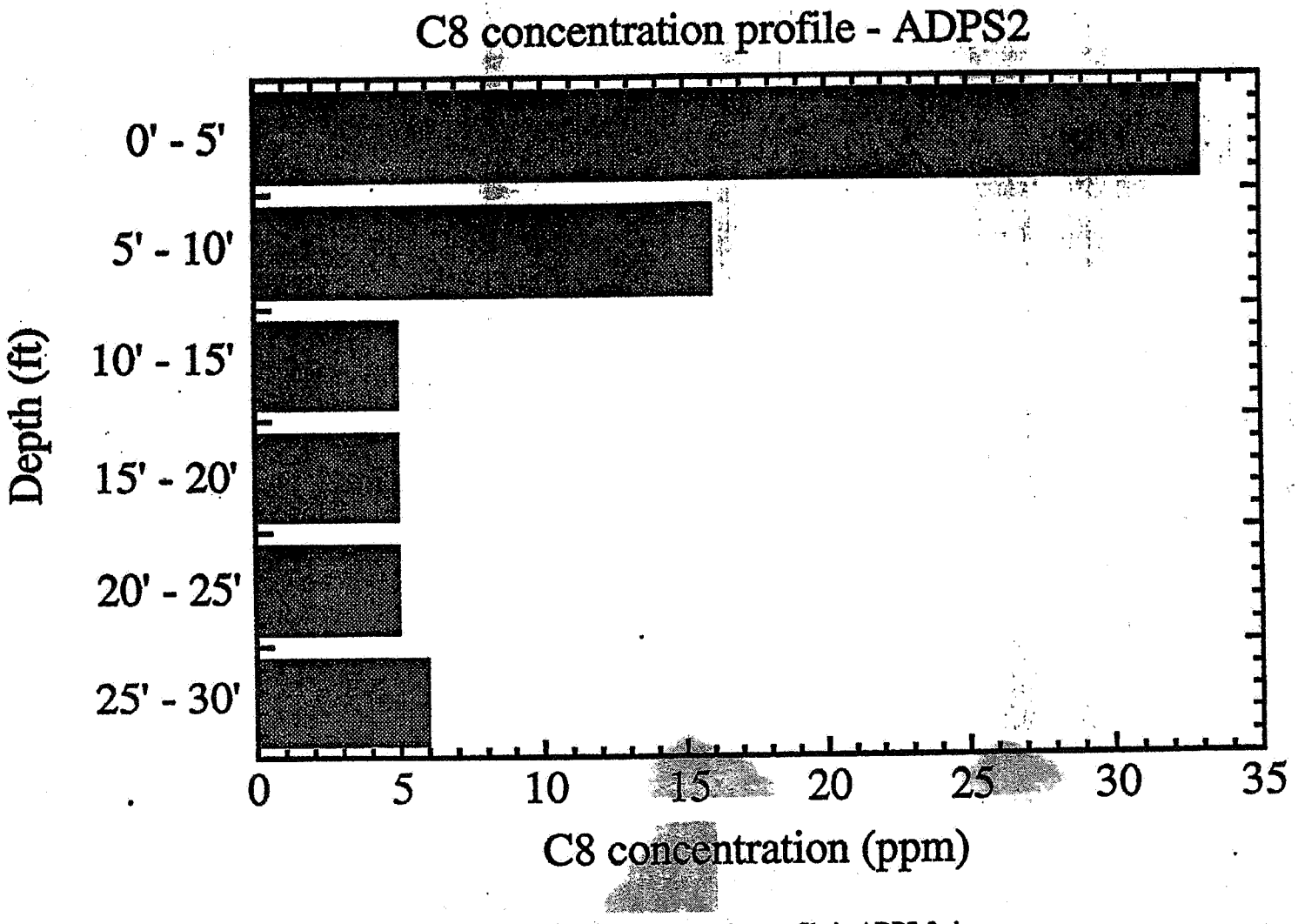

Figure 39. C8 concentration profile in ADPS-2 site.

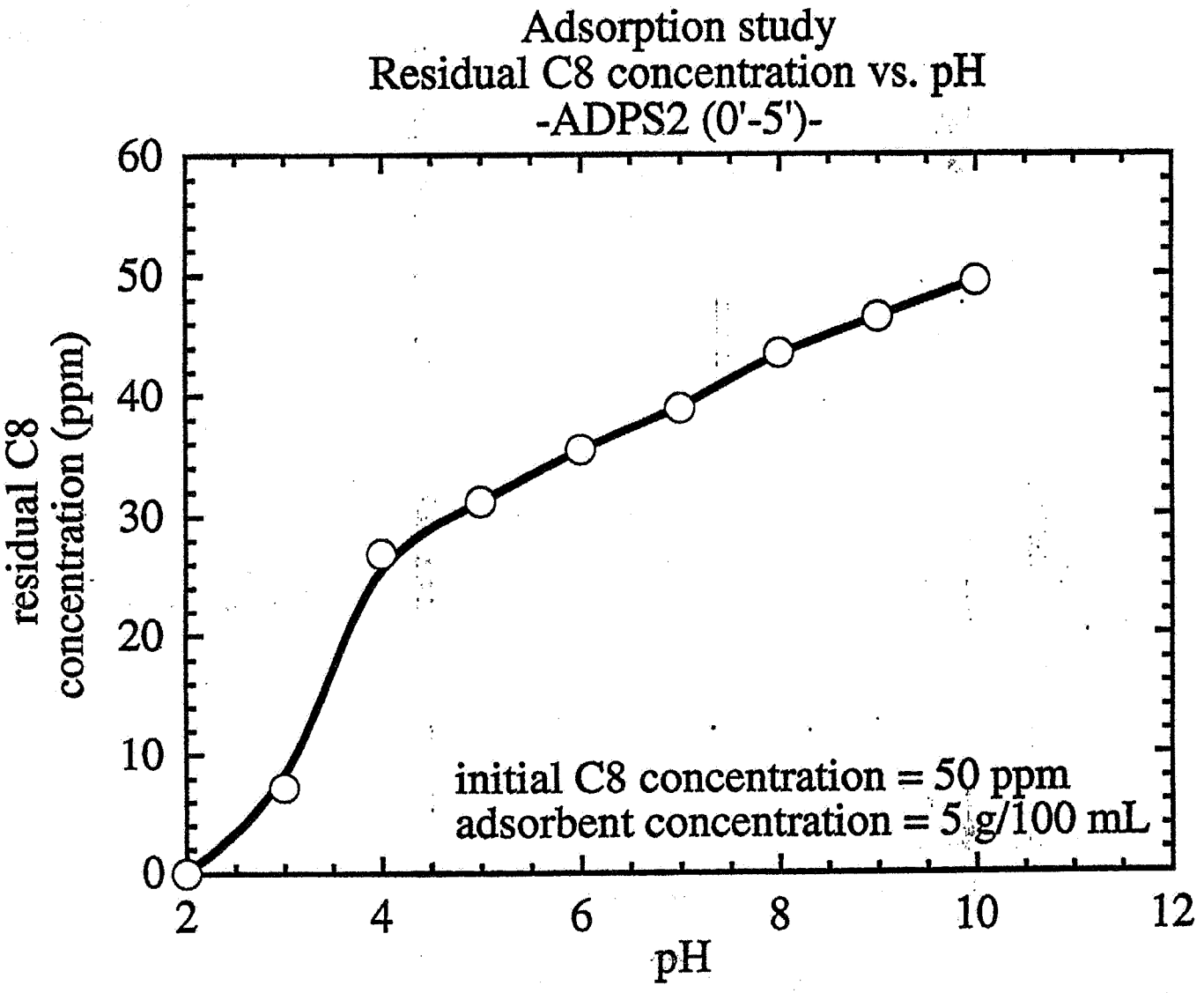

Figure 40. Residual C8 concentration as a function of pH.
Soil sample: ADPS2 (0'-5').
Experimental conditions: initial C8 concentration = 50 mg/L;
soil/water ratio = 0.05 g/mL; ionic strength = 0.1 M $NaClO_4$.

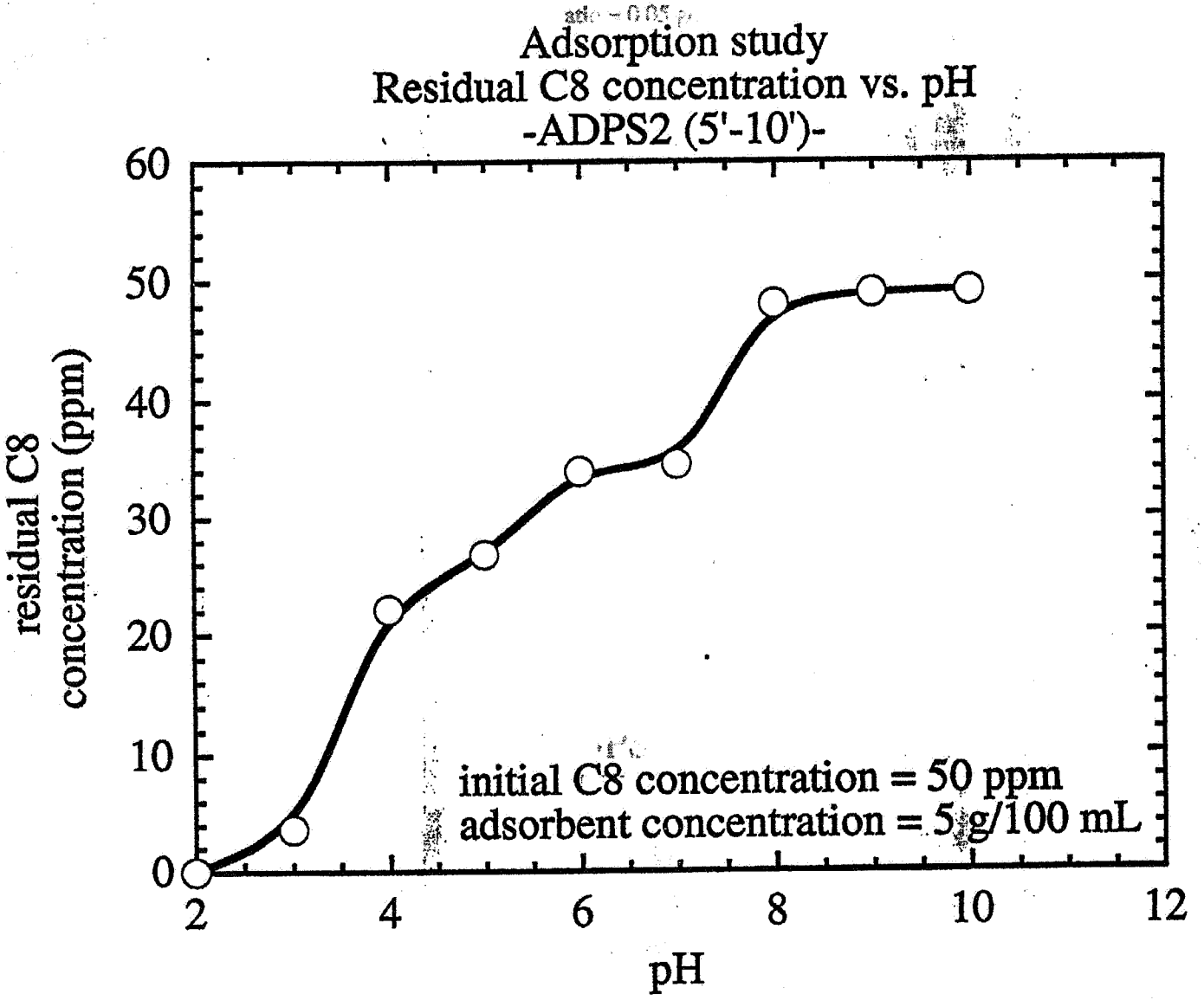

Figure 41. Residual C8 concentration as a function of pH.
Soil sample: ADPS2 (5'-10').
Experimental conditions are the same as in Figure 40.

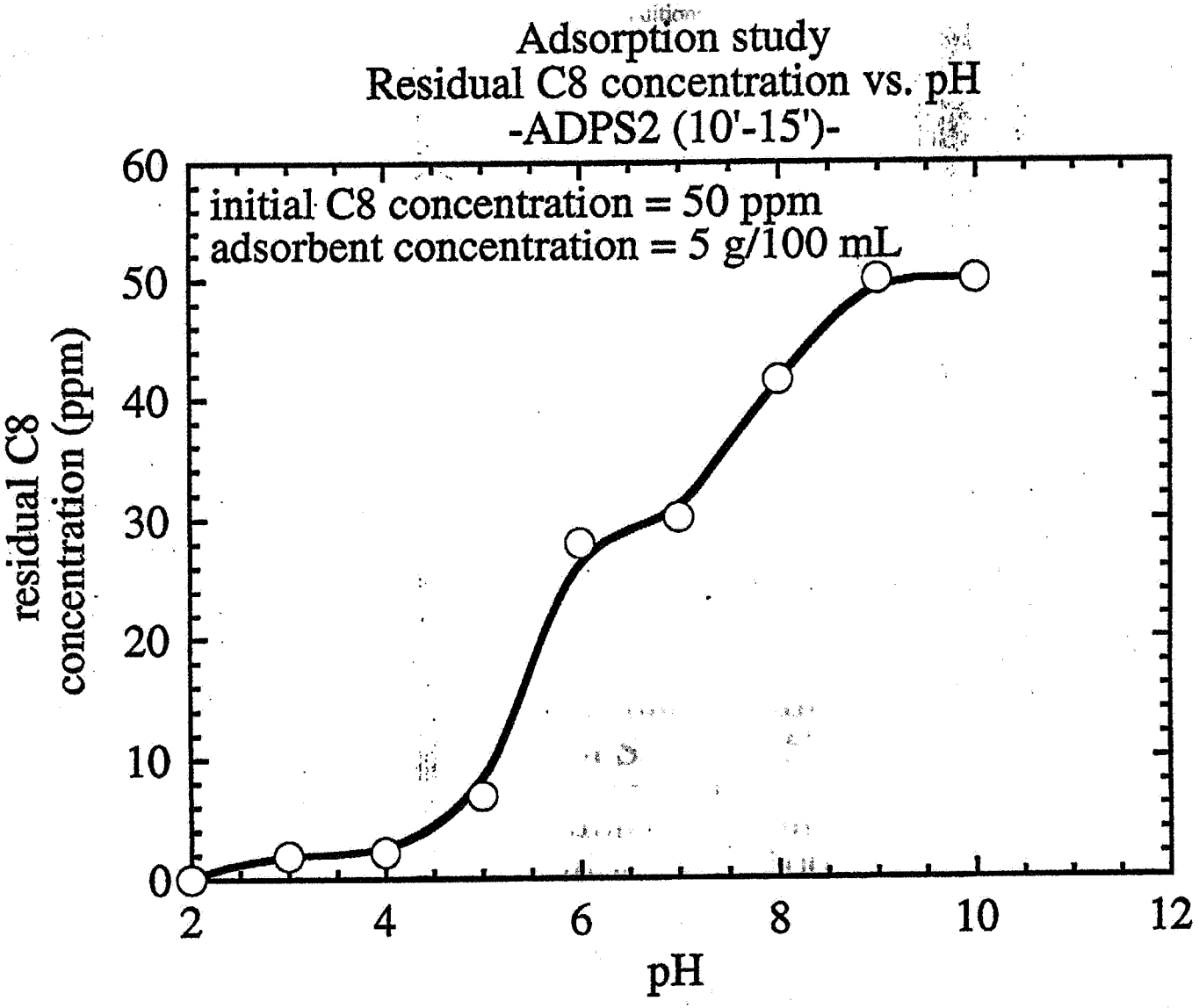

Figure 42. Residual C8 concentration as a function of pH.
Soil sample: ADPS2 (10'-15').
Experimental conditions are the same as in Figure 40.

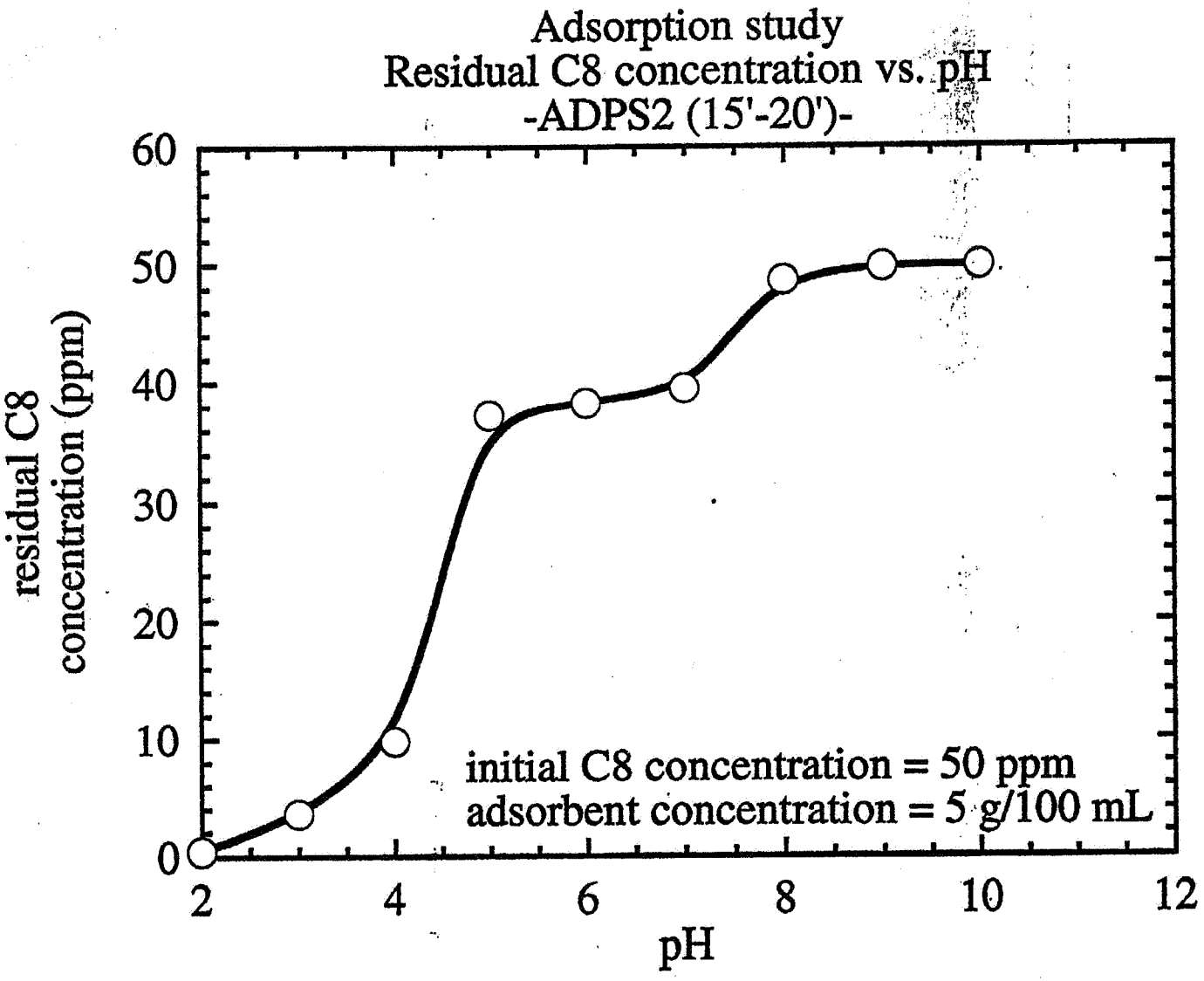

Figure 43. Residual C8 concentration as a function of pH.
Soil sample: ADPS2 (15'-20').
Experimental conditions are the same as in Figure 40.

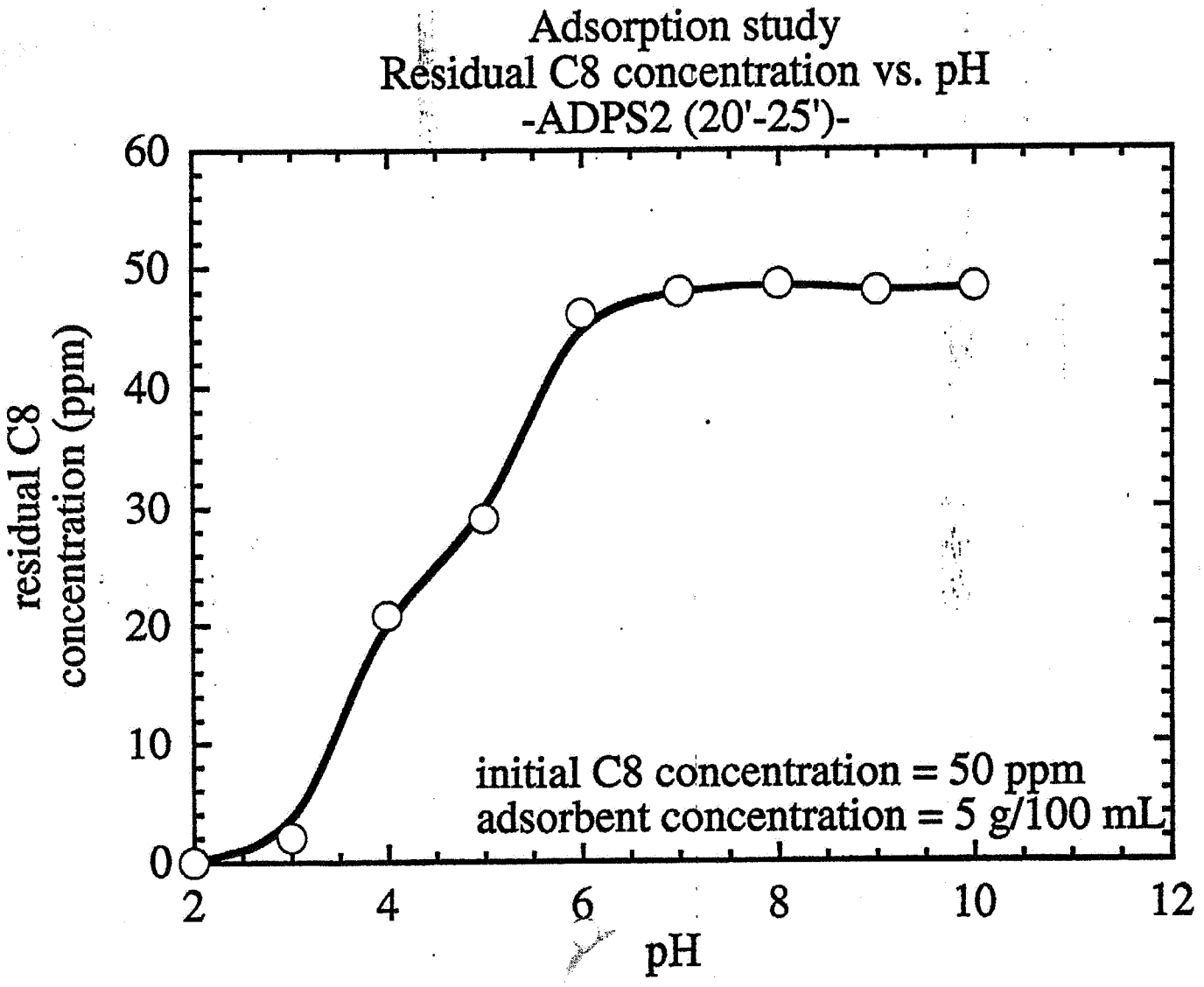

Figure 44. Residual C8 concentration as a function of pH.
Soil sample: ADPS2 (20'-25').
Experimental conditions are the same as in Figure 40.

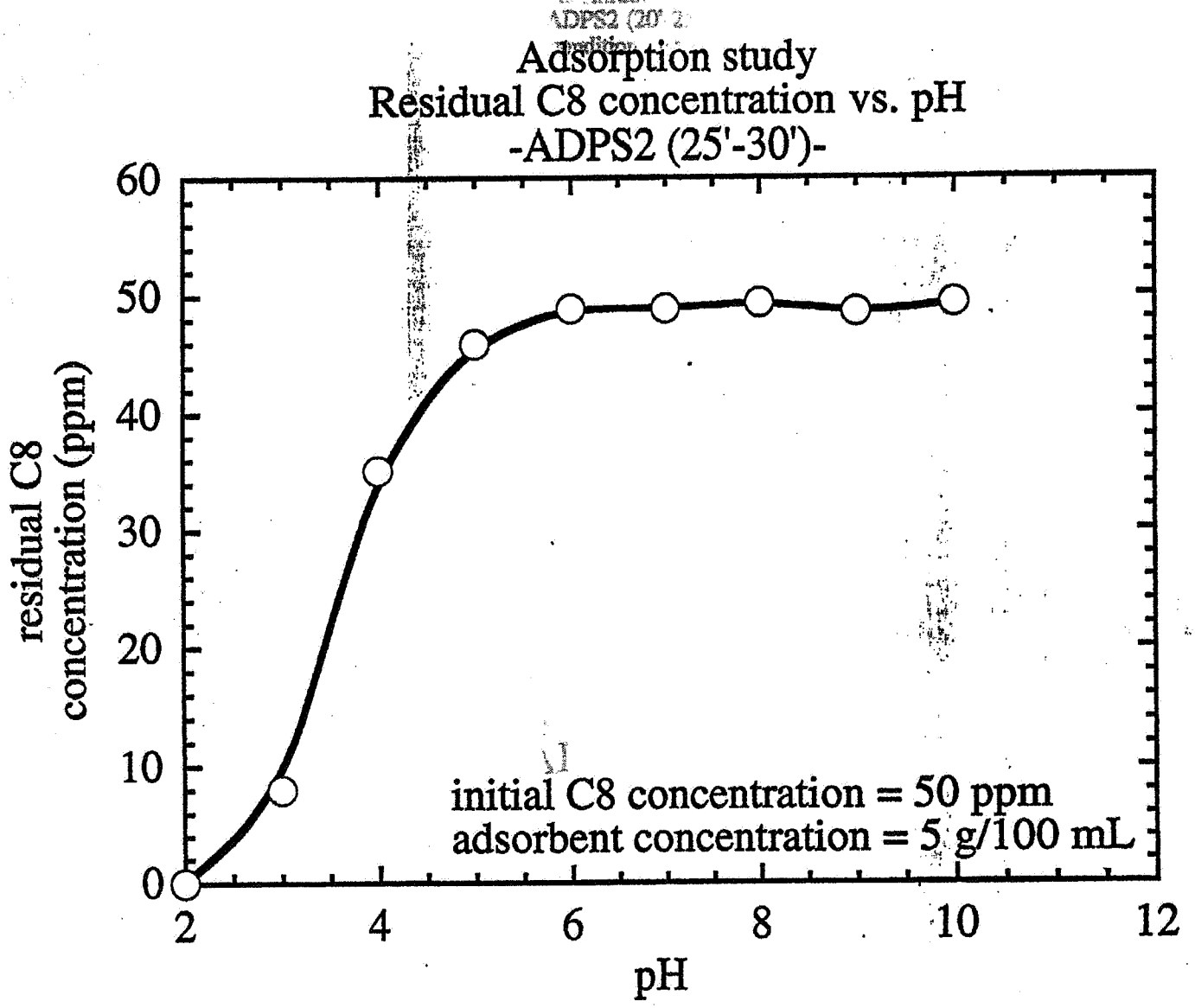

Figure 45. Residual C8 concentration as a function of pH.
Soil sample: ADPS2 (25'-30').
Experimental conditions are the same as in Figure 40.

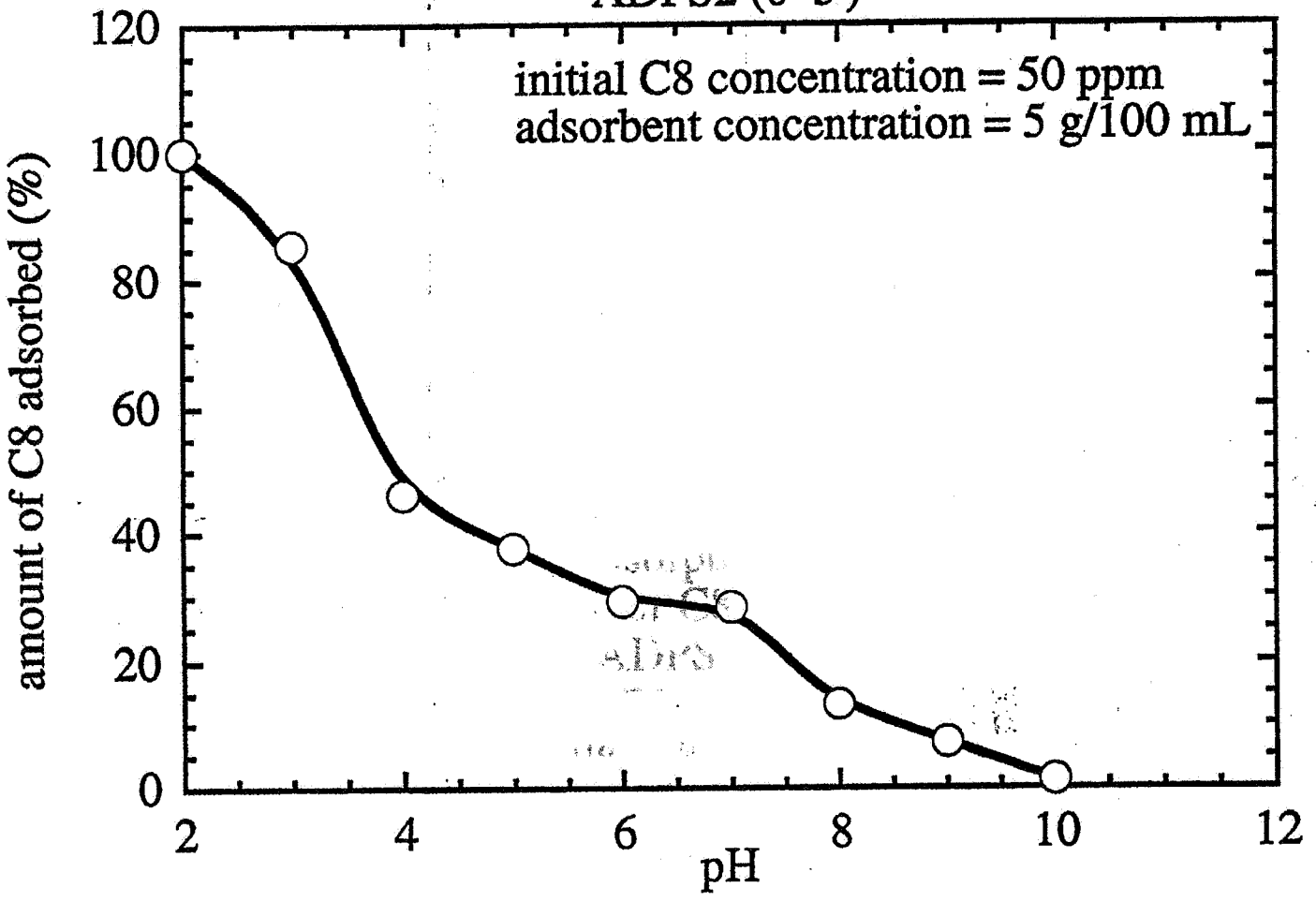

Figure 46. Percentage of C8 adsorbed as a function of pH.
Soil sample: ADPS2 (0'-5').
Experimental conditions: initial C8 concentration = 50 mg/L;
soil/water ratio = 0.05 g/mL; ionic strength = 0.1 M $NaClO_4$.

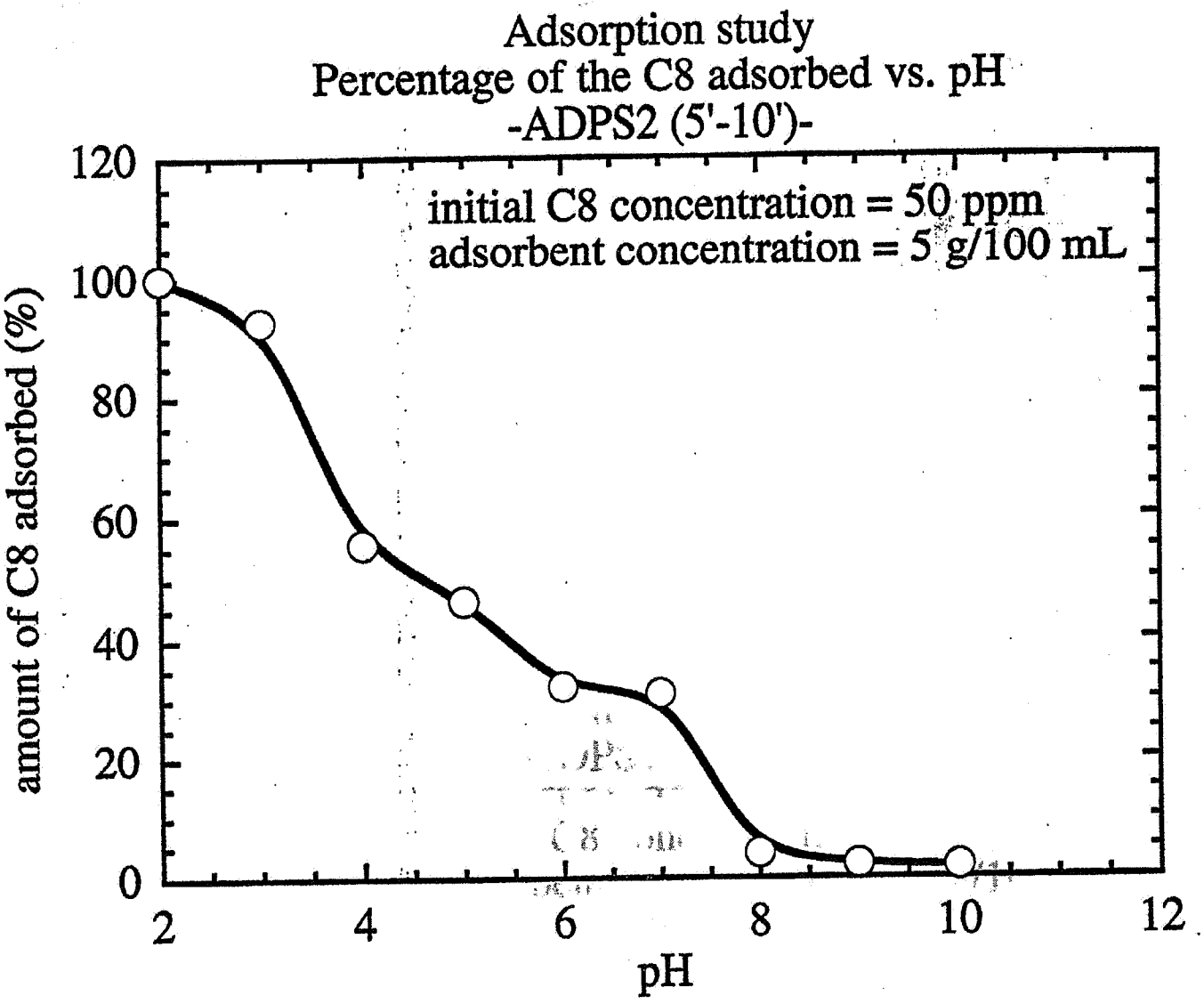

Figure 47. Percentage of C8 adsorbed as a function of pH.
Soil sample: ADPS2 (5'-10').
Experimental conditions are the same as in Figure 46.

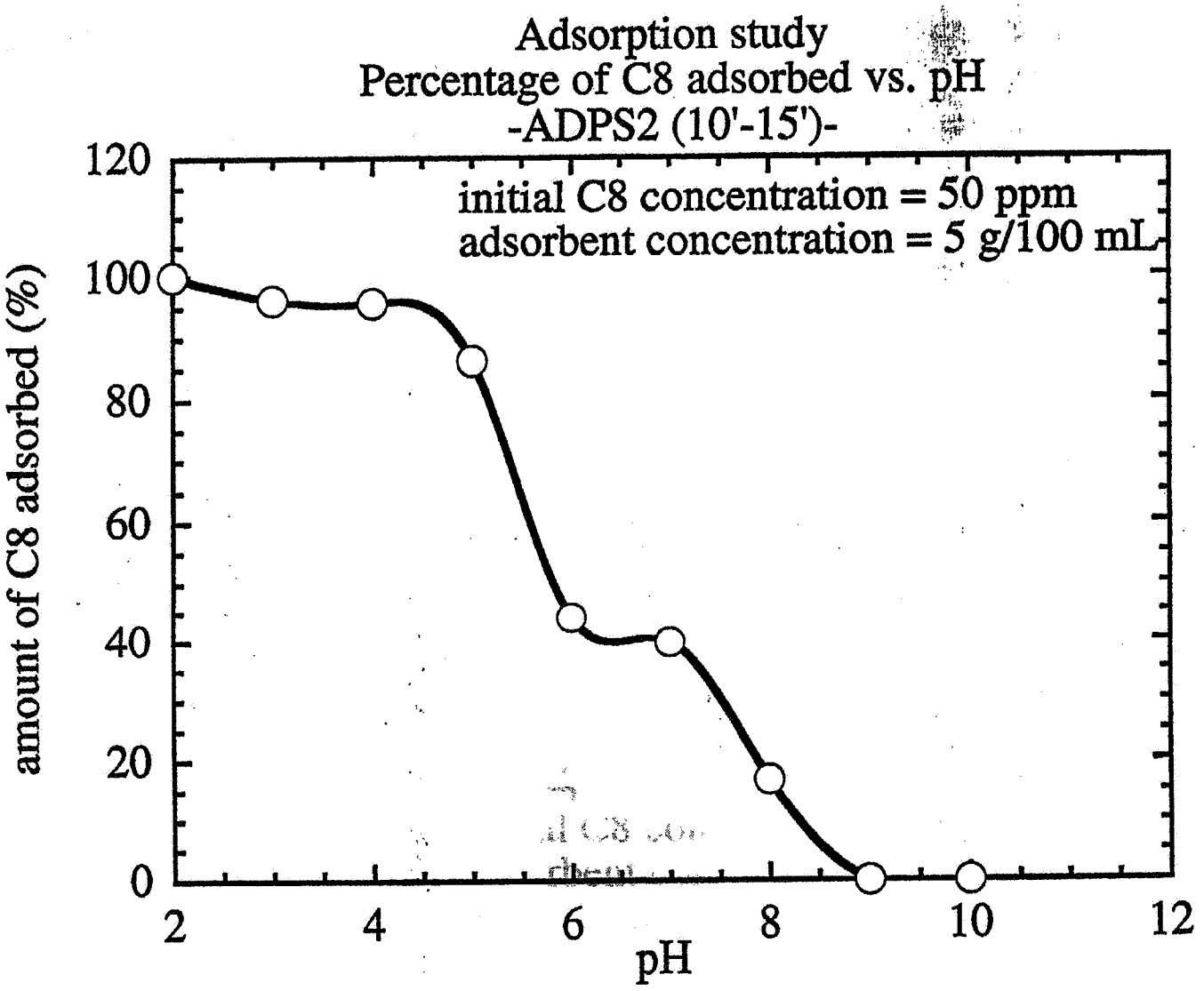

Figure 48. Percentage of C8 adsorbed as a function of pH.
Soil sample: ADPS2 (10'-15').
Experimental conditions are the same as in Figure 46.

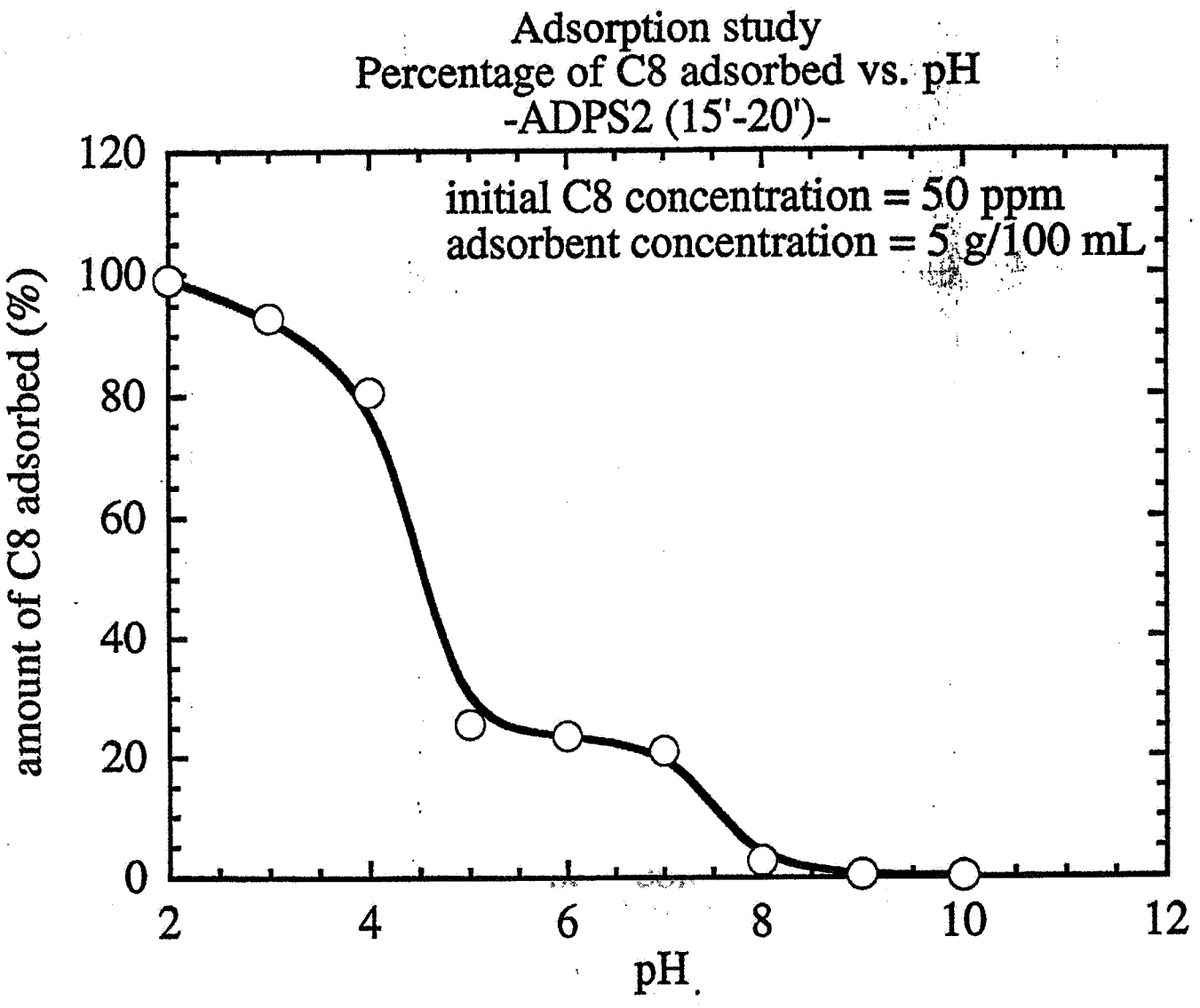

Figure 49. Percentage of C8 adsorbed as a function of pH.
Soil sample: ADPS2 (15'-20').
Experimental conditions are the same as in Figure 46.

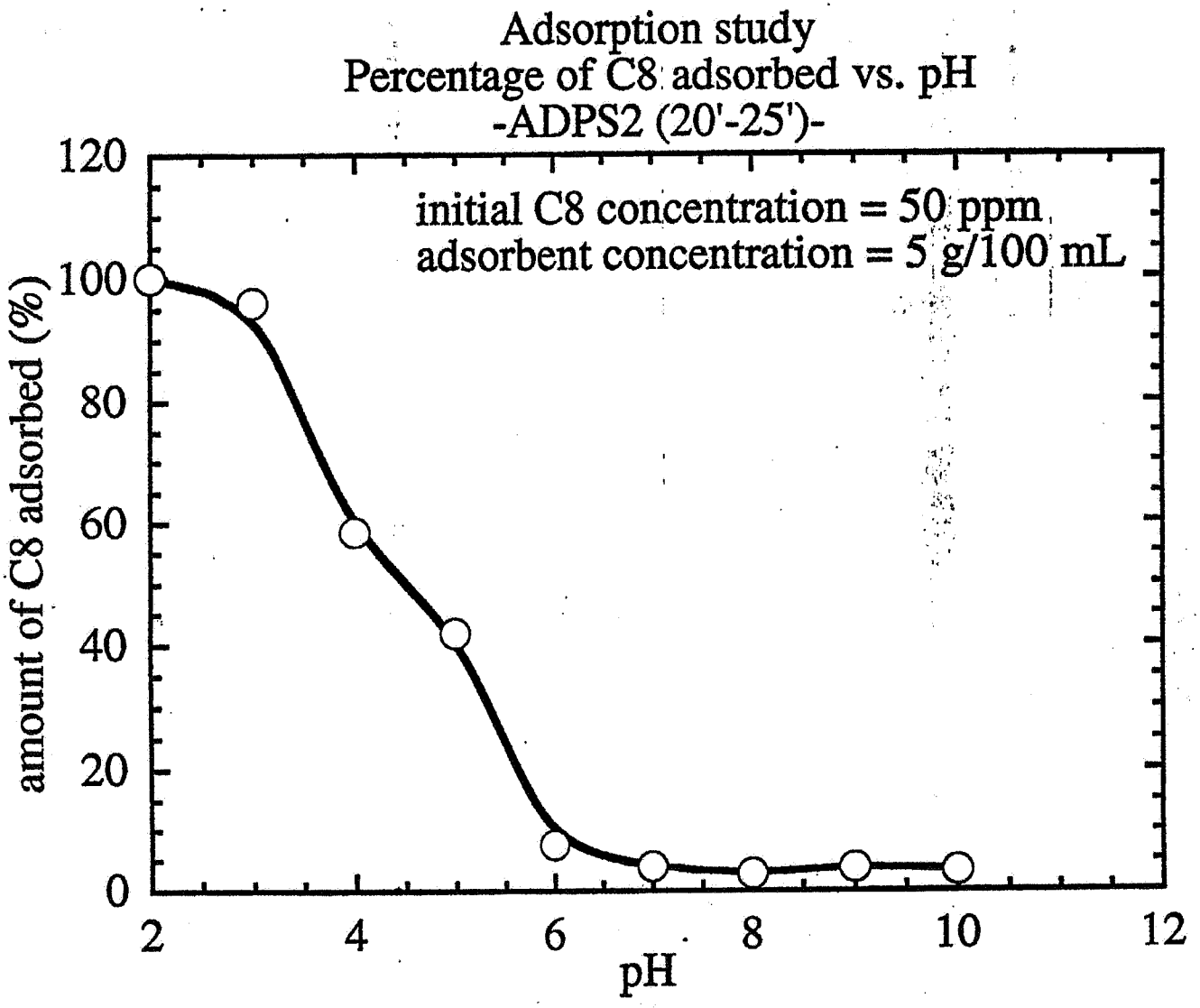

Figure 50. Percentage of C8 adsorbed as a function of pH.
Soil sample: ADPS2 (20'-25').
Experimental conditions are the same as in Figure 46.

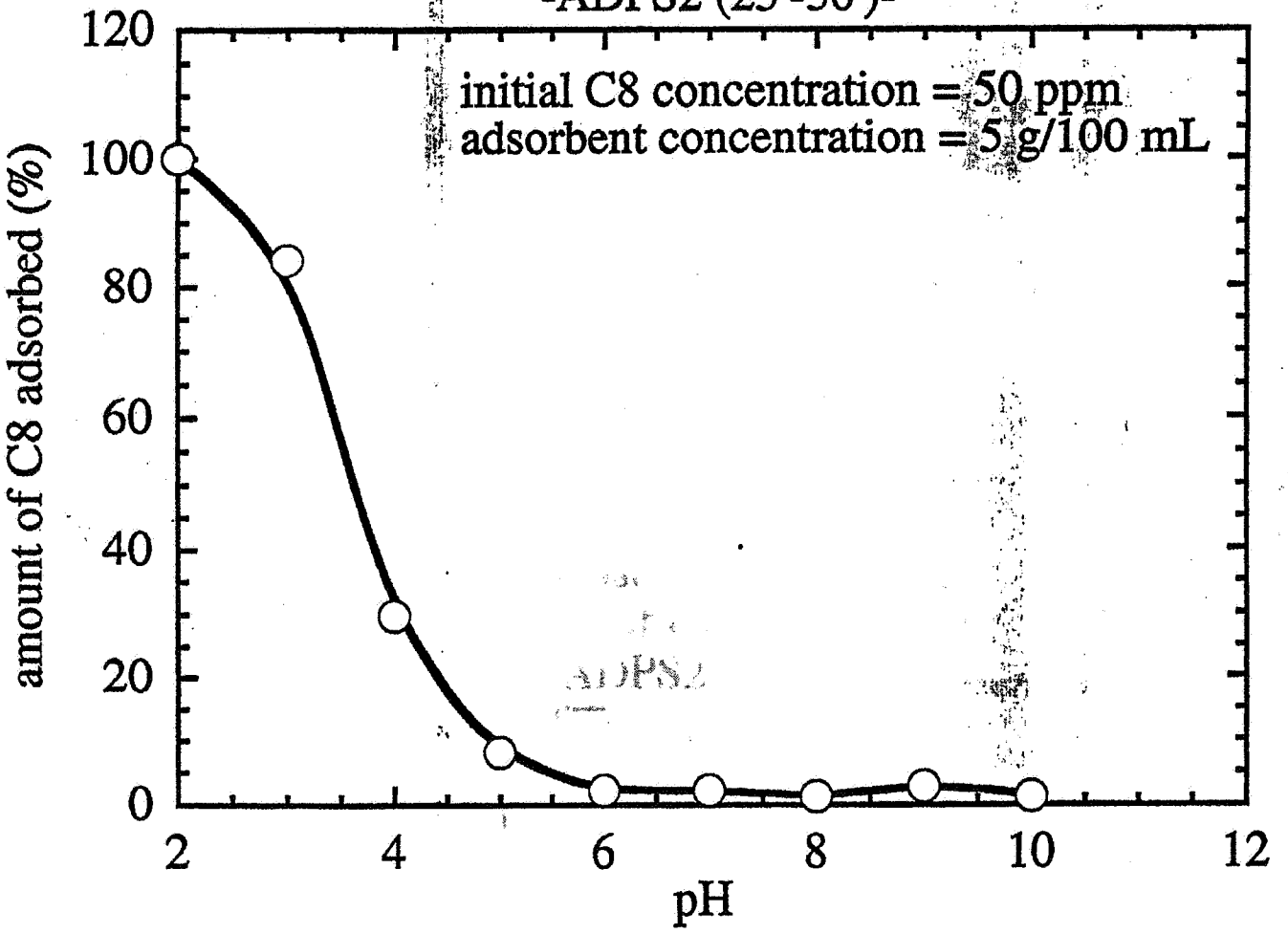

Figure 51. Percentage of C8 adsorbed as a function of pH.
Soil sample: ADPS2 (25'-30').
Experimental conditions are the same as in Figure 46.

Equilibrium diagram of C8 species

$$C_7F_{15}COOH \longrightarrow C_7F_{15}COO^- + H^+ \qquad pKa = 2.9$$

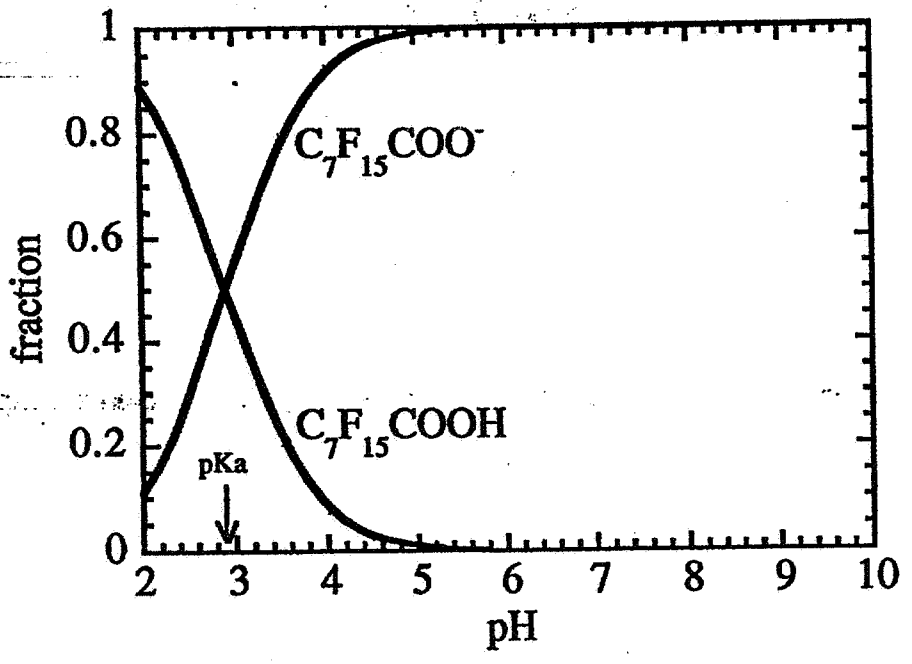

Figure 52. Equilbrium diagram of C8 species.

ASH010722

$$\overline{SOH}_2^+ \leftrightarrow \overline{SOH} + H^+ \qquad K_{a1}^{int}$$

$$\overline{SOH} \leftrightarrow \overline{SO}^- + H^+ \qquad K_{a2}^{int}$$

$$pH_{ZPC} = \frac{1}{2}(pK_{a1}^{int} + pK_{a2}^{int})$$

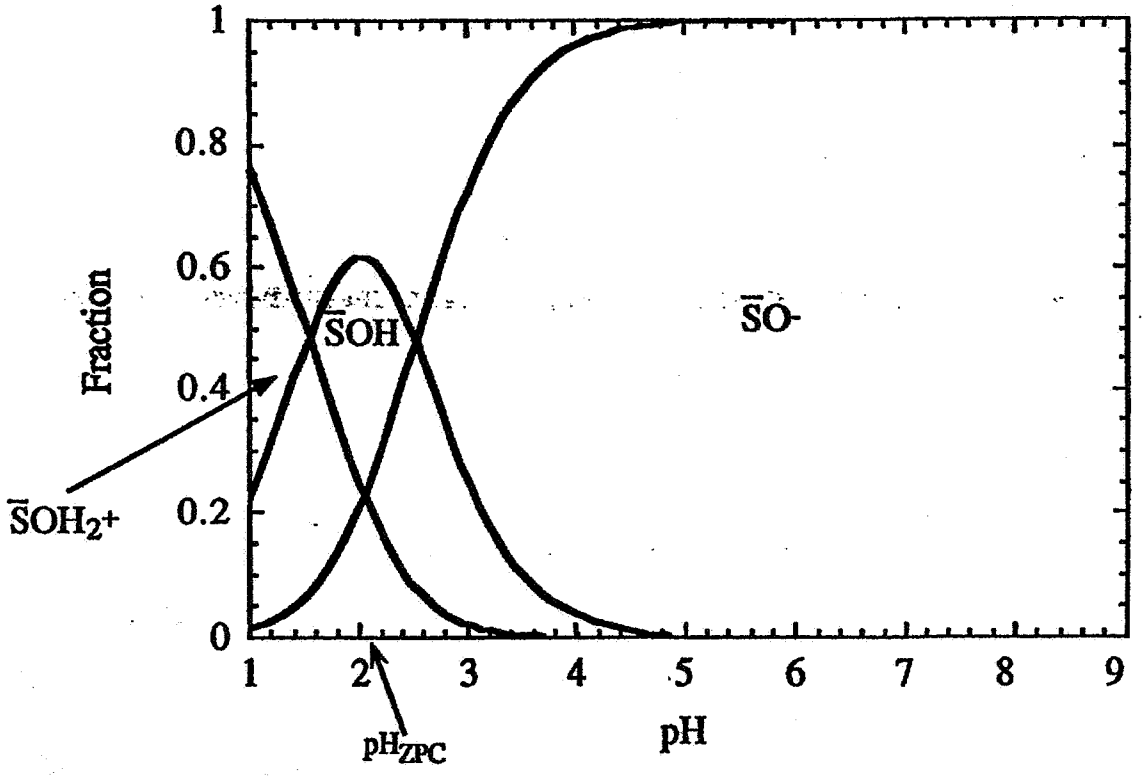

ASH010723

Figure 53. The fraction of protonated species vs. pH.

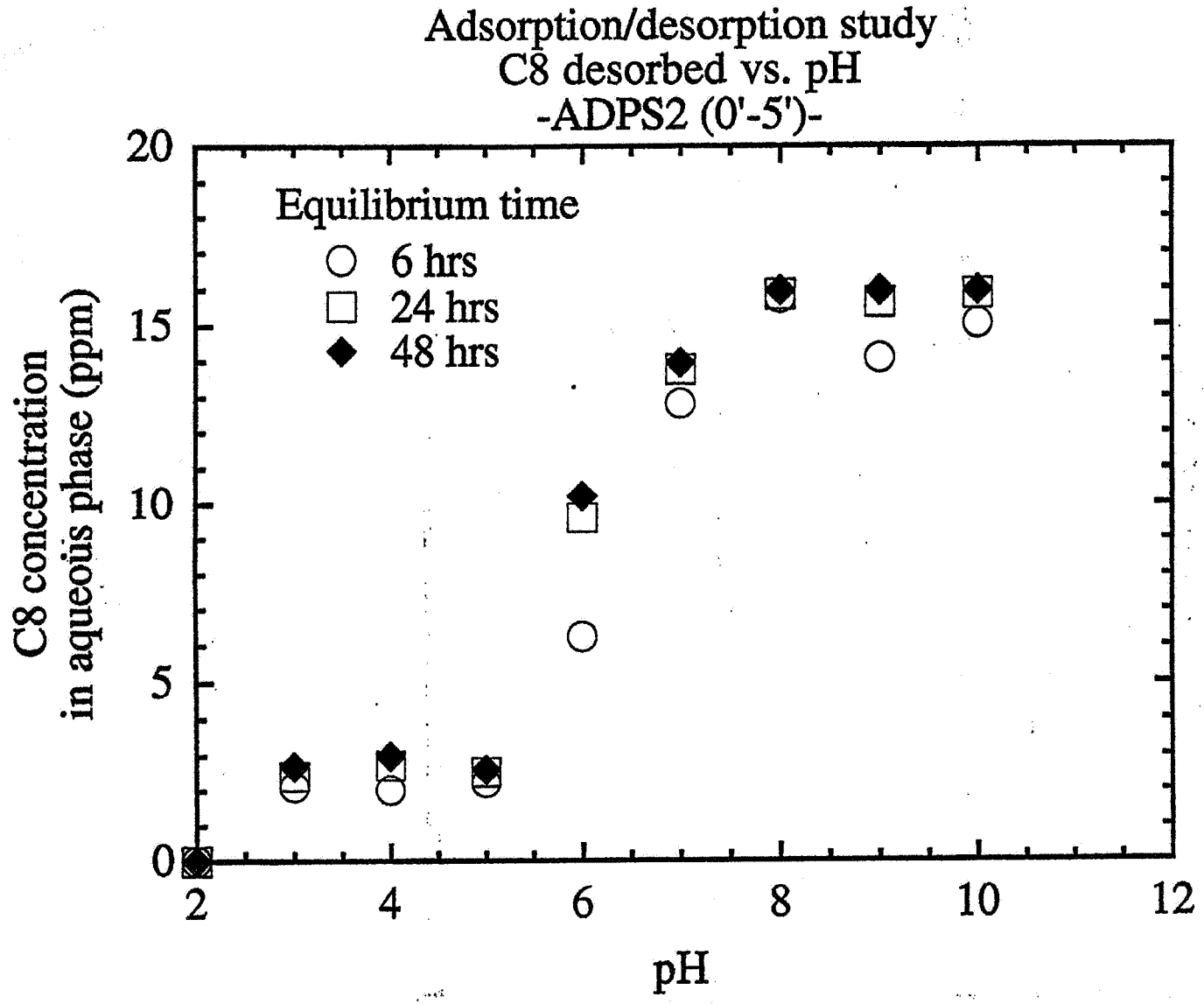

Figure 54a. The amount of C8 desorbed from ADPS2 (0' - 5') vs. pH.
Experimental conditions: initial C8 concentration in solid phase = 1.0 mg/g;
soil/water ratio = 0.05 g/mL; ionic strength = 0.1 M $NaClO_4$.

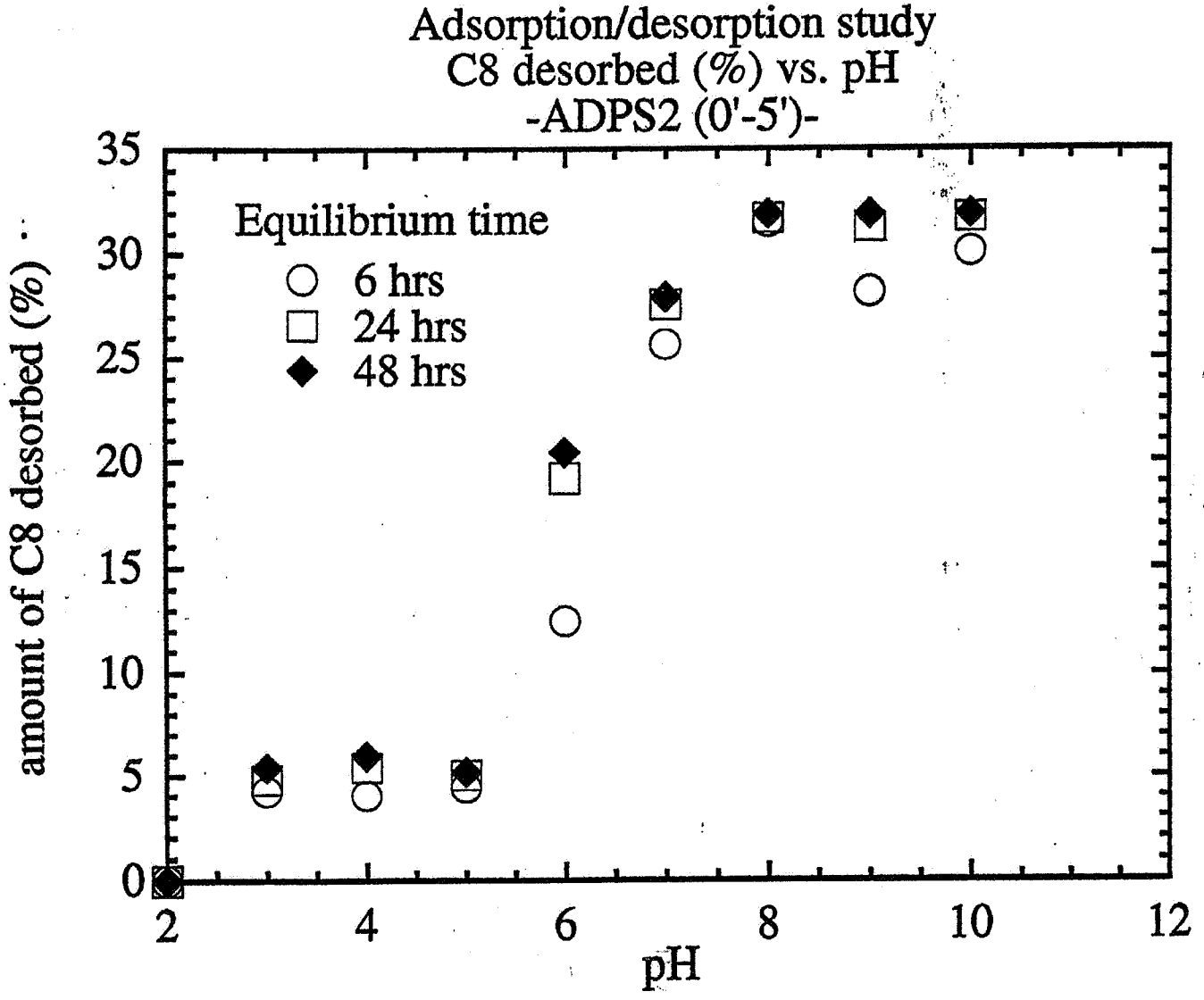

Figure 54b. The percentage of C8 desorption from ADPS2 (0' - 5') vs. pH.
Experimental conditions: initial C8 concentration in solid phase = 1.0 mg/g;
soil/water ratio = 0.05 g/mL; ionic strength = 0.1 M $NaClO_4$.

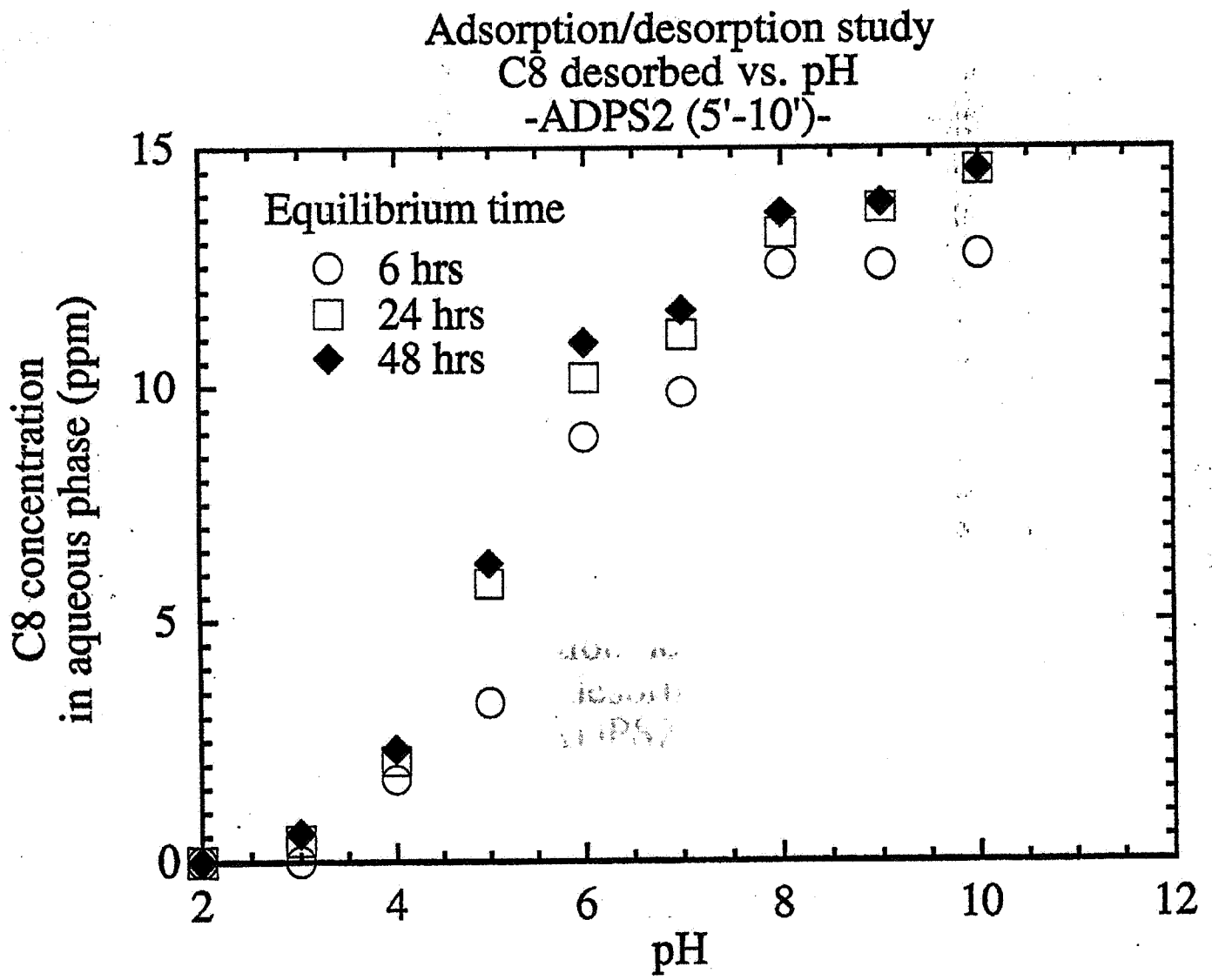

Figure 55a. The amount of C8 desorbed from ADPS2 (5' - 10') vs. pH.
Experimental conditions: initial C8 concentration in solid phase = 1.0 mg/g;
soil/water ratio = 0.05 g/mL; ionic strength = 0.1 M $NaClO_4$.

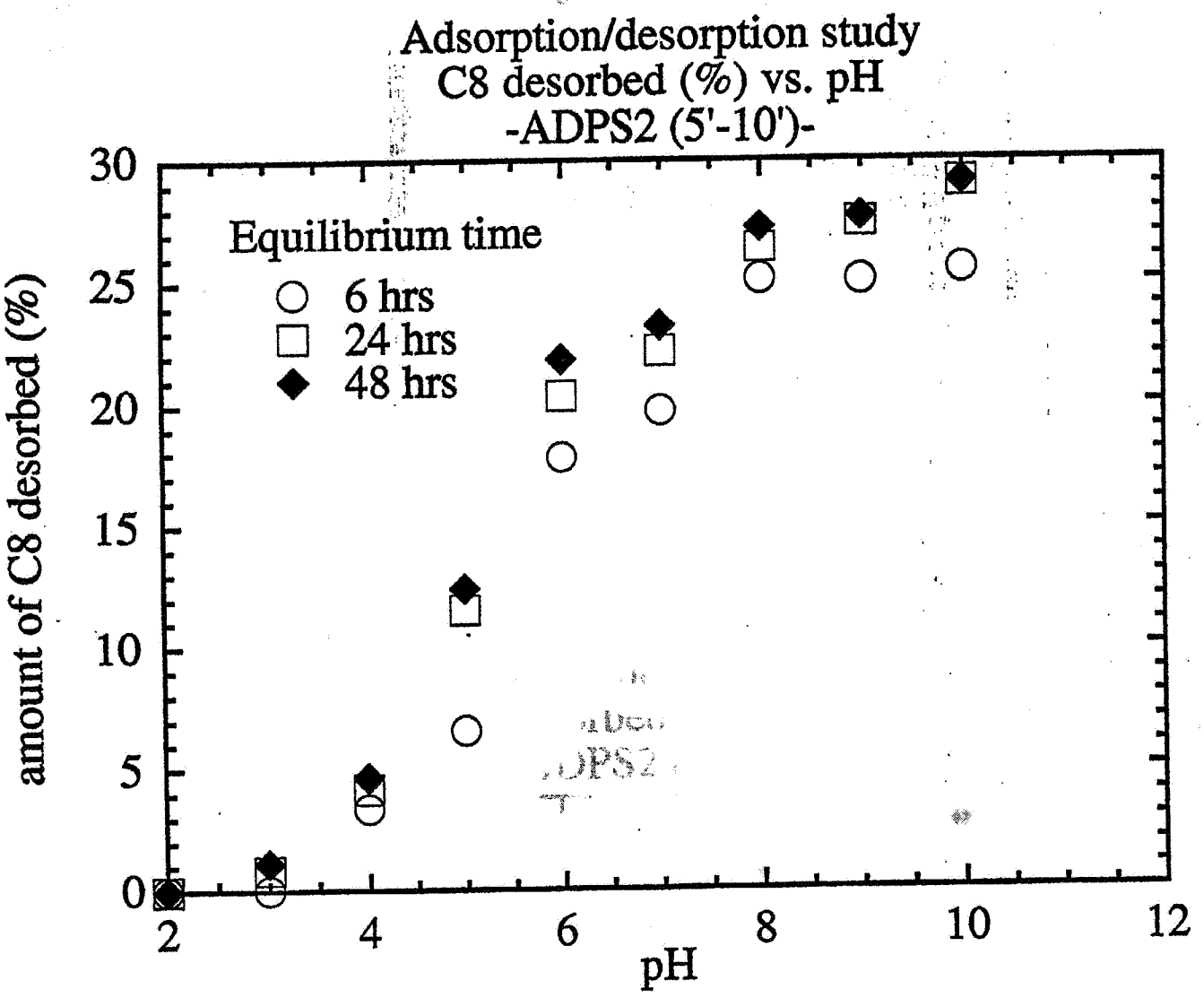

Figure 55b. The percentage of C8 desorption from ADPS2 (5' - 10') vs. pH. Experimental conditions: initial C8 concentration in solid phase = 1.0 mg/g; soil/water ratio = 0.05 g/mL; ionic strength = 0.1 M $NaClO_4$.

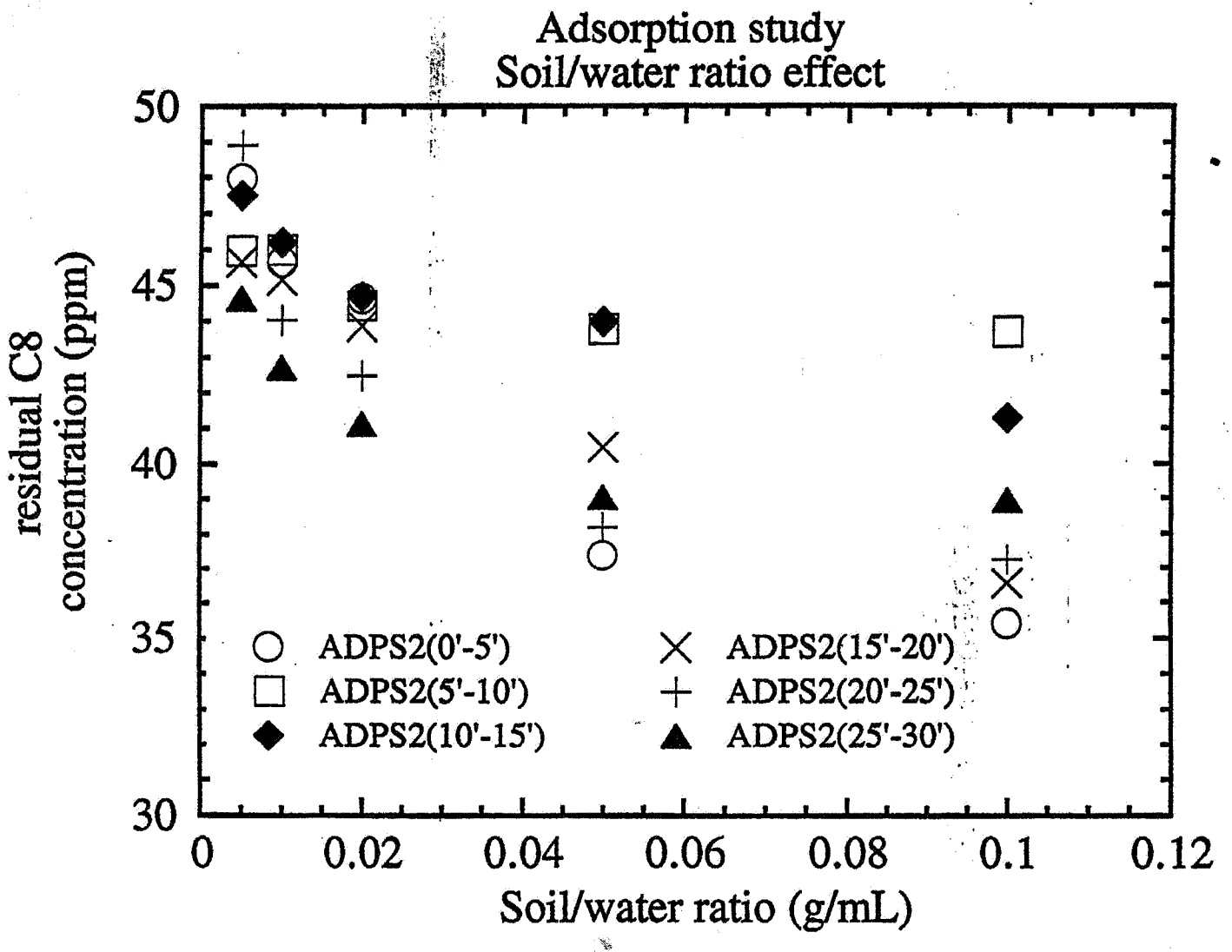

Figure 56. The soil water ratio effect on the C8 adsorption for six soil samples from the ADPS2 site
Experimental conditions: initial C8 concentration = 50 mg/L; pH =7.0; ionic strength = 0.1 M $NaClO_4$.

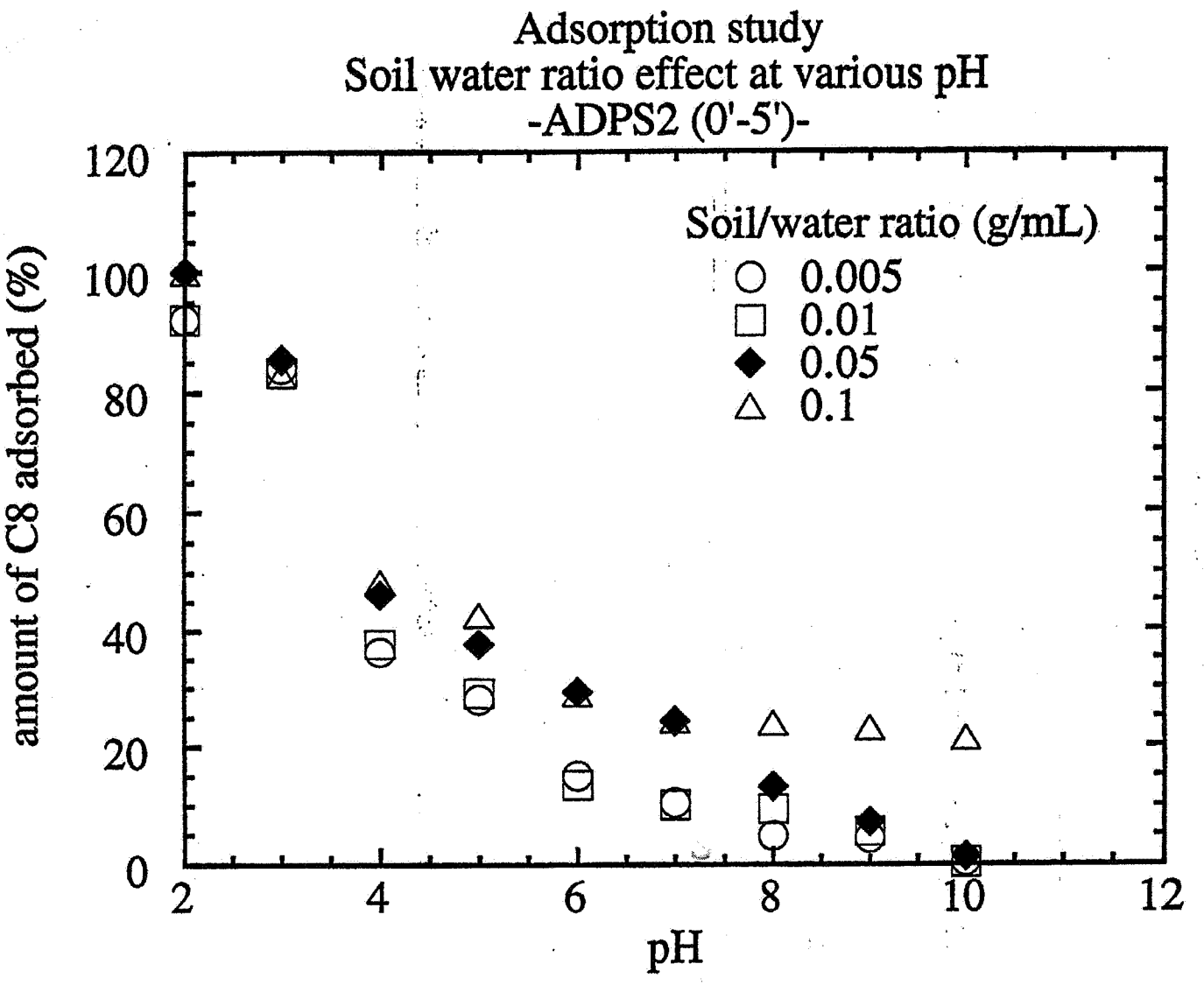

Figure 57. The soil water ratio effect on the C8 adsorption.
soil sample: ADPS2 (0' - 5').
Experimental conditions: initial C8 concentration = 50 mg/L;
ionic strength = 0.1 M $NaClO_4$.

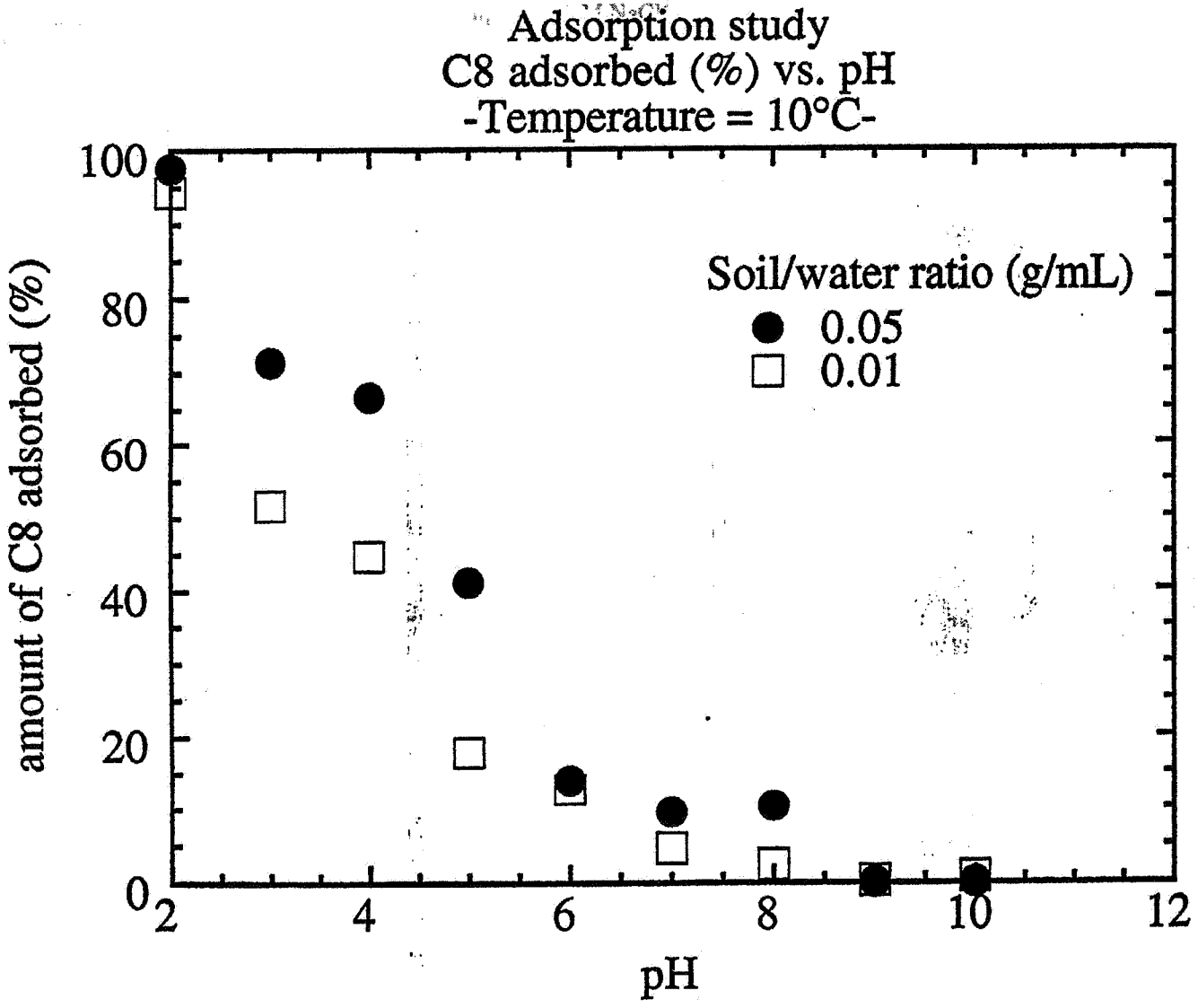

Figure 58. Percentage of C8 adsorbed as a function of pH.
Soil sample : ADPS2 (0' - 5').
Experimental conditions : initial C8 concentration = 50 mg/L;
Temperature = 10 °C; ionic strength = 0.1 M $NaClO_4$.

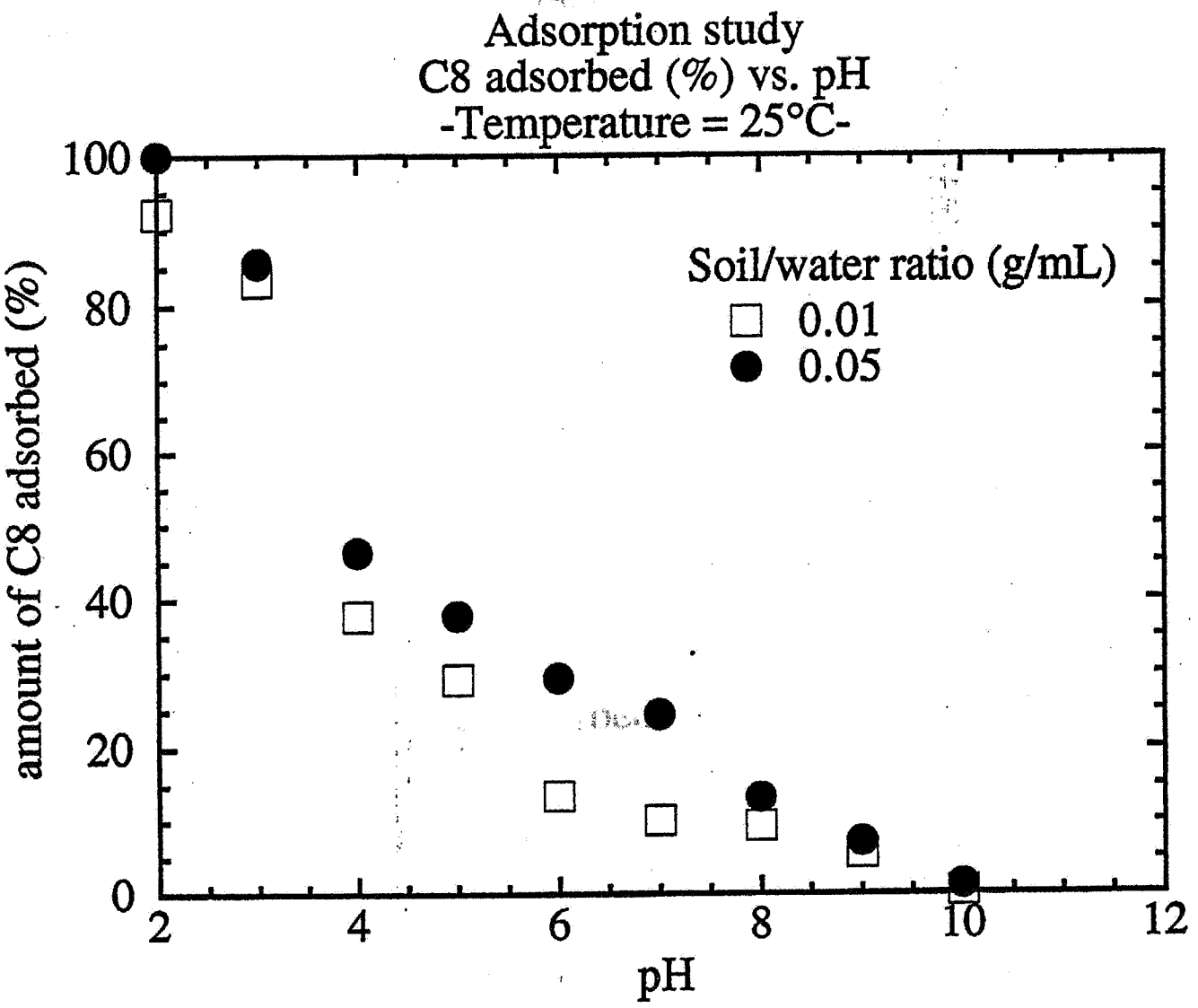

Figure 59. Percentage of C8 adsorbed as a function of pH.
Soil sample : ADPS2 (0' - 5').
Experimental conditions : initial C8 concentration = 50 mg/L;
Temperature = 25 °C; ionic strength = 0.1 M $NaClO_4$.

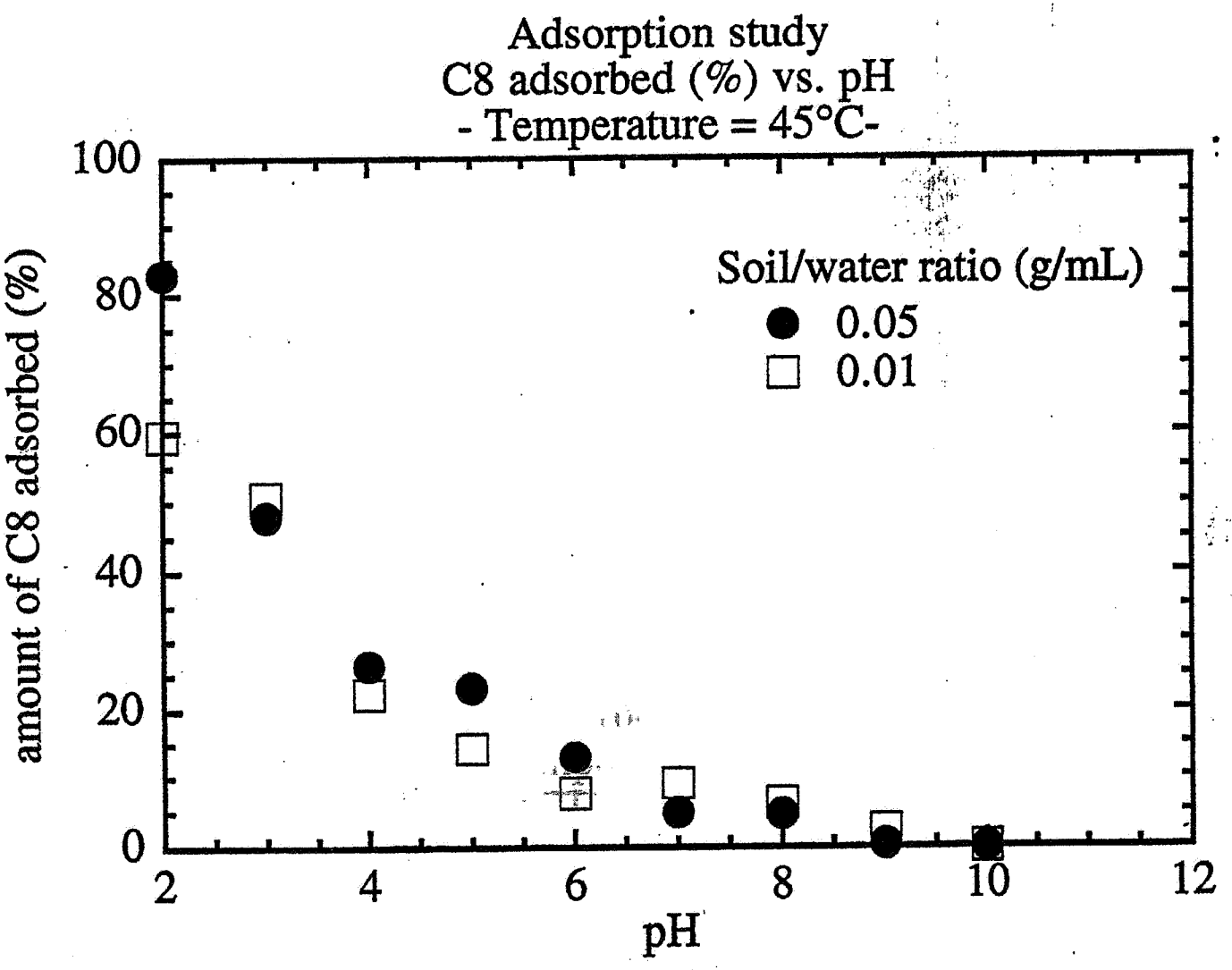

Figure 60. Percentage of C8 adsorbed as a function of pH.
Soil sample : ADPS2 (0' - 5').
Experimental conditions : initial C8 concentration = 50 mg/L;
Temperature = 45°C; ionic strength = 0.1 M $NaClO_4$.

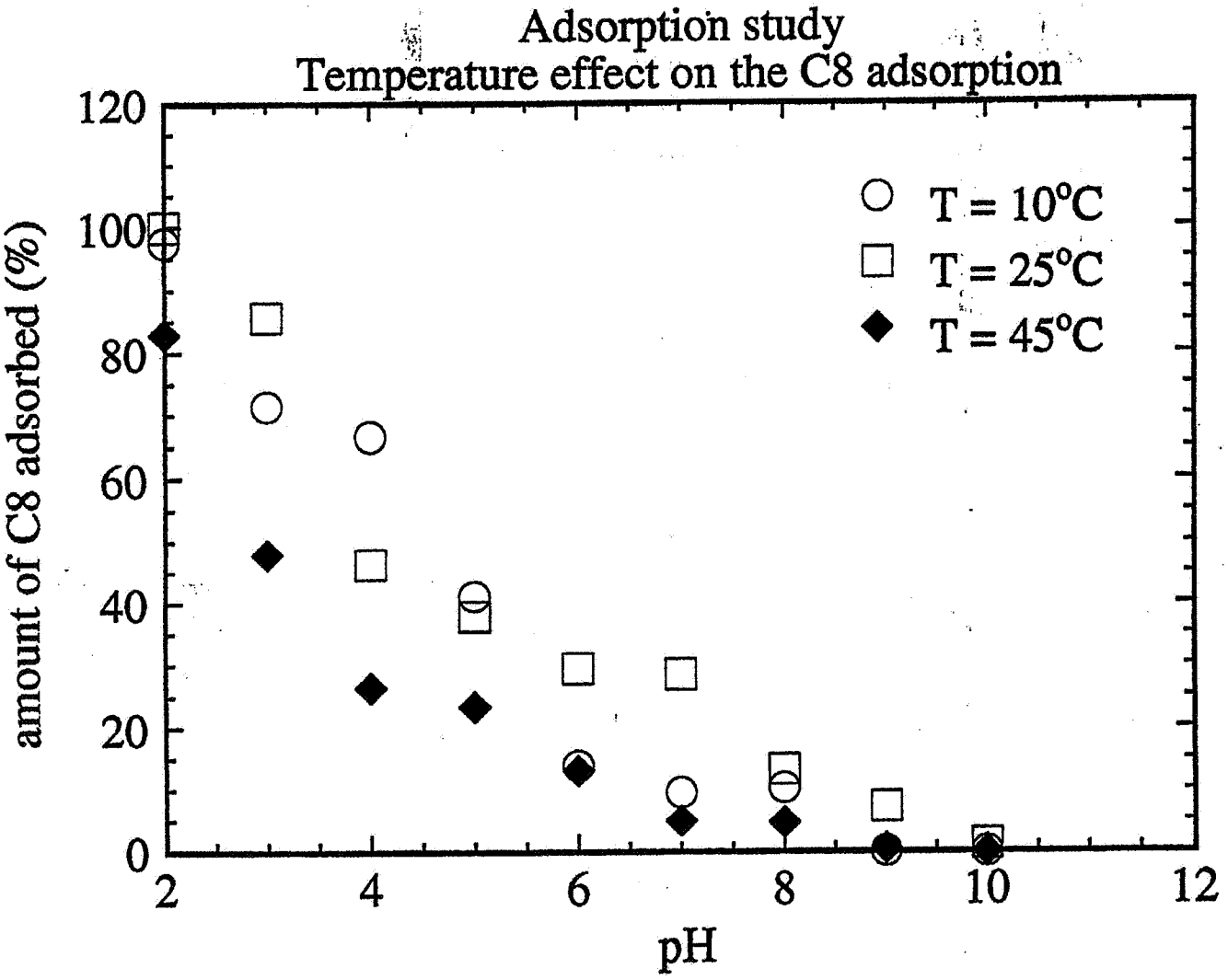

Figure 61. The temperature effect on the C8 adsorption.
Soil sample: ADPS2 (0'-5').
Experimental conditions: initial C8 concentration = 50 mg/L;
ionic strength = 0.1M $NaClO_4$.

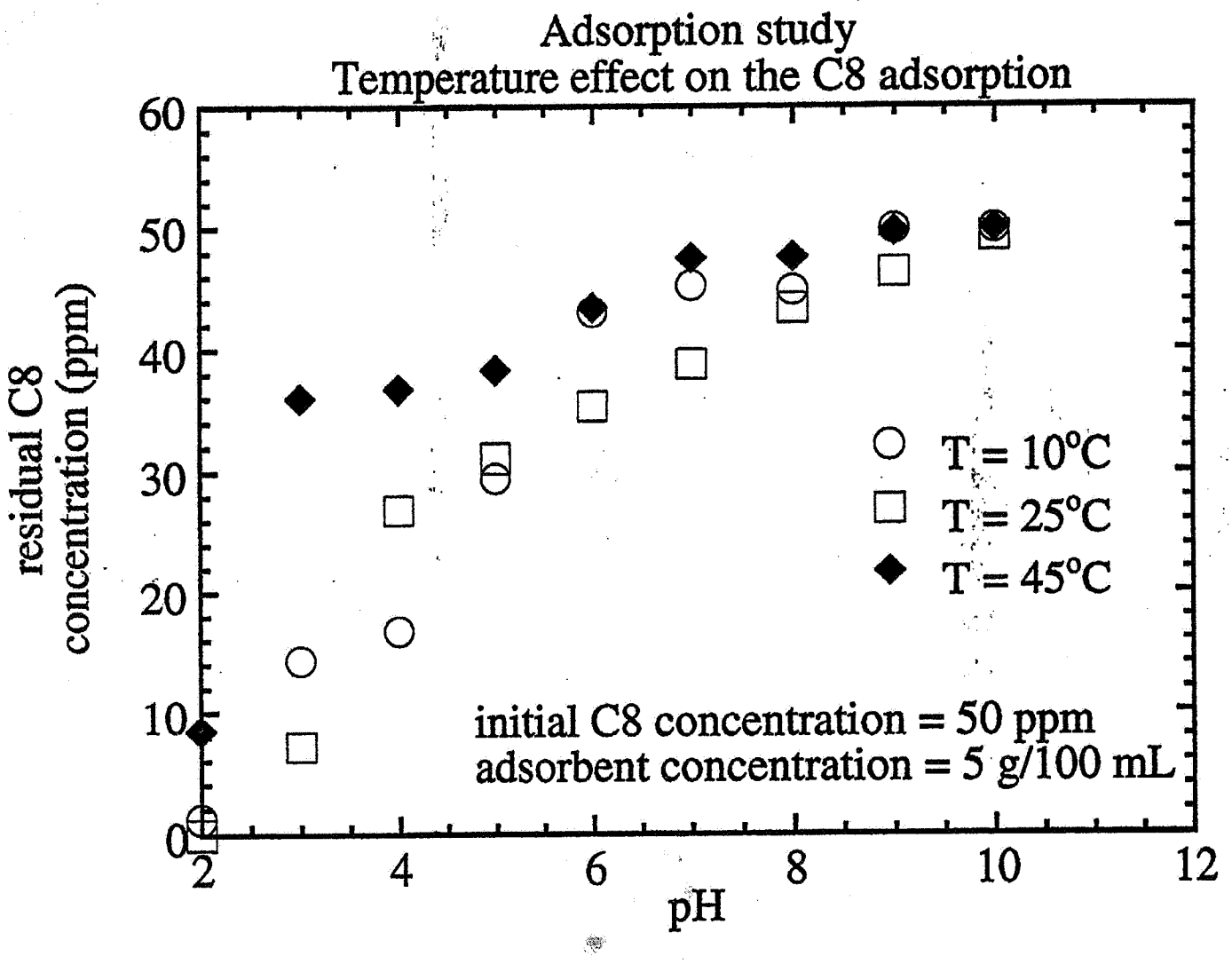

Figure 62. The temperature effect on the residual C8 concentration after the C8 adsorption.
Soil sample: ADPS2 (0' - 5').
Experimental conditions : initial C8 concentration = 50 ppm.
ionic strength = 0.1 M $NaClO_4$.

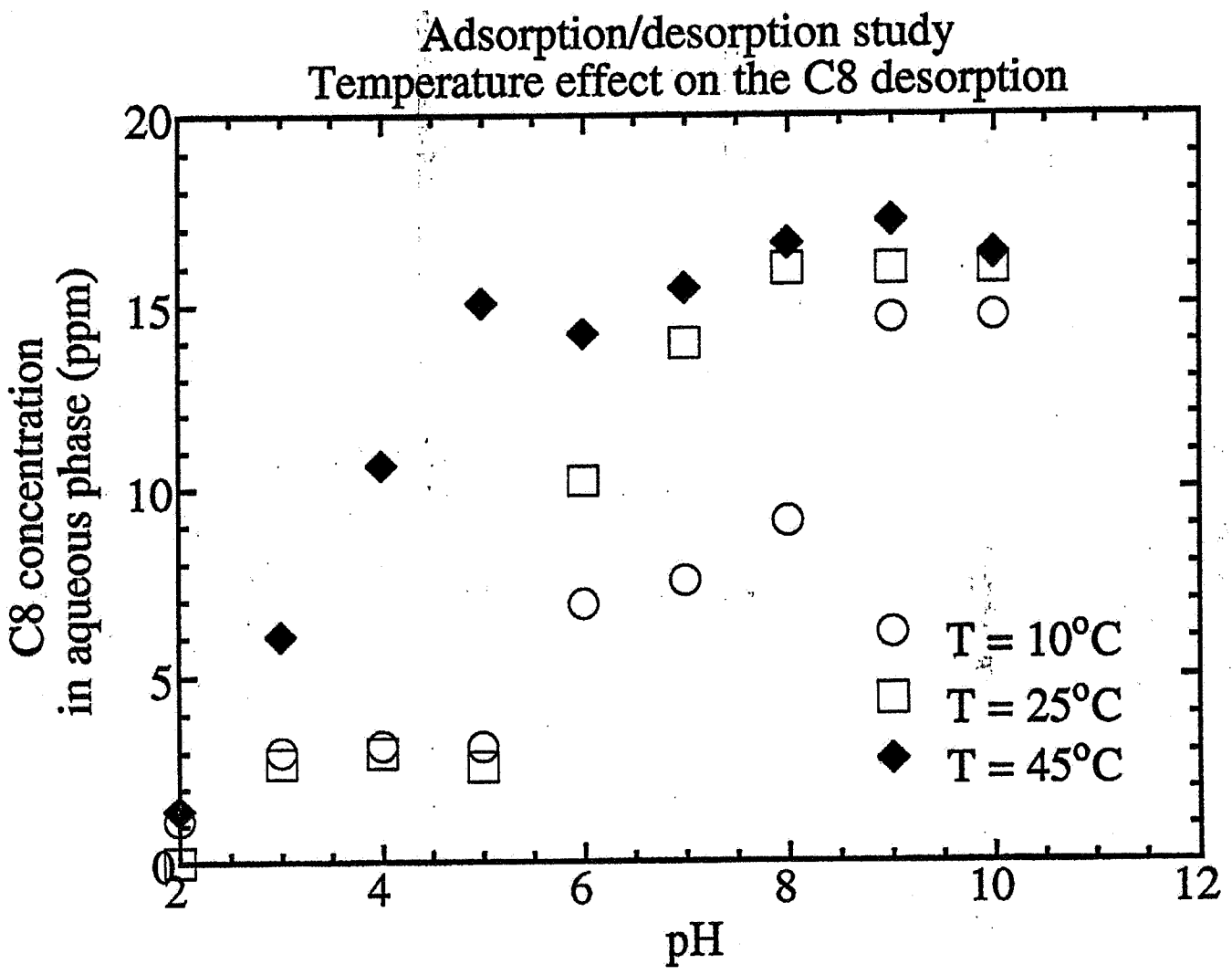

Figure 63. The temperature effect on the C8 desorption.
Soil sample: ADPS2 (0' - 5').
Experimental conditions : initial C8 concentration = 50 ppm.
ionic strength = 0.1 M $NaClO_4$.

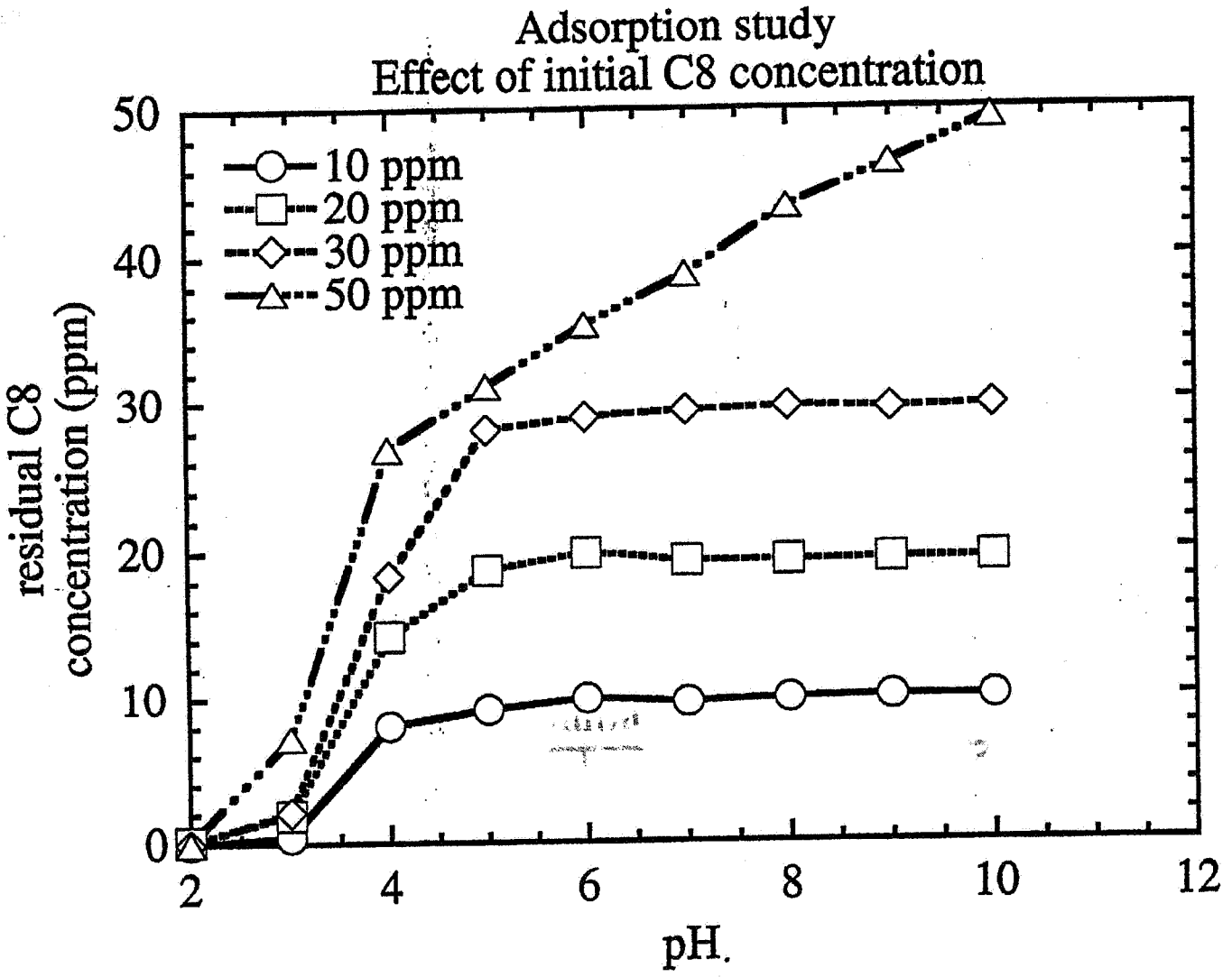

Figure 64. The residual C8 concentration as a function of pH at initial C8 concentration below 50 ppm;
soil sample: ADPS-2(0'-5').
Experimental conditions: ionic strength = 0.1 M $NaClO_4$.

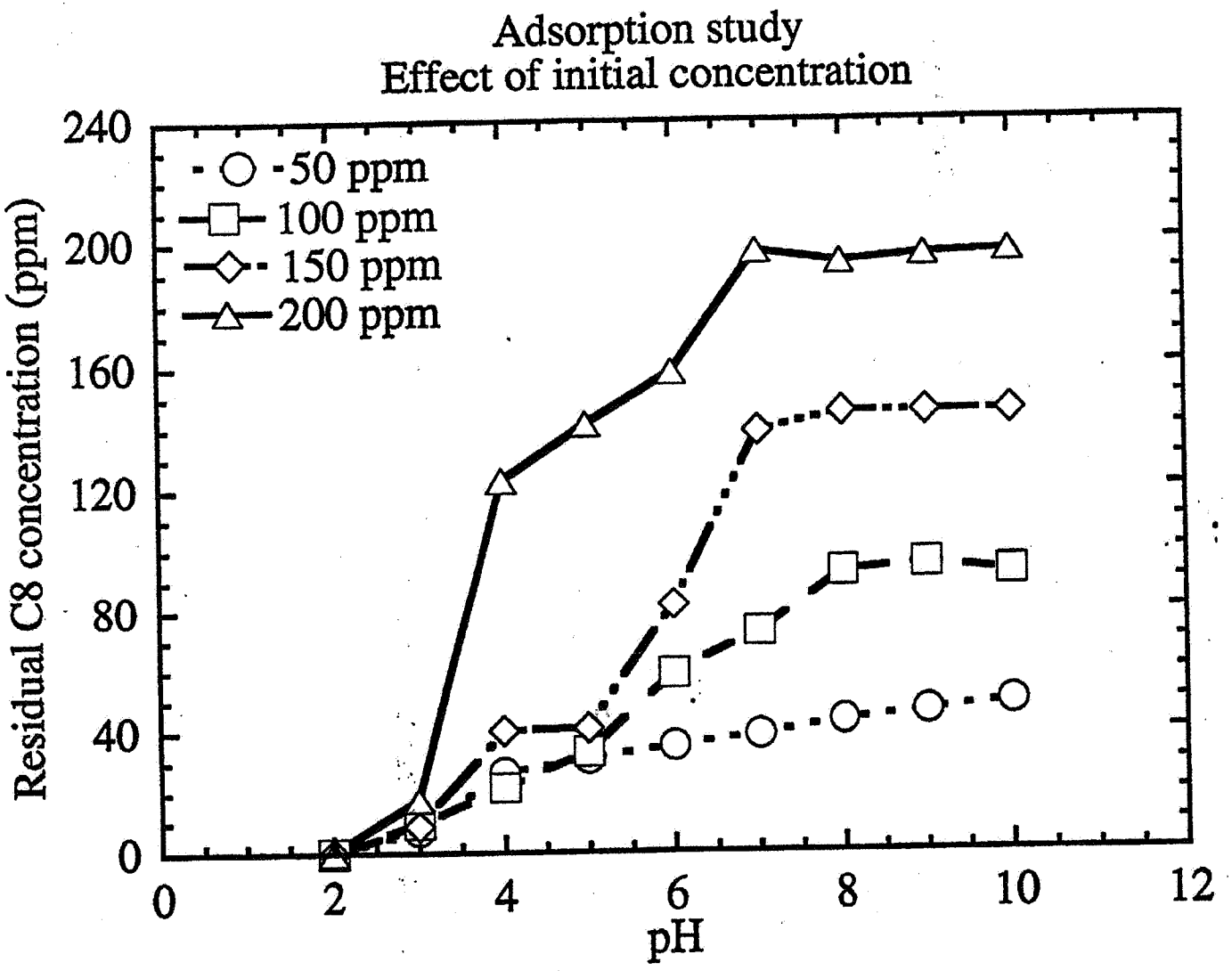

Figure 65. The residual C8 concentration as a function of pH
at initial C8 concentration above 50 ppm;
Soil sample: ADPS-2(0'-5').
Experimental conditions: ionic strength = 0.1 M $NaClO_4$.

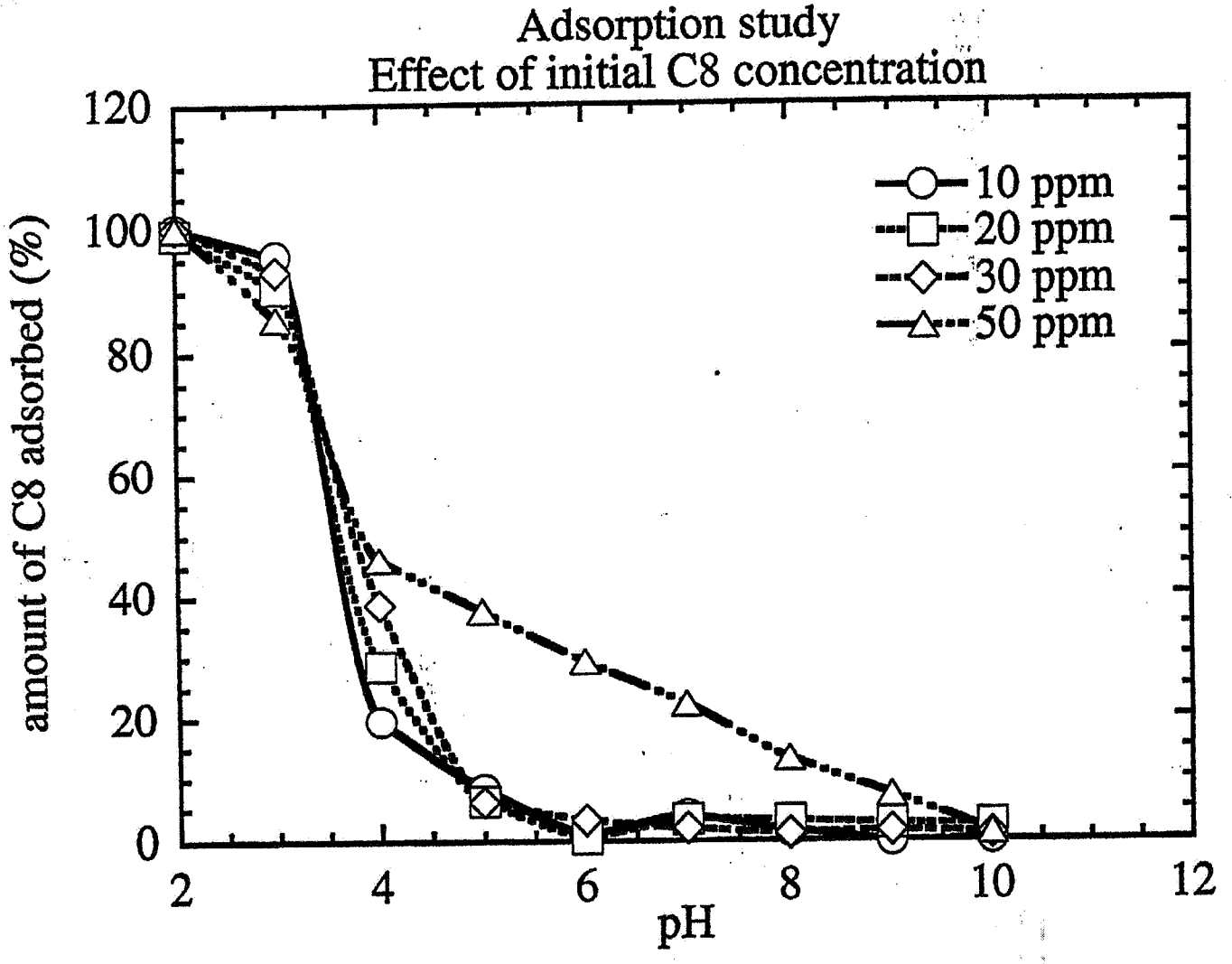

Figure 66. Percentage of C8 adsorbed as a function of pH
at various initial C8 concentration.
Soil sample: ADPS2 (0'-5').
Experimental conditions: pH =7.0; ionic strength = 0.1 M $NaClO_4$.

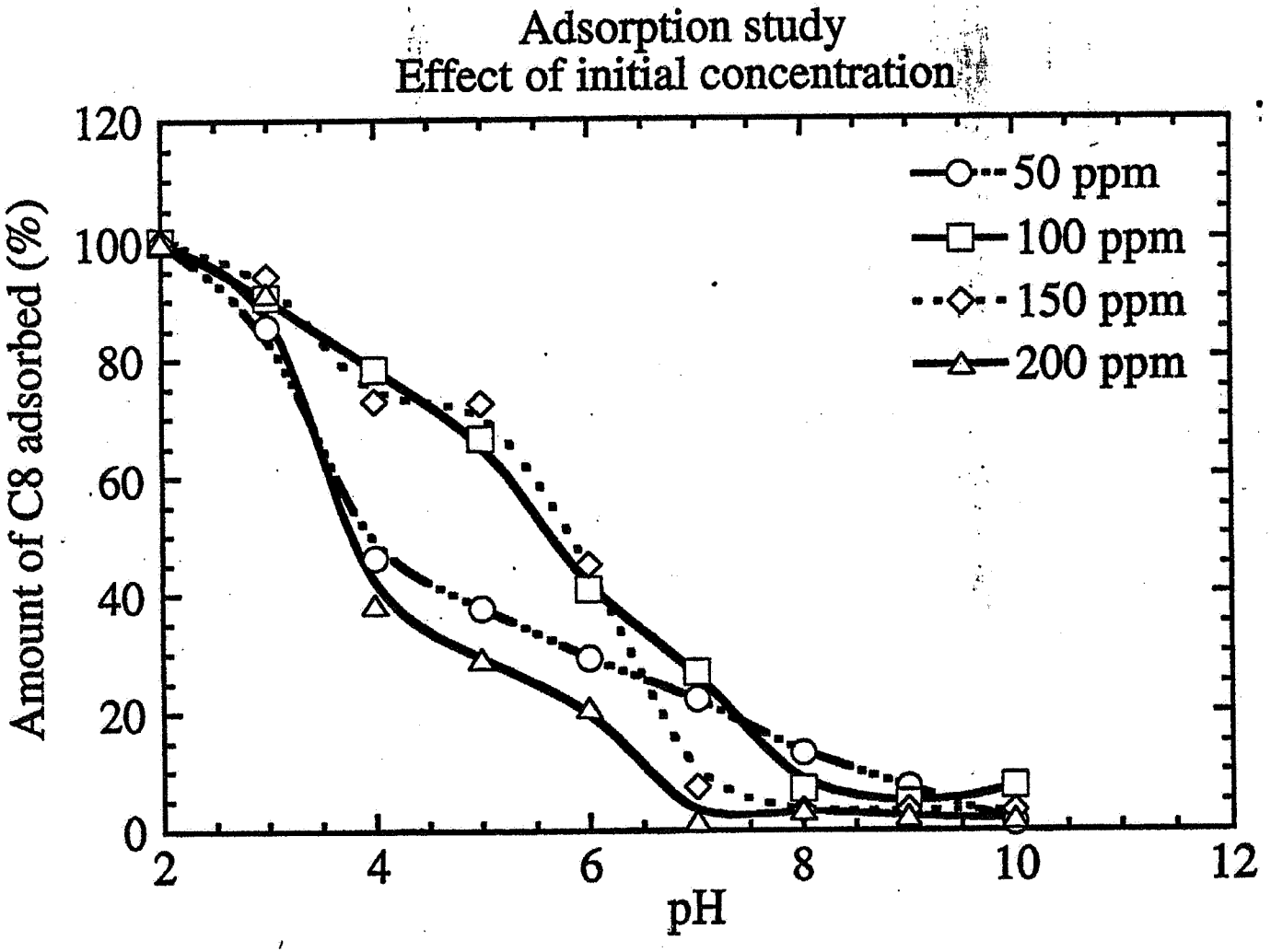

Figure 67. Percentage of C8 adsorbed as a function of pH
at initial C8 concentation above 50 ppm.
Soil sample: ADPS2 (0'-5').
Experimental conditions: pH = 7.0; ionic strength = 0.1 M $NaClO_4$.

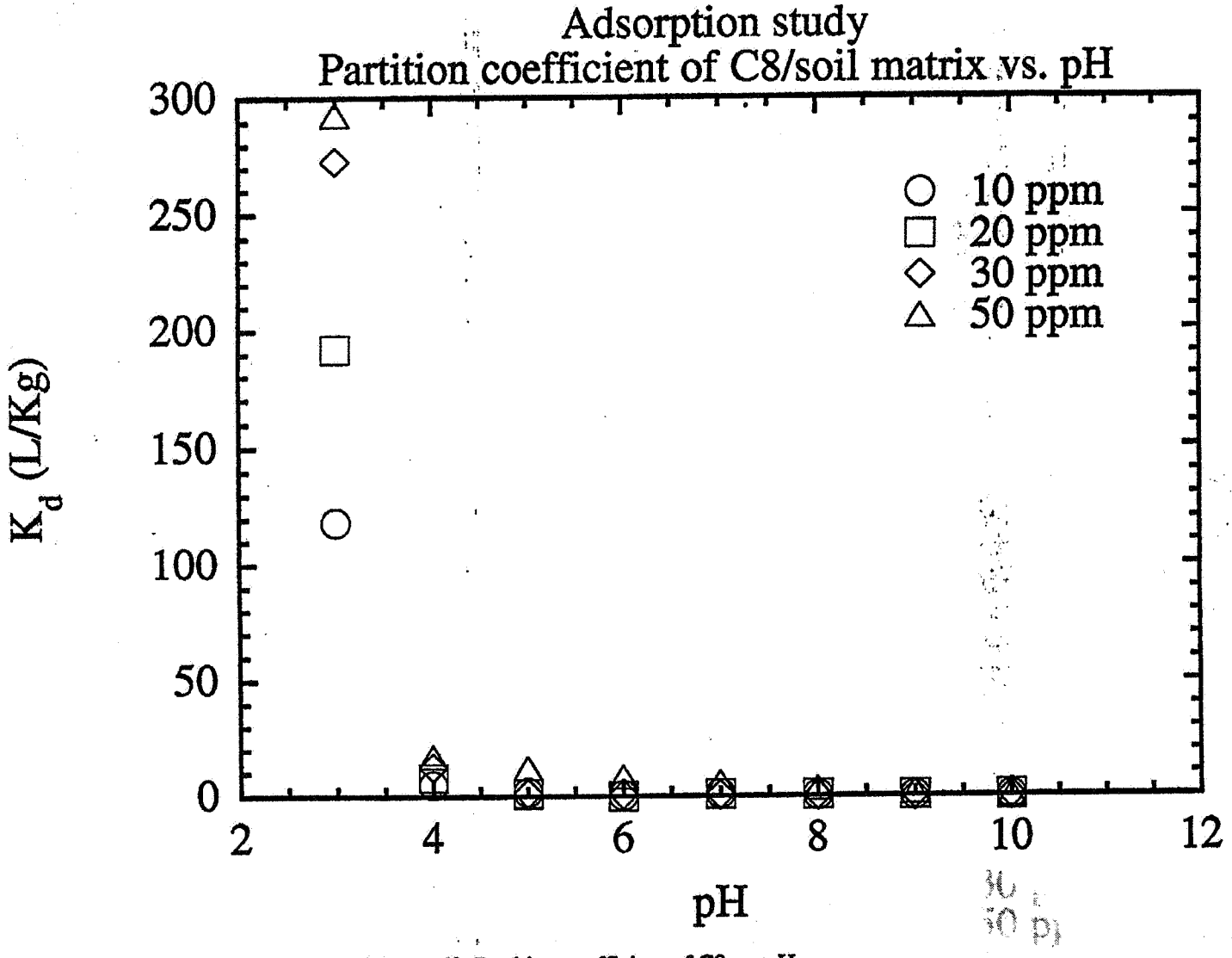

Figure 68. Partition coefficient of C8 vs. pH
at initial concentration below 50 ppm;
soil sample: ADPS-2 (0'-5').
Experimental conditions: Soil/water ratio = 0.05 mg/L;
ionic strength = 0.1 M $NaClO_4$.

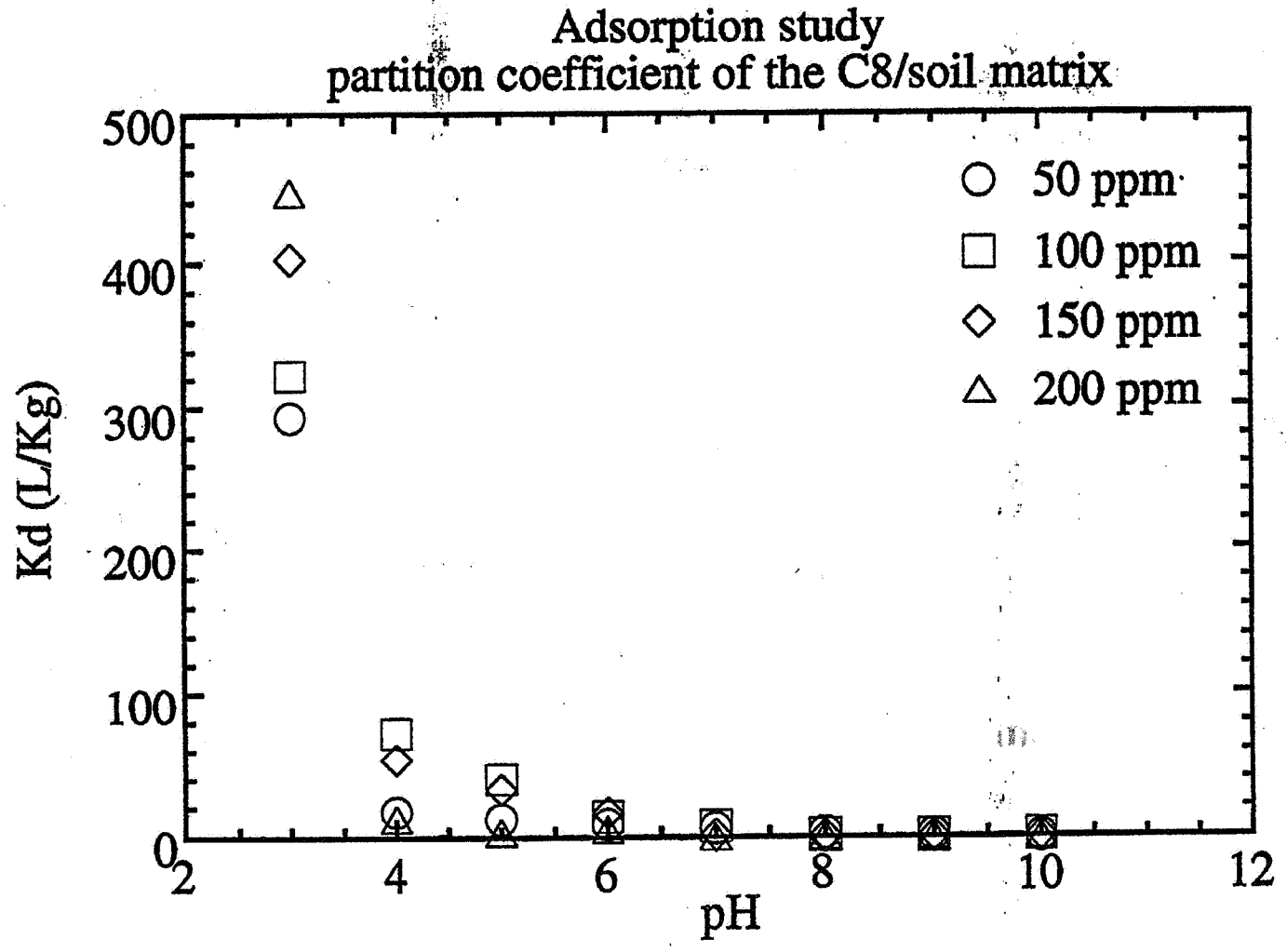

Figure 69. Partition coefficient of C8 vs. pH
at initial concentration 50-200 ppm;
soil sample: ADPS-2 (0'-5').
Experimental conditions: Soil/water ratio = 0.05 mg/L;
ionic strength = 0.1 M $NaClO_4$.

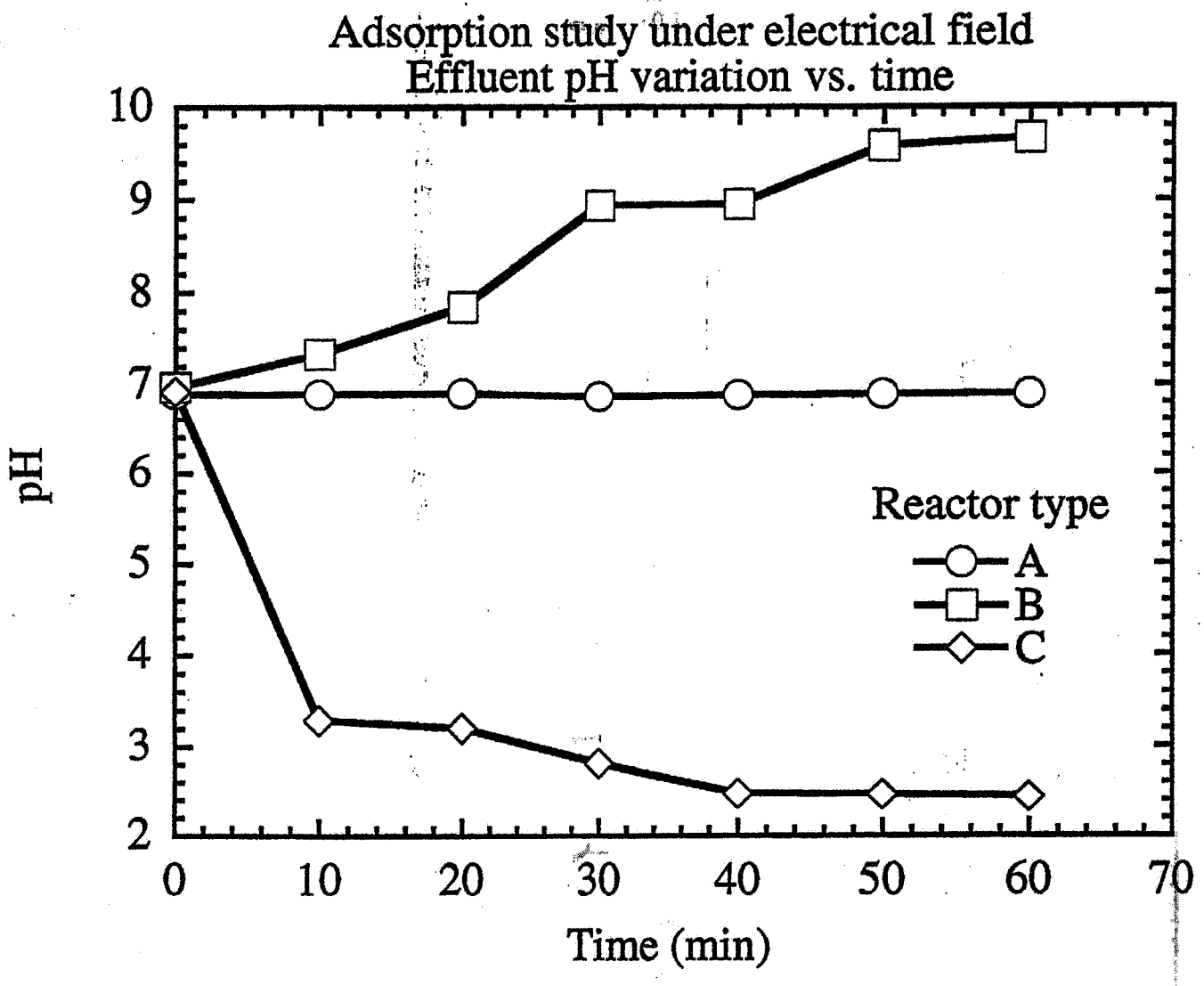

Figure 70. The pH of effluent from the continuous flow apparatus. Experimental conditions: initial C8 concentration = 50 mg/L, ionic strength = 0.1 M, weight of soil = 200 g.

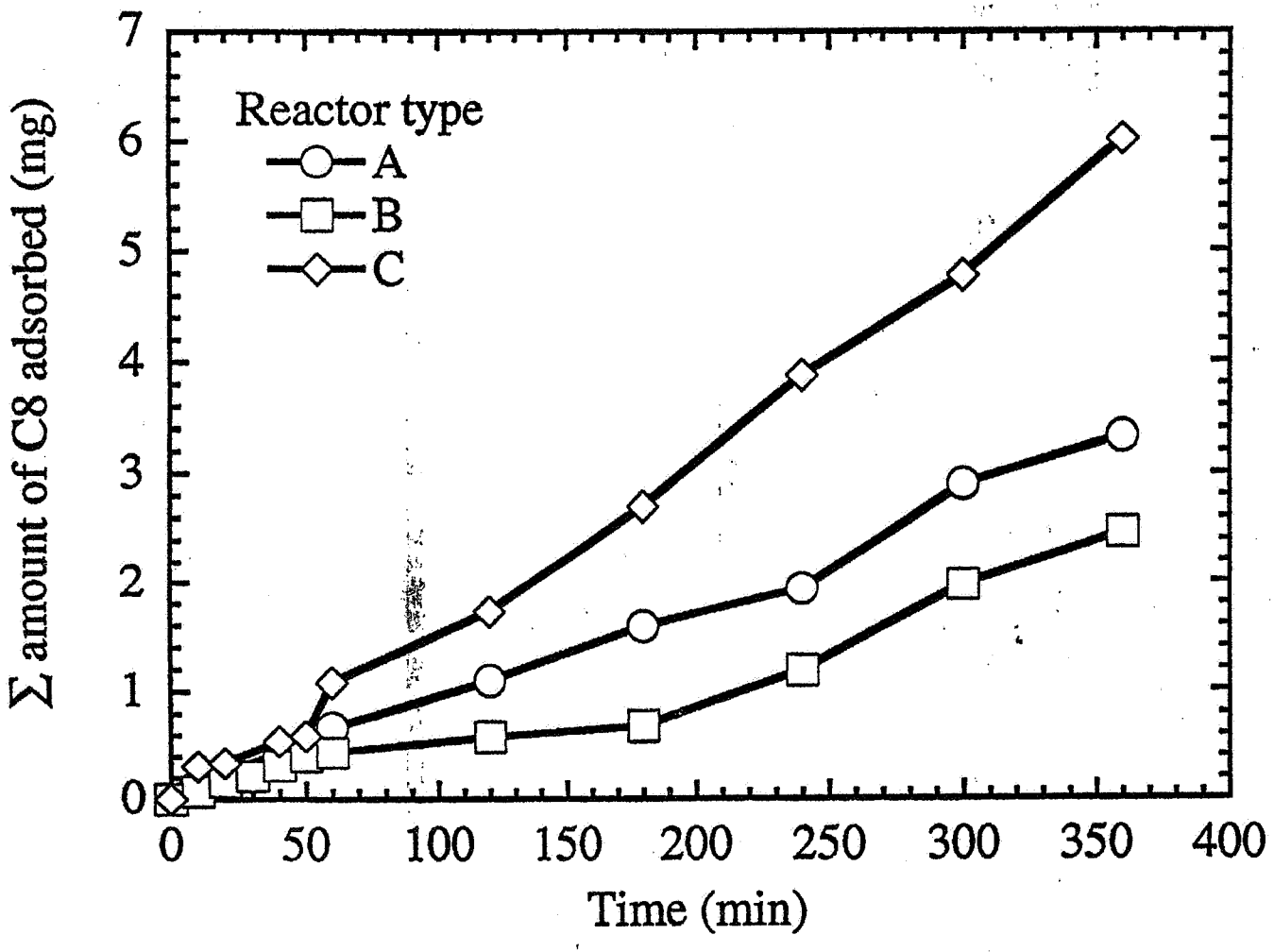

Figure 71. The amount of C8 retained in the soil vs. time.
Experimental conditions are the same as in Figure 70.

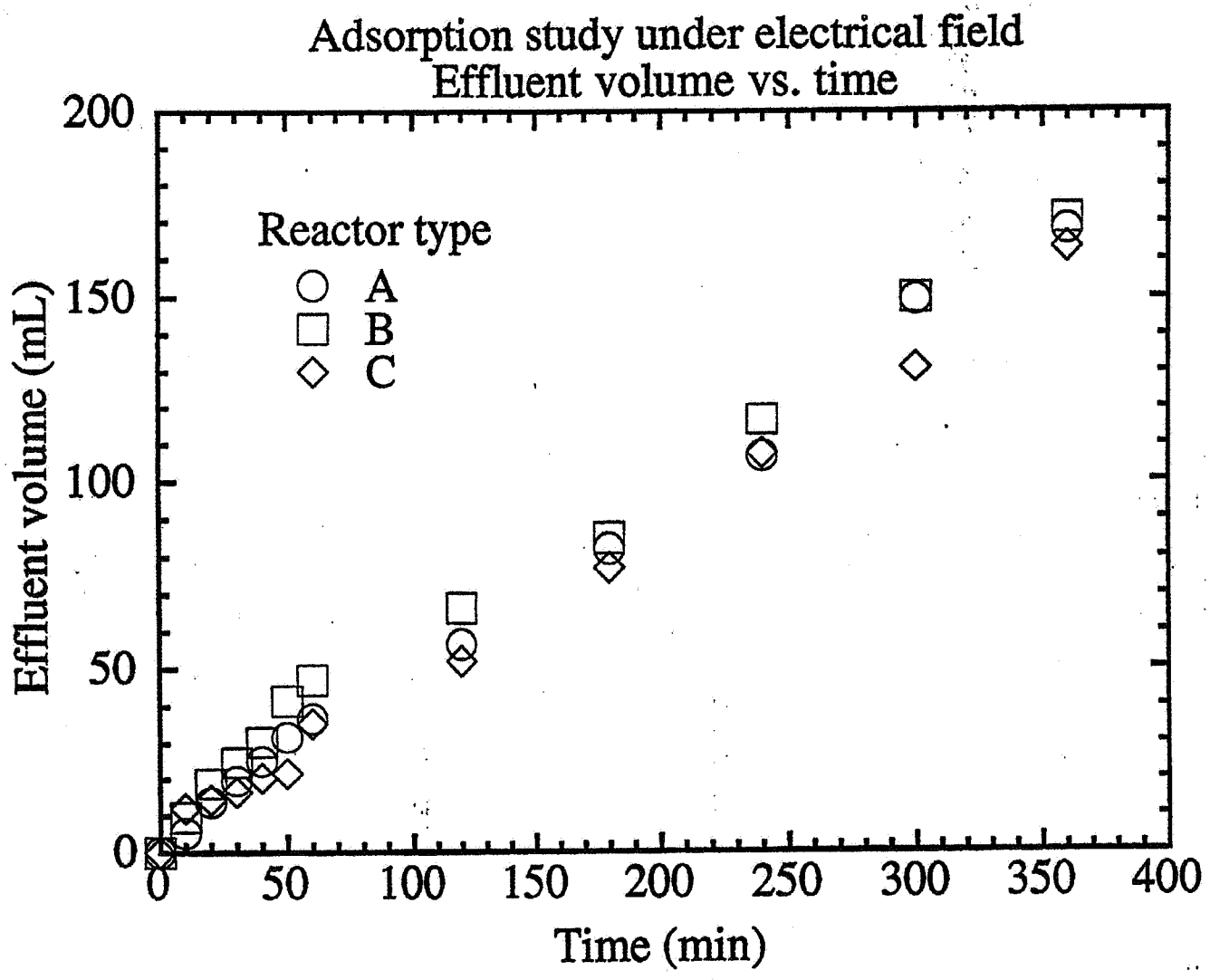

Figure 72. Effluent volume vs. time.
Experimental conditions are the same as in Figure 70.

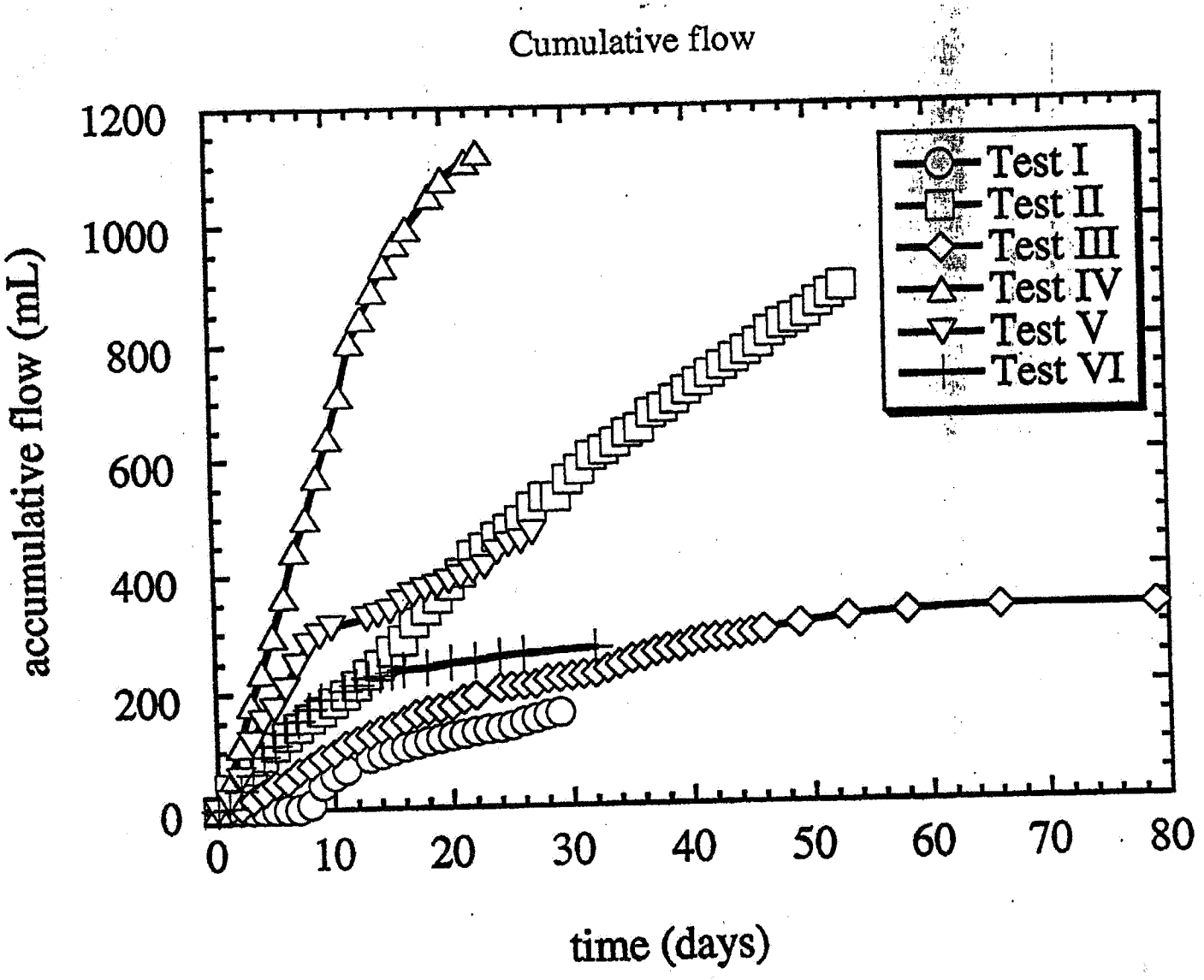

Figure 73. Electro-osmosis experiments.
Accumulative electro-osmotic water flow as a function of time.

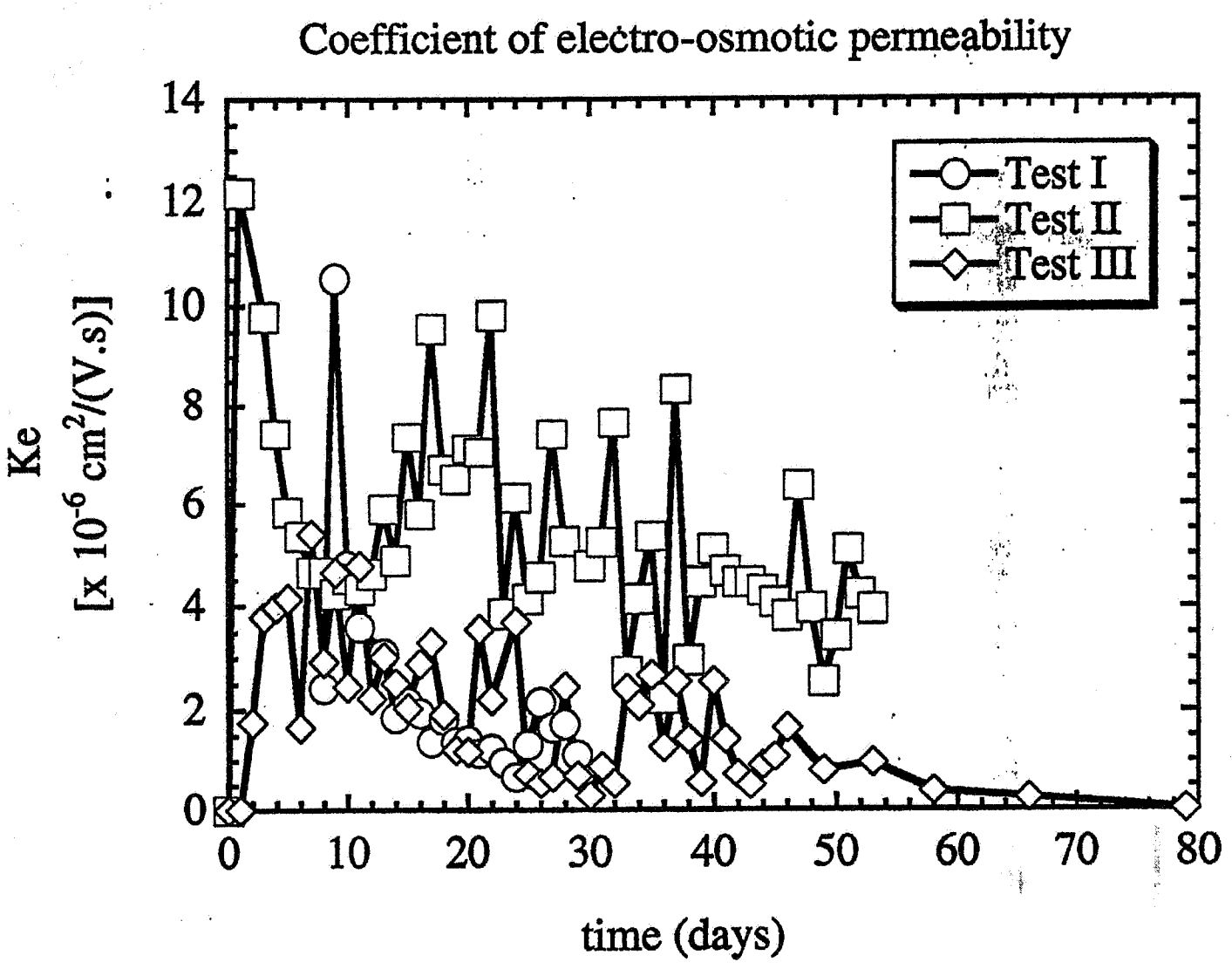

Figure 74a. Electro-osmosis experiments.
Coefficient of electro-osmotic permeability (k_e) as a function of time for Tests I, II and III.

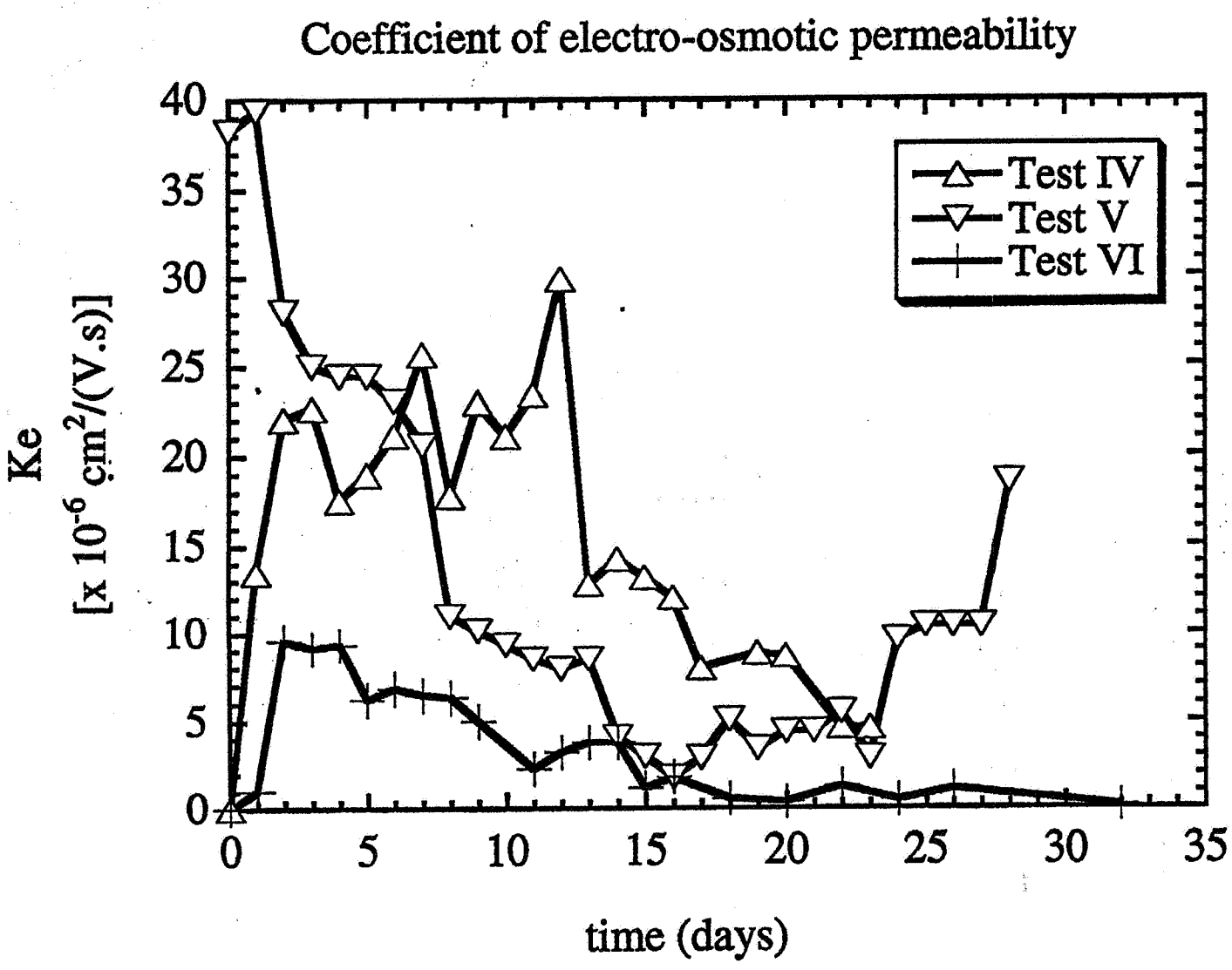

Figure 74b. Electro-osmosis experiments.
Coefficient of electro-osmotic permeability (k_e) as a function of time for Tests IV, V and VI.

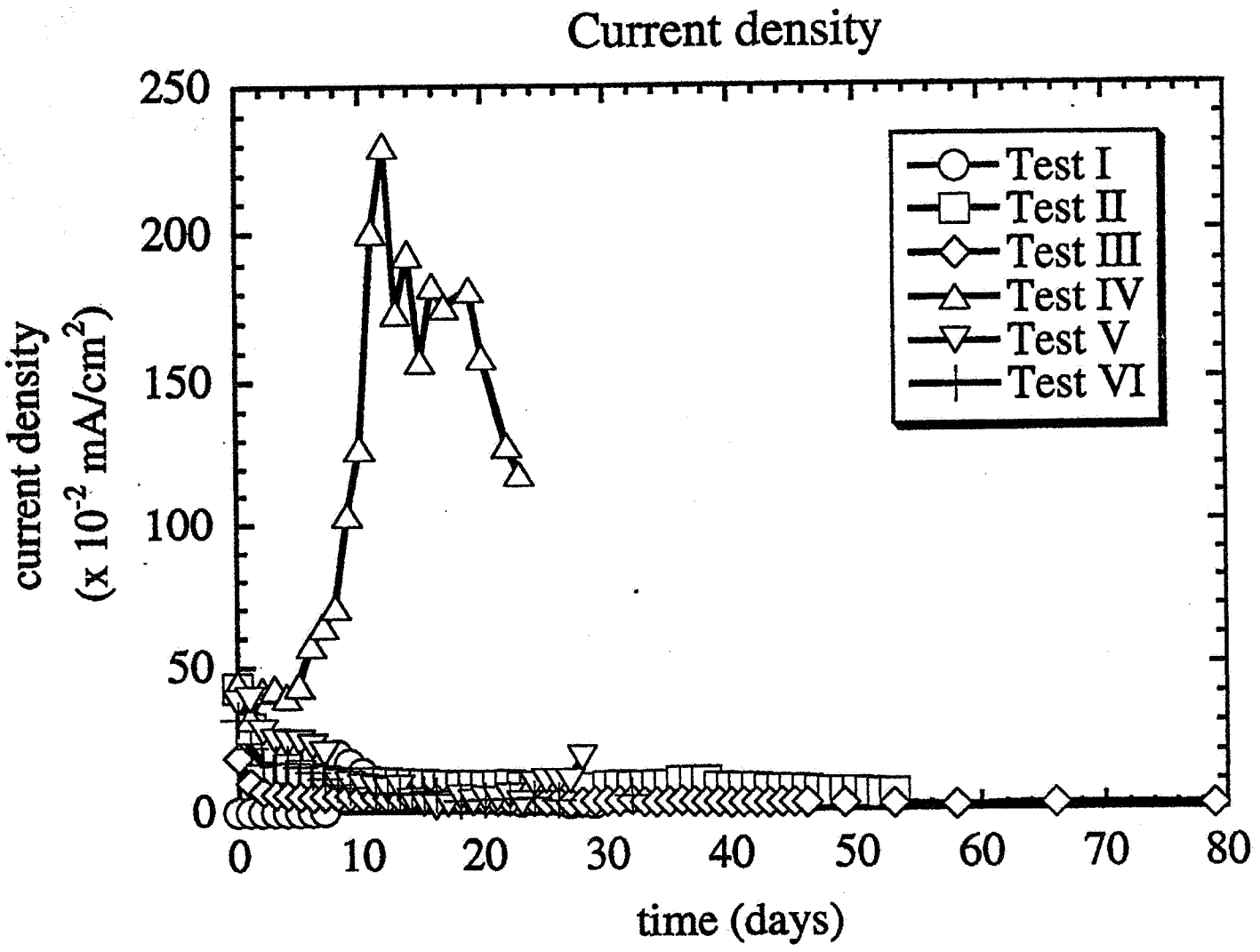

Figure 75. Electro-osmosis experiments.
Current density as a function of time.

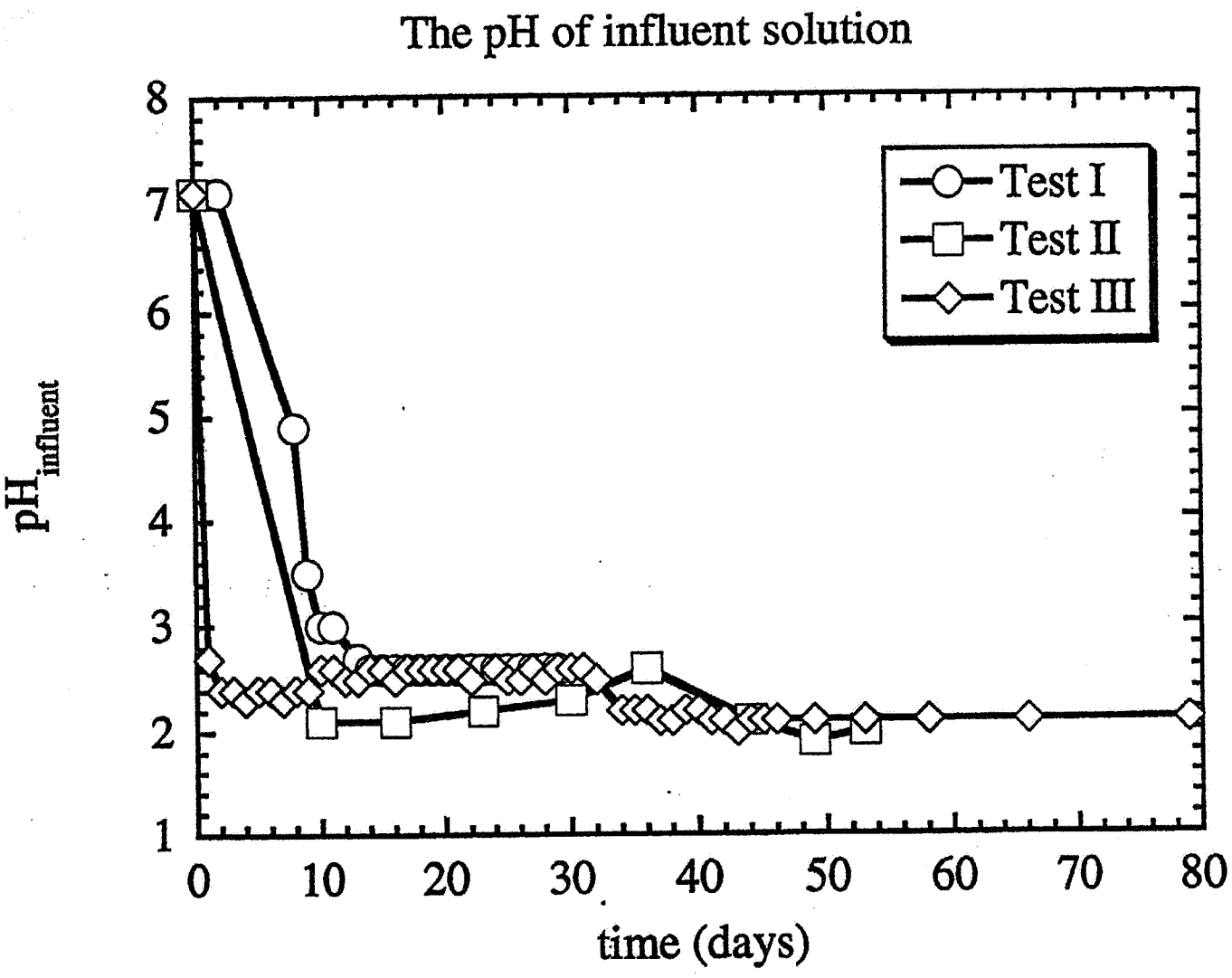

Figure 76a. Electro-osmosis experiments.
The pH of influent solution as a function of time for Tests I, II and III.

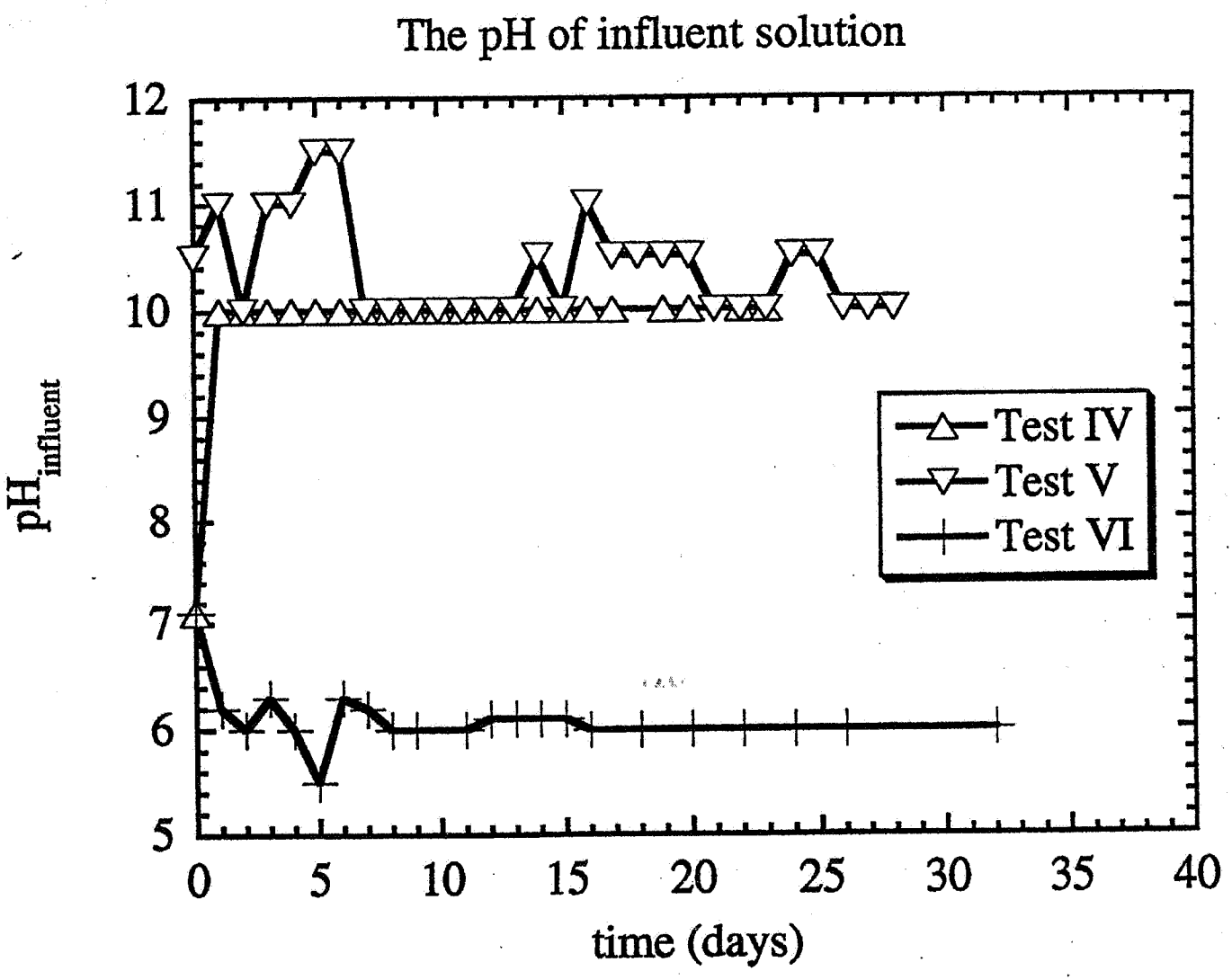

Figure 76b. Electro-osmosis experiments.
The pH of influent solution as a function of time for Tests IV, V and VI.

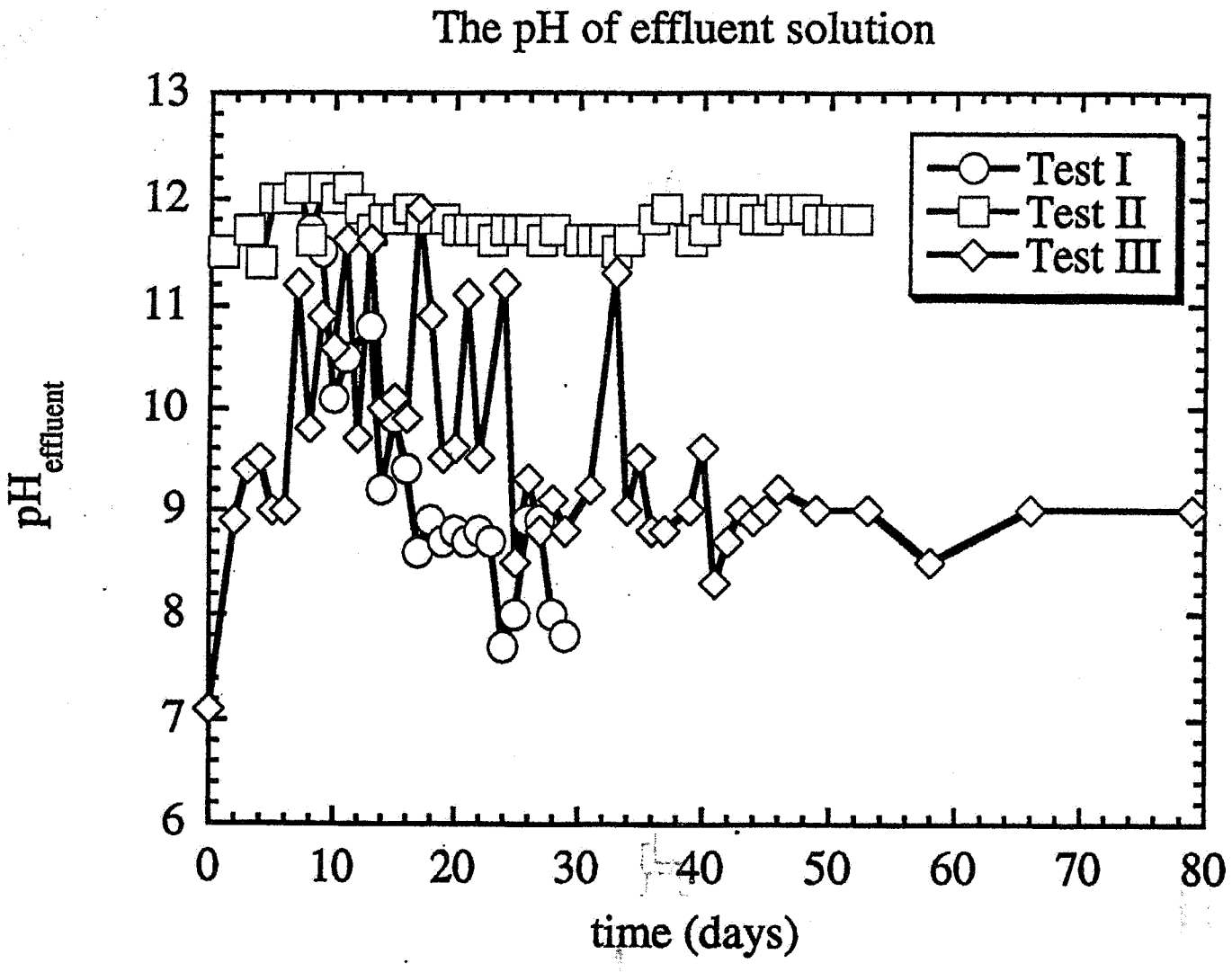

Figure 77a. Electro-osmosis experiments.
The pH of effluent solution as a function of time for Tests I, II and III.

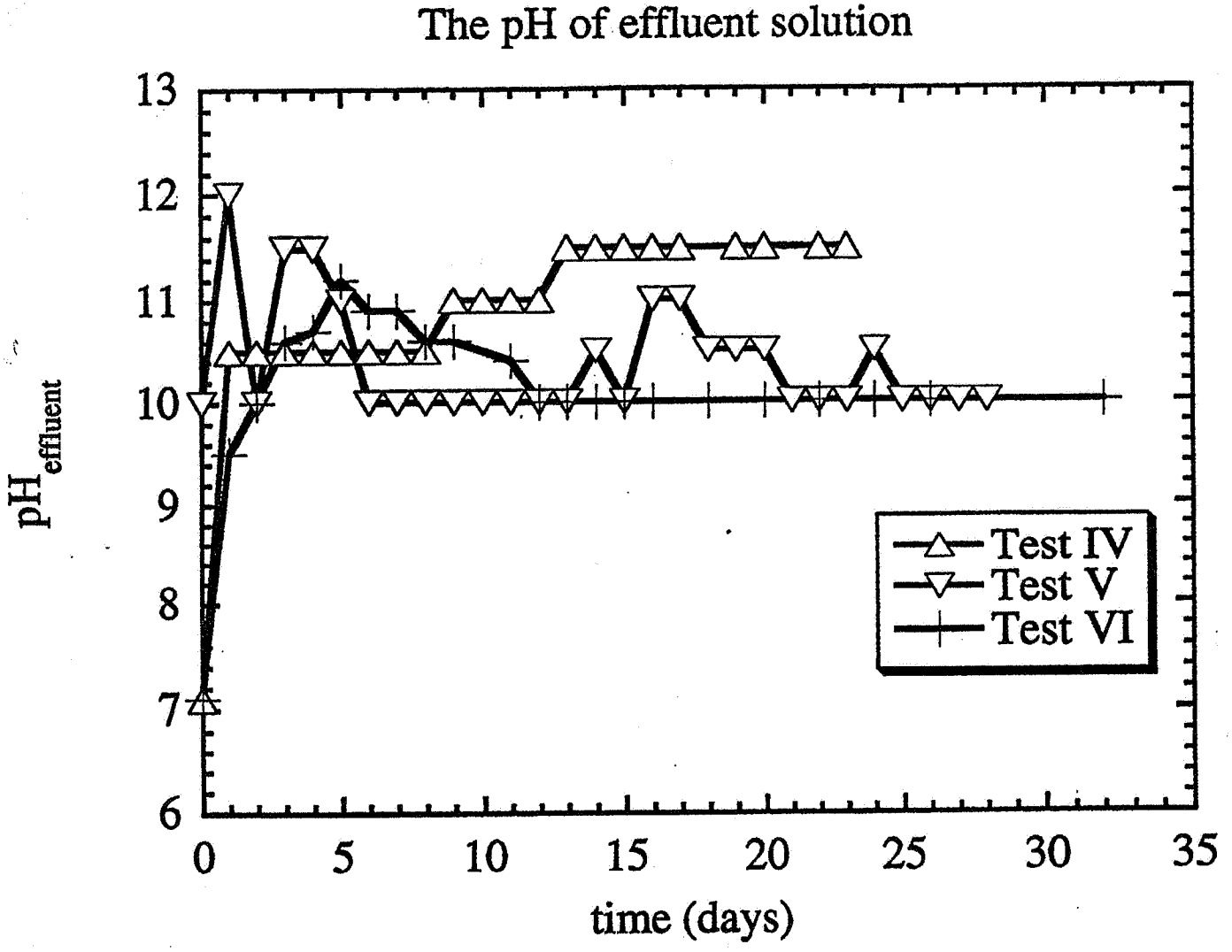

Figure 77b. Electro-osmosis experiments.
The pH of effluent solution as a function of time for Tests IV, V and VI.

ASH0107S2

EID103334

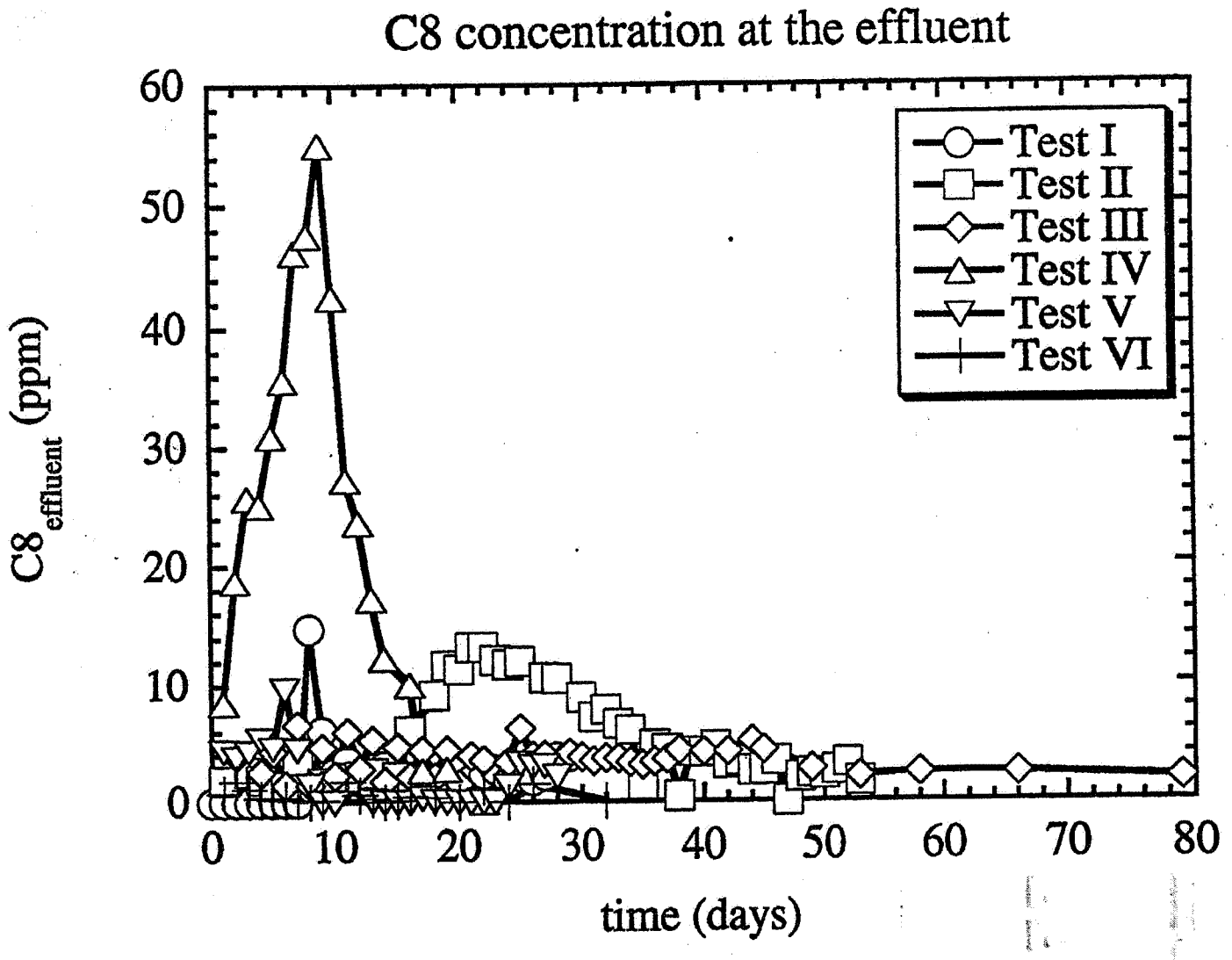

Figure 78. Electro-osmosis experiments.
C8 concentration at the effluent solution as a function of time.

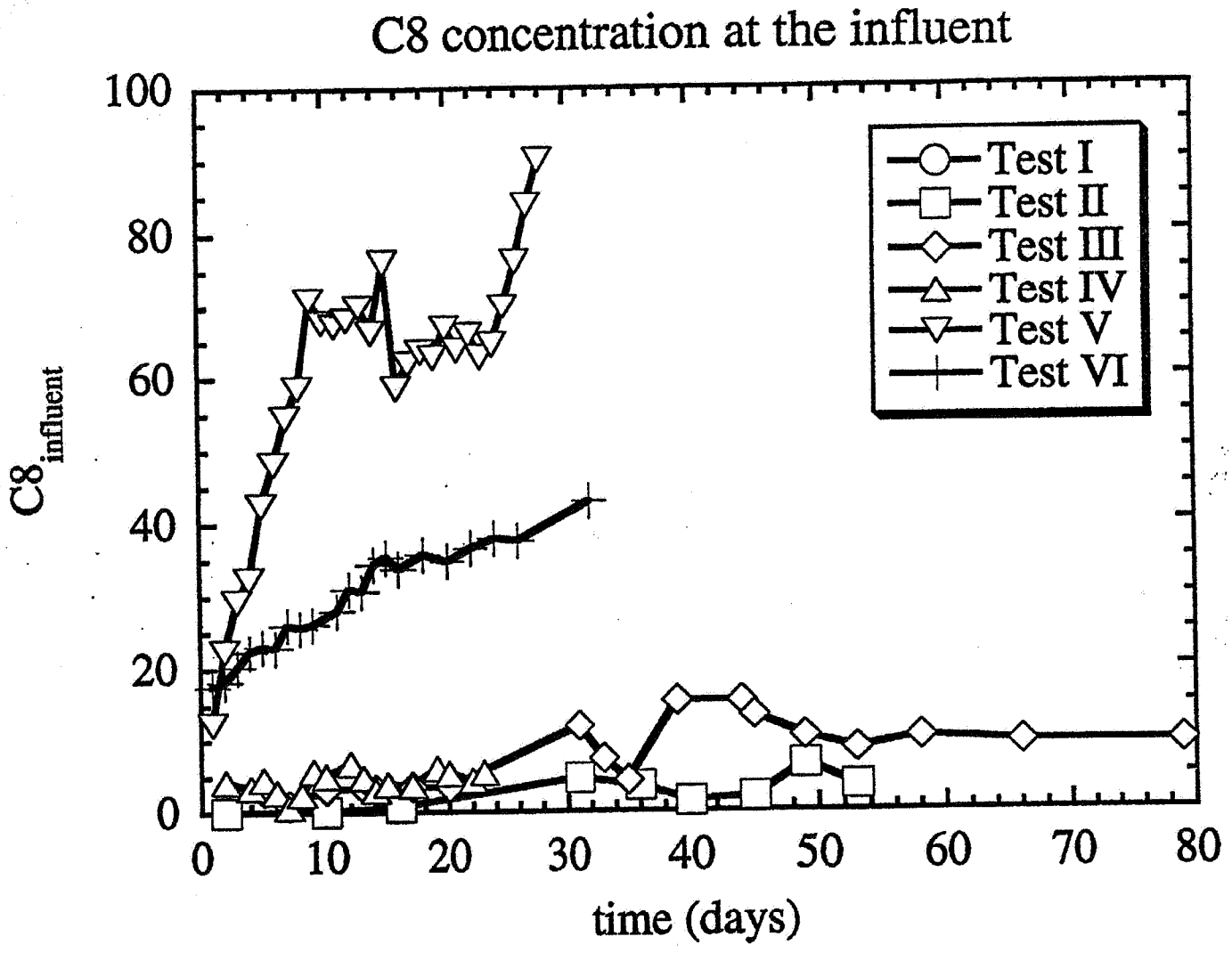

Figure 79. Electro-osmosis experiments.
C8 concentration at the influent solution as a function of time.

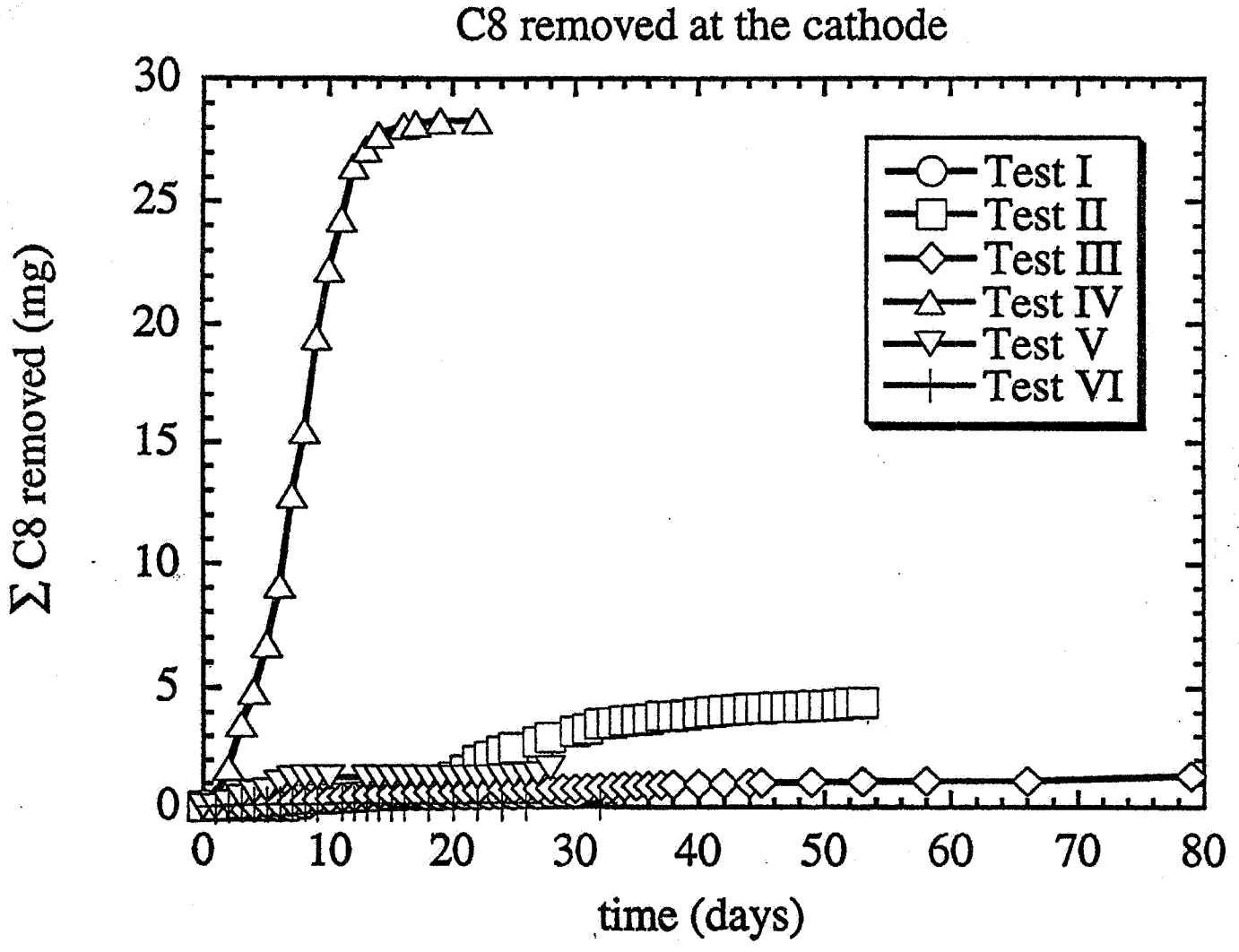

Figure 80. Electro-osmosis experiments.
Cumulative C8 removed at the cathode (in milligrams) as a function of time.

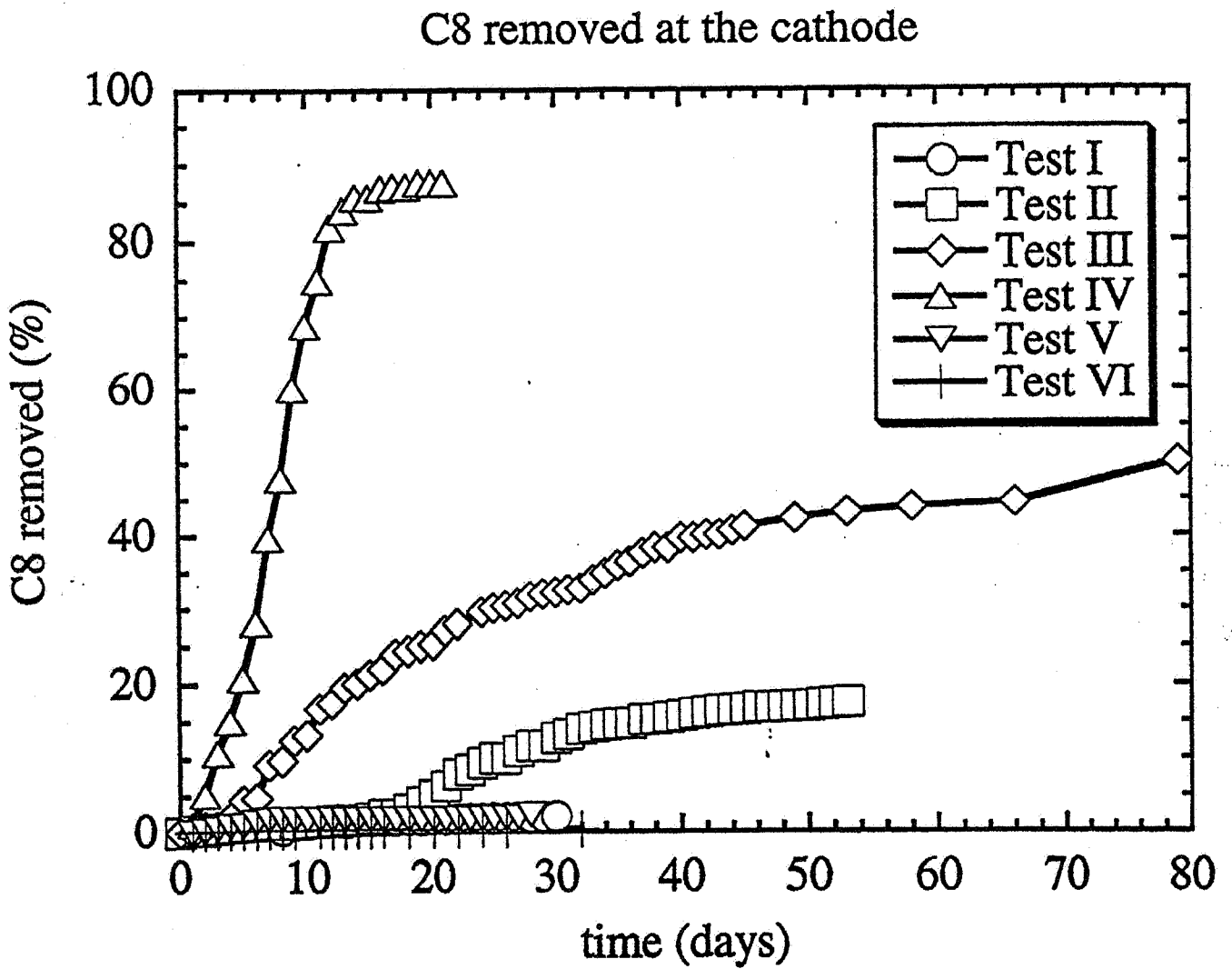

Figure 81. Electro-osmosis experiments.
Cumulative C8 removed at the cathode (in percentage) as a function of time.

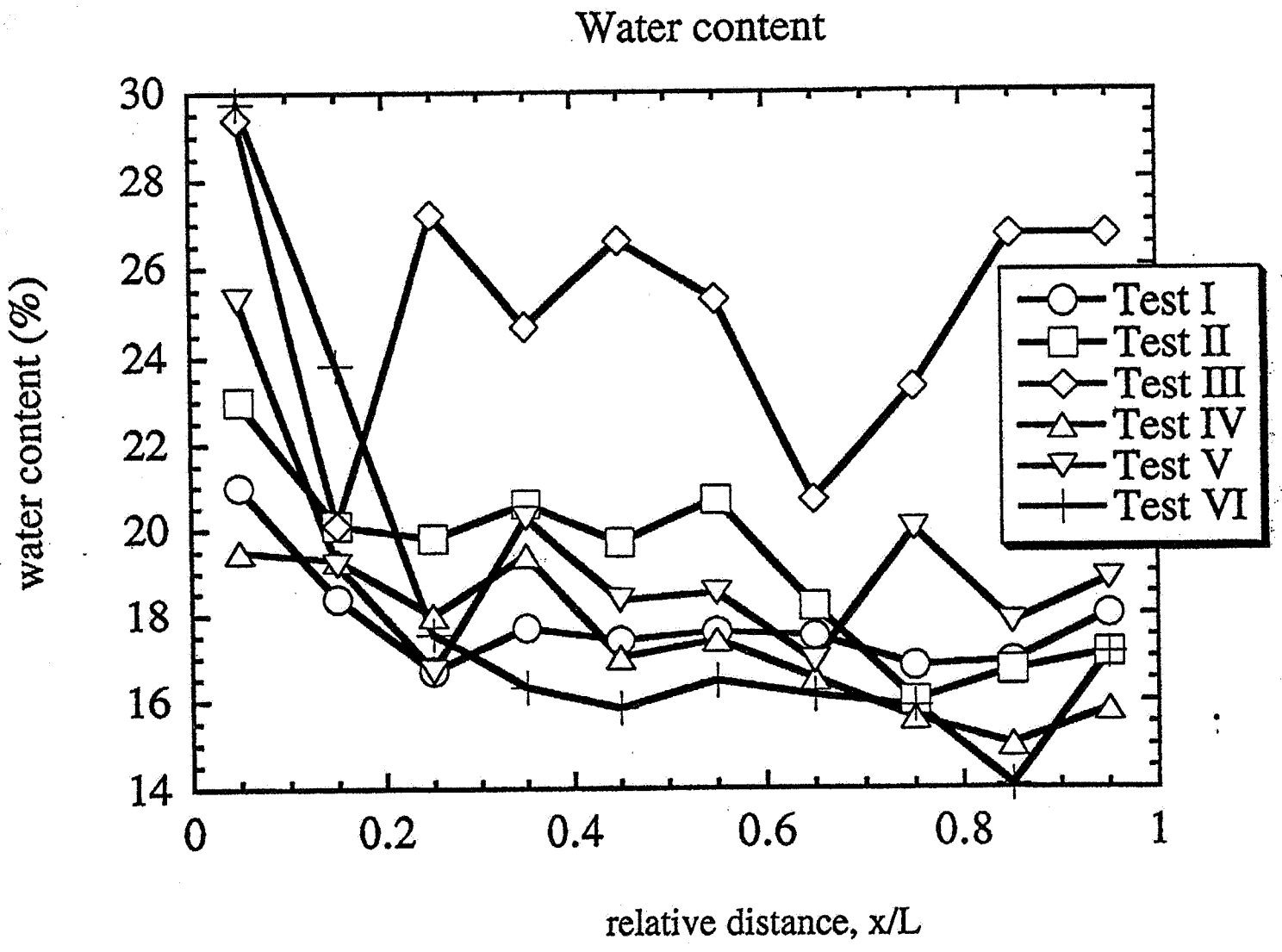

Figure 82. Electro-osmosis experiments.
Water content distribution Vs. relative distance .
x: distance to the anode (cm) ; L: total length of soil column (cm).

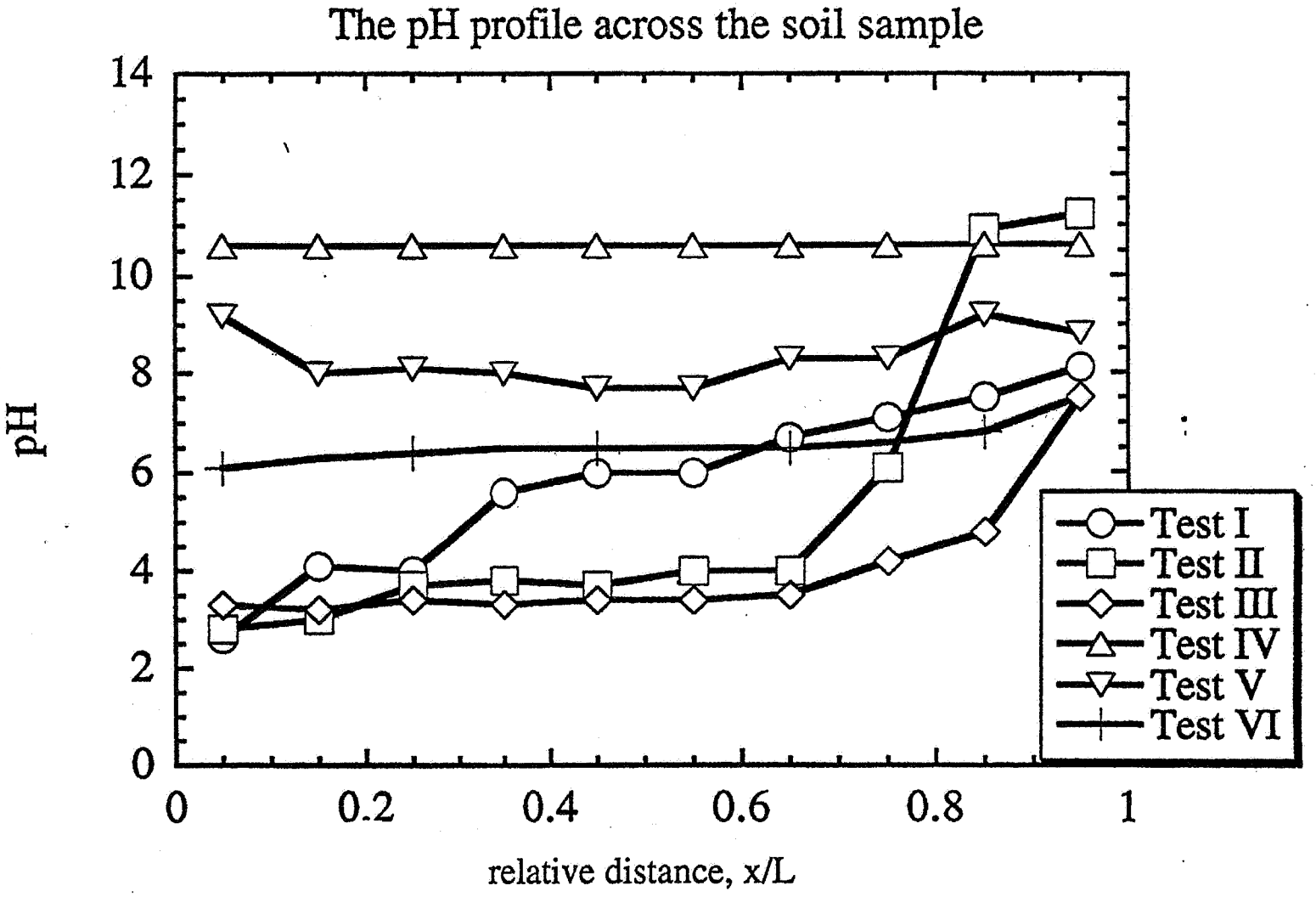

Figure 83. Electro-osmosis experiments.
The soil pH Vs. relative distance .
x: distance to the anode (cm) ; L: total length of soil column (cm).

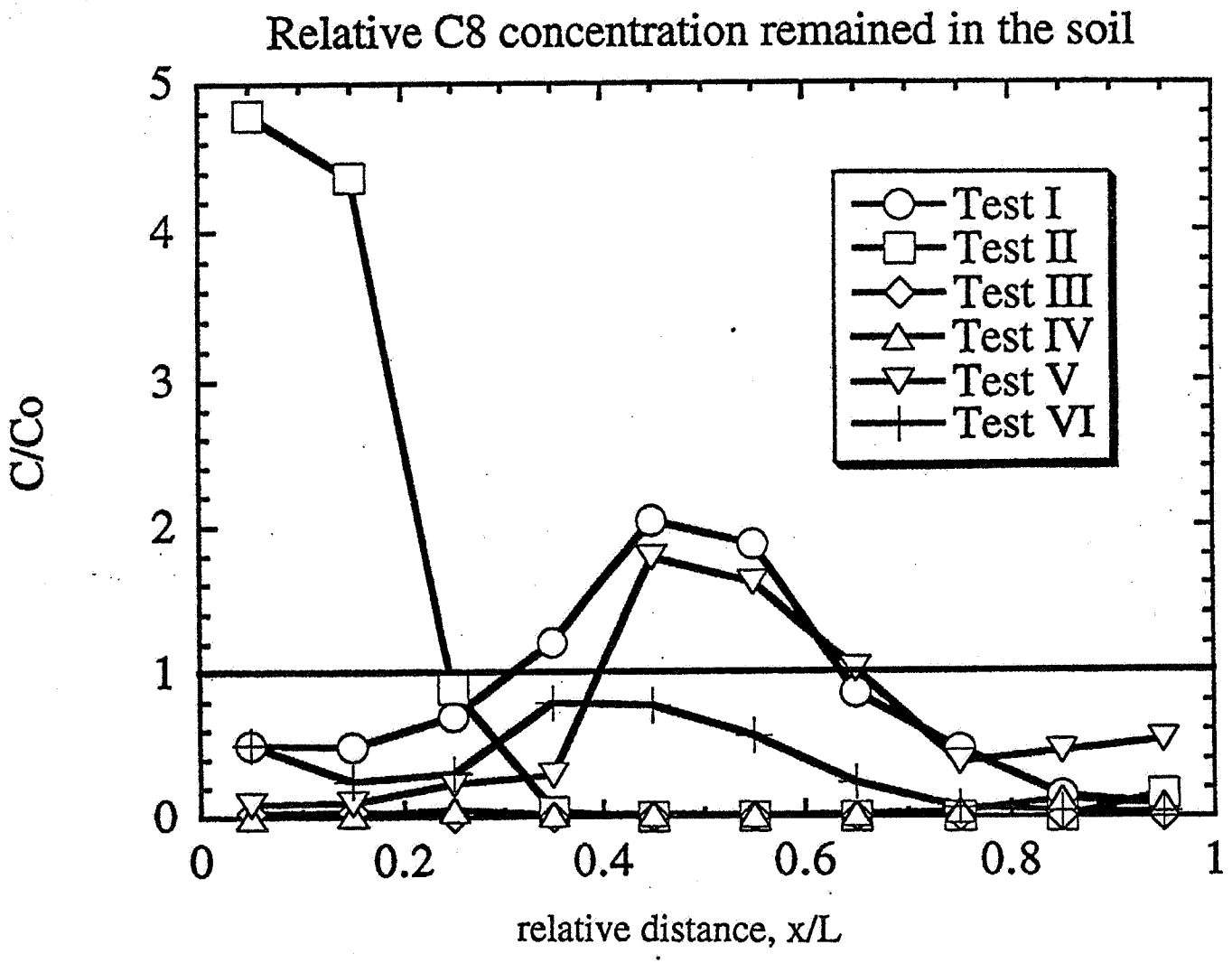

Figure 84. Electro-osmosis experiments.
Relative C8 concentration measued in the soil Vs. relative distance.
x: distance to the anode (cm) ; L: total length of soil column (cm).

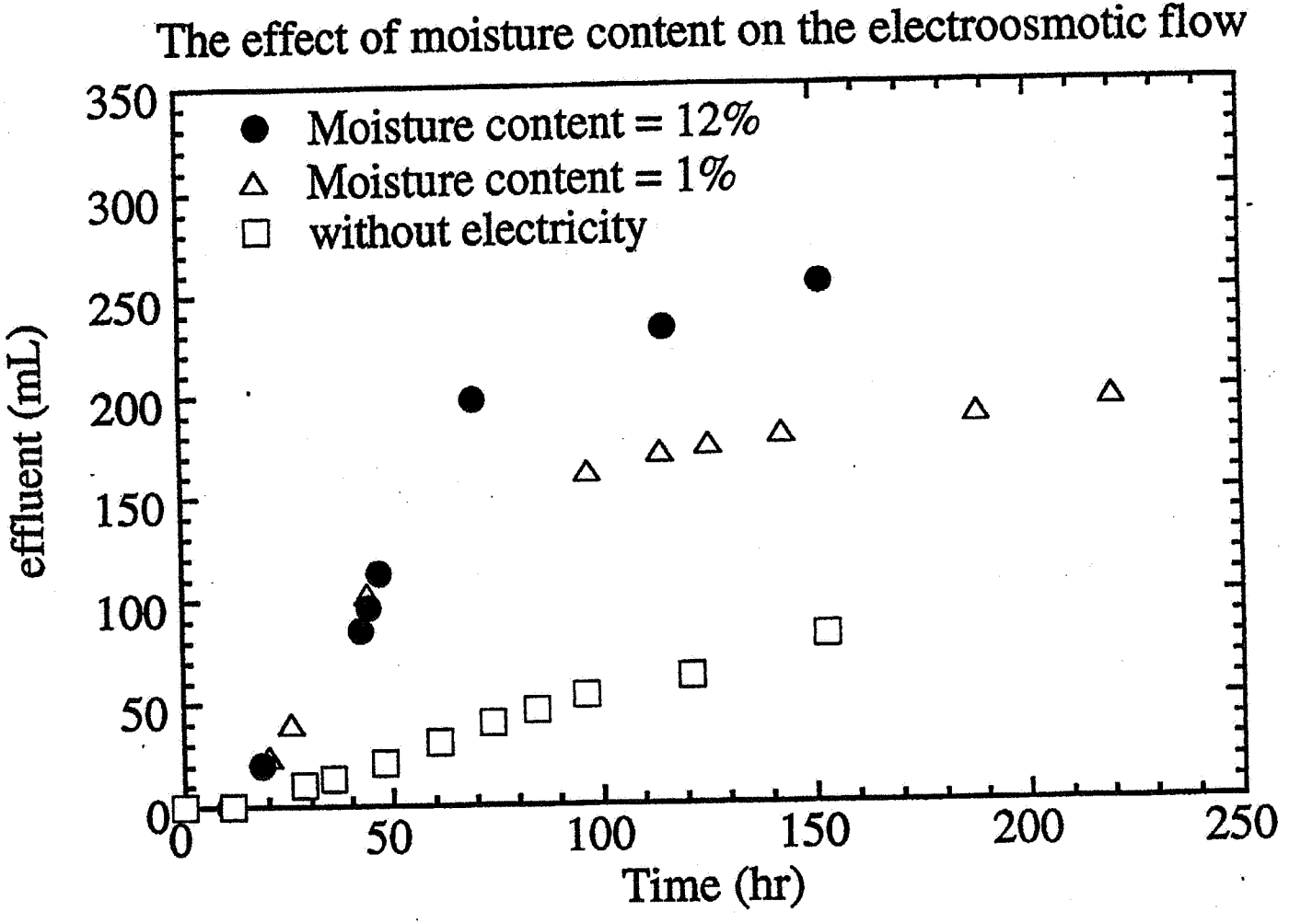

Figure 85. The effect of moisture content on the electro-osmotic flow.
Soil sample: RBLMW2 (10'-12').